Interplay between the bacterial nucleoid protein H-NS and macromolecular crowding in compacting DNA

Kathelijne Wintraecken

Thesis committee

Promoters

Prof.dr.ir. F.A.M. Leermakers
Personal chair at the Laboratory for Physical Chemistry and Colloid Science
Wageningen University

Co-promoters

Prof.dr. T. Odijk
Full professor Complex Fluids Theory group
Delft University of Technology

Dr. R.J. de Vries
Assistant professor at the Laboratory for Physical Chemistry and Colloid Science
Wageningen University

Other members

Prof.dr. J. van der Oost, Wageningen University
Dr. R. Spurio, Università degli Studi di Camerino, Italy
Dr. R.T. Dame, Leiden University
Dr. M.M.A.E. Claessens, University of Twente, Enschede

This research was conducted under the auspices of the graduate school VLAG (Advanced studies in Food Technology, Agrobiotechnology, Nutrition and Health Sciences).

Interplay between the bacterial nucleoid protein H-NS and macromolecular crowding in compacting DNA

Kathelijne Wintraecken

Thesis

submitted in fulfilment of the requirements for the degree of doctor

at Wageningen University

by the authority of the Rector Magnificus

Prof.dr. M.J. Kropff,

in the presence of the

Thesis committee appointed by the Academic Board

to be defended in public

on Friday the 21st of September 2012

at 1.30 p.m. in the Aula.

Kathelijne Wintraecken
Interplay between the bacterial nucleoid protein H-NS and macromolecular crowding in compacting DNA
Thesis, Wageningen University, Wageningen, The Netherlands
With references, contains summaries in English and Dutch
ISBN 978-94-6173-302-3

To my mother

Table of contents

Chapter 1

Introduction

1.1 Motivation

This thesis is concerned with the role of the DNA binding protein H-NS (Histone-like Nucleoid Structuring protein) in condensing bacterial DNA. The condensation of the bacterial genomic DNA and its associated proteins into a structure called the bacterial nucleoid is ill understood at present, but it has been suggested that some of the proteins associated with DNA play a crucial role. H-NS is a bacterial nucleoid protein that is thought to be crucially important as a global regulator of gene expression and as a modulator of nucleoid structure. In this thesis, we use approaches from physical chemistry and biochemistry to elucidate the role of H-NS in condensing DNA, with excursions into related topics: the influence of H-NS self-association on its DNA binding properties, and the role of the archaeal nucleoid protein Sso7d (from *Sulfolubus Solfataricus*) in condensing DNA. In this introductory chapter we discuss basic concepts underlying the later chapters of this thesis.

We first briefly review current ideas about the organization of genomic DNA in prokaryotes (especially bacteria) and point out some of the gaps in our knowledge about this topic. Next, we introduce the behaviour of DNA as a polymer, and models for DNA compaction/condensation. A short summary of the literature on H-NS as a nucleoid-associated protein focuses on its self-association behaviour, its DNA-binding properties and its possible role in DNA compaction. This is followed by a brief overview of some other abundant bacterial and archaeal nucleoid proteins. Many new insights into the physical properties of nucleoid proteins and their binding to DNA have been derived from recent single molecules studies. Therefore we briefly introduce some of these techniques and some results relating to nucleoid-associated proteins (NAPs). Finally, we introduce light scattering, the technique most extensively used in this thesis, and its applications to the characterisation of DNA, proteins and DNA-protein complexes.

1.2 Organization of DNA in bacteria

The structure of DNA in bacteria and other prokaryotes is very different from the organization of the genome in eukaryote cells: prokaryotes lack a nuclear envelope or membrane and histones. Bacterial genomes are also much smaller; they typically contain several thousands of genes and range in size from roughly 0.5 to 10×10^6 base pair (bp) (Krawiec and Riley, 1990). The bacterial genome is especially small compared to the human genome, which is ~3 Gbp (genome sizes are generally expressed in base pairs) and contains

~30,000 genes. If stretched out, the average bacterium's genomic DNA would be millimetres long. This is far longer than a typical bacterium such as *E. coli* , which is 2 to 4 μm long, depending on growth conditions (Aarsman *et al*., 2005).

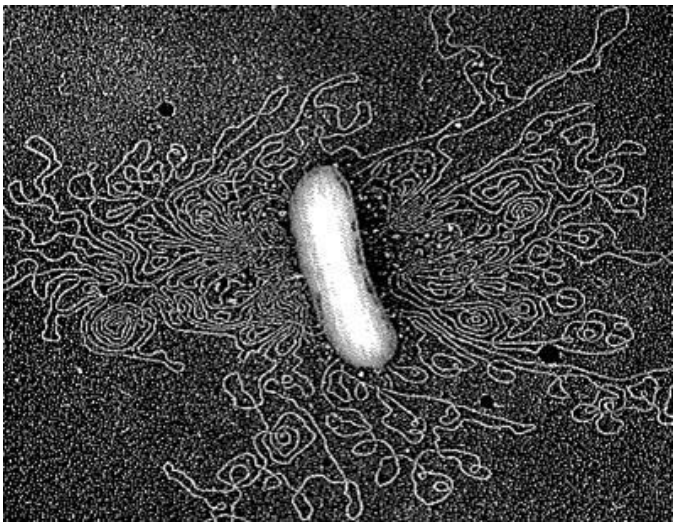

Figure 1.1: *E. coli* with ghost and rosette DNA
This electron micrograph shows the *E. coli* ghost in the middle, surrounded by its circular chromosome in looped random coils. The *E. coli* ghost is ~2 μm long. Picture credits: Dr. Gopal Murti/Science photo library.

The amount of DNA in the smallest bacterial genome would be far too large to be contained inside even the largest bacteria if the DNA polymer was a random coil (Figure 1.1). Bacteria, like all organisms, must reduce the volume of their genomic material in order for it to fit into the cell. DNA is a stiff polymer, so random coils occupy very large volumes if they are not constrained somehow. DNA also has a high negative charge, which causes self-repulsion. Despite these characteristics, genomic DNA occupies only a part of the bacterial cell, forming a body called the nucleoid. The nucleoid is distinct from the rest of the intracellular fluid (in this thesis, we will refer to the bacterial cytoplasm not occupied by the nucleoid as cytosol), and yet is not separated from the cytosol by a membrane barrier. The size of the nucleoid compared to the whole cell varies strongly between species, and even between cells of the same species under different growth conditions (Borgnia *et al*., 2008). In some small bacteria the nucleoid is difficult to detect even by phase contrast and fluorescence microscopy, and some doubt was raised the universal existence of nucleoid structures in prokaryotes, in view of difficulties to detect nucleoids in *Caulobacter crescentus* (Jensen, 2006). Nucleoids can also be identified indirectly as a differently textured area without ribosomes in electron microscopy (Borgnia *et al*., 2008; Eltsov and Dubochet, 2005), and

these studies have been important in eliminating doubts about the universality of nucleoid bodies in prokaryotes.

In this thesis, we refer to the volume reduction of DNA that is required for nucleoid formation as compaction or condensation, and use the terms interchangeably. The bacterial DNA coil must be compacted by a factor of 1×10^3-10^4 times to fit in the cell. Chromatin organization and compaction is one of the rare areas where our knowledge of bacteria is inferior to eukaryotes; the way DNA wraps around histones and forms fibres in eukaryotes is described in any textbook on biochemistry, but in bacteria there is no consensus model. Most literature agrees that supercoiling, macromolecular crowding and architectural proteins (or NAPs, sometimes also called histone-like proteins, though there is no homology) all play a role in this fascinating, but poorly understood topic: we are still far from understanding the relative contributions of each of the factors that has been suggested to contribute to nucleoid formation, let alone from a more or less quantitative description.

Part of the problem in studying bacterial chromatin is the difficulty of detecting the nucleoid optically compared to the eukaryote nucleus, due to the absence of membranes that provide contrast and the nucleoid's much smaller size, which is close to the detection limit of modern confocal microscopes. However, staining nucleoids is a trivial procedure at present. Most current *in vivo* detection methods use some sort of immunological stain, fused fluorescent proteins or a dye, for example the blue-fluorescing DNA-binding dye DAPI used in our microscopy studies. This allows us to determine nucleoid size quantitatively (Cunha *et al*., 2001). New optical microscopy techniques are just starting to map structural details within bacterial nucleoids (Wang *et al*., 2011).

Most bacterial genomes consist of a single circular chromosome. In *E. coli* the nucleoid localizes to the centre of the cell, and has an elongated shape during rapid growth. Factors that influence the shape and size of the nucleoid include transcription (causing nucleoid expansion (Dworsky and Schaechter, 1973)) and translation (which compacts the nucleoid (Woldringh, 2002)), structural maintenance proteins (which make the nucleoid diffuse (Niki *et al*., 1992)) and NAPs, whose effects will be discussed in §1.3.

Chromatin condensation becomes even more interesting if partial unfolding of DNA due to replication and translation is taken into account; even though this does not contribute strongly to the coil volume, the genome has to function while strongly compacted. The amount of nucleic acids in a nucleoid is also considerably larger than one would expect given a cell's genome size, because the DNA constantly replicates itself under most circumstances. There are multiple replication forks in the chromatin during fast growth and cells often

contain several different highly copied plasmids, though plasmids are not necessarily restricted to the nucleoid. Nucleoids also contain RNA in the process of being transcribed. Although this makes the total nucleic acid content of a bacterium hard to predict, a rough determination can be made using flow cytometry experiments. In this thesis we focus on *in-vitro* experiments to understand the role of nucleoid proteins in condensing DNA. This means that dynamic phenomena such as cell division are outside the scope of our approach, even though they must have an influence on DNA compaction.

The bacterial chromosome is organized into regions with special properties called domains. The existence of these domains was initially discovered as a heterogeneity in the sensitivity to enzymatic degradation and other physical processes between different regions in the nucleoid. Domains are thought to be insulated from each other by transient barriers (Staczek and Higgins, 1998), which influence the chromosome's physical properties and its behaviour as an information carrier. Domains are often represented as loops, because of the rosette-like structure of isolated nucleoids (Figure 1.1, Kavenoff and Bowen, 1976). Possible loop formation by NAPs has been investigated, but it was shown to lead to loops smaller than ~10 kbp in size (Dame *et al*., 2006, Garcia-Russell *et al*., 2004). Therefore, the issue whether or not large-scale domains are indeed due to NAPs has not been completely resolved yet.

The organization and compaction of DNA inside a bacterium poses major questions for both biologists, chemists and physicists. Physico-chemical models can contribute much to our understanding of how DNA behaves as a polymer rather than an information carrier, and models for DNA compaction (both experimental and theoretical) are now becoming available for circumstances more and more similar to the situation *in vivo* (de Vries, 2010).

1.2.a *Similarities between chromatin organization in archaea and bacteria*

Like bacteria, archaea have no nuclear membrane that encloses the DNA, and still their DNA forms a nucleoid, segregated from the rest of the cytoplasm. Unlike eukaryotes which all use the widely studied and relatively well-understood histones, neither archaea nor bacteria have universally conserved nucleoid-associated proteins, though they share the same need to compact their chromatin. DNA compaction in prokaryotes has received significant interest, but until recently, most attention was focused on bacteria. Those results can also be useful in the study of archaea, because genome sizes and cell volumes are similar.

Here we focus on the Crenarchaeota and the Euryarchaeota, two phyla from the archaeal kingdom. The latter phylum possesses histone homologues that form nucleosomes

(Pereira *et al*., 1997), but these histone tetramers wrap less DNA then eukaryote nucleosomes, only ~90 bp (Bailey *et al*., 1999) and are always combined with other NAPs. The best known Crenarchaeota are extremophiles, such as *Sulfolubus*. These phyla share many DNA-binding proteins, but they have no truly universal architectural proteins, like the eukaryote histones. All Crenarchaea are thought to have DNA bending and DNA bridging proteins, a trait they are thought to share with bacteria. Mechanisms for DNA condensation are thought to be shared too (Driessen *et al*., 2011). But unlike bacteria, archaea do modulate their NAPs with posttranslational modifications, such as lysine methylation (Edmondson and Shriver, 2001) or acetylation (Bell *et al*., 2002). In this thesis we will consider the role of the small basic DNA-bending protein Sso7d from *Sulfolobus Solfataricus* in condensing DNA to compare it to our main subject; the role of H-NS in condensing bacterial DNA.

1.3. *In vitro* studies of DNA condensation

1.3.a *DNA as a semiflexible polyelectrolyte*

The physical properties of DNA are important to its function as an information carrying molecule: DNA is a polymer, made up from two strands that form an antiparallel double helix (Watson and Crick, 1953). Its chemical composition and other properties are described in any textbook of biochemistry or molecular biology, so here we focus on relevant physicochemical characteristics.

First of all, the double helix can take several helical configurations. B-DNA is by far the most common form in living cells. If B-DNA with a typical base pair composition is measured under physiological circumstances, the distance between base pairs is 0.34 nm measured along the helix axis, with a rotation of ~34°. This results in a helical repeat of ~10.5 bp or 3.5 nm. We will use these standard numbers for all calculations in this thesis. More details on DNA structure, function and properties as a polymer can be found in various reference manuals and textbooks (e.g. Calladine *et al*., 2004).

Secondly, DNA is highly soluble in aqueous solutions. When the polymer is dissolved, the phosphate groups on the backbone carry a large negative charge. This makes DNA a polyelectrolyte. The behaviour of polyelectrolytes in solution depends on the solvent quality, the polymer concentration, and the concentration of low molecular weight salts (Khokhlov and Khachaturian, 1982) and other counter charges. While monovalent cations typically associate rather weakly with the phosphate charges, forming a diffuse electrical double layer,

multivalent cations associate much stronger and may lead to DNA neutralization and insolubility.

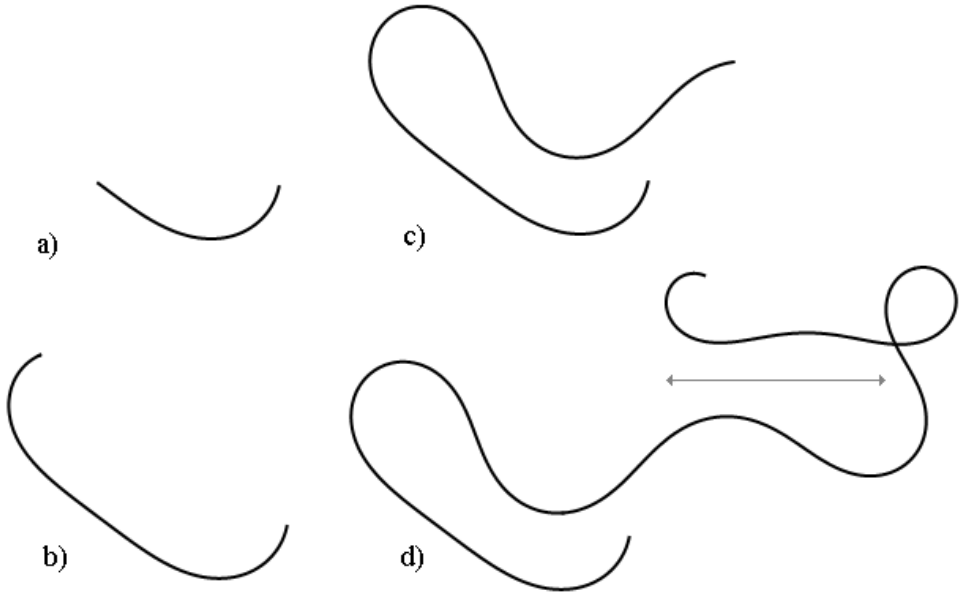

Figure 1.2: The persistence length of DNA
DNA is a stiff polymer, with a persistence length (l_p) of 46-50 nm (or 140-150 bp). This schematic picture shows random DNA coils of different lengths a) 1 l_p, b) 2 l_p, c) 4 l_p and d) 8 l_p (1.1 kbp). The grey arrow is 1 l_p long.

A third important characteristic is the bending rigidity of DNA. A single strand is highly flexible, but the double helix is not. Indeed, double stranded DNA is often used as an example of a particularly stiff polymer, and can be considered a rod-like object for lengths of a few dozen bp (Figure 1.2). Within the context of the so-called worm-like chain model (Yamakawa, 1971) the material property characterizing the stiffness of the polymer chain is the so-called persistence length. Strictly speaking, it is a correlation length characterizing the decay of orientational correlations between distant points on the chain. A consensus value for the persistence length l_p of DNA is approximately 140-150 bp or 46-50 nm. Only chains with contour length of many times the persistence length coil up due to thermal motion, whereas chains of a few persistence lengths or less are rod-like (Figure 1.2). Controversial new research has shown that circular pieces of DNA ~100 bp long (Cloutier and Widom, 2004) are formed much easier than expected on the basis of the consensus value for the l_p of DNA. Other effects may play a role here, such as partial unwinding (Travers, 2005). We continue to use a value of 50 nm for the l_p of unconstrained dsDNA throughout this thesis.

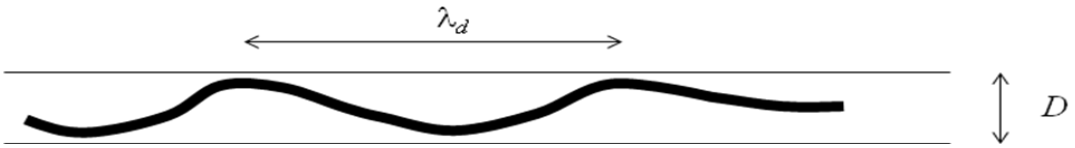

Figure 1.3 Confined DNA
dsDNA is confined in a narrow tube of diameter D. The typical distance between deflections is the so-called deflection length λ_d.

For freely coiling DNA (as in Fig 1.2), the typical size of a segment may be identified with the persistence length of DNA. This no longer the case when DNA is not freely coiling, but confined by surrounding molecules or surfaces. Consider for example the case of a DNA molecule confined in a narrow tube of diameter *D*. This can be used as a model for a highly concentrated DNA solution, in which the molecules align, and each DNA molecule is surrounded by a "tube" formed by neighbouring polymers. For tube diameters $D < l_p$ deflections of the DNA chain from the tube wall occur over smaller distances than the persistence length: the DNA chain looks rippled (Figure 1.3). The characteristic distance between deflections is called the deflection length λ_d, and depends more on the tube diameter than by the persistence length (Odijk, 1998):

$$\lambda_d = D^{2/3} l_p^{1/3} \qquad (1.1)$$

Finally, we present some estimates of DNA coil sizes using simple polymer models. Polymer coil sizes in solution are typically determined using scattering techniques (such as light- neutron- or X-ray scattering) and for a distribution of coil sizes, this gives an average value that is called the gyration radius R_g. For the worm-like chain model of DNA, the gyration radius (ignoring any interactions between DNA segments) is given by

$$R_g^2 = \frac{l_p L}{3} \qquad (1.2)$$

where *L* is the contour length. In order to illustrate typical DNA coil sizes, we consider two cases: a plasmid which is a few kbp long, and the bacterial chromosome, which measures several Mbp. In this thesis, we use the 2686 bp long plasmid pUC18. When linearized, it has a contour length of 886 nm, corresponding to about 18-19 times the l_p. This results in a gyration

radius for the linearized plasmid of $R_g \approx 120$ nm according to equation 1.2. In contrast, the 4.6 Mbp long *E. coli* genome has over 30,000 persistence-length segments and a contour length of 1.5 mm. When linearized, the expected R_g would be 4.8-5 μm, corresponding to a coil volume of 470-530 μm^3. The volume of an intact *E. coli* cell is ~1.5 μm^3 during non-exponential growth, and its nucleoid occupies only ~15% of that volume, or 0.1-0.3 μm^3 (Woldringh and Nanninga, 1985). Hence the genomic DNA must be compacted 10^3-10^4 times in volume compared to the linearized molecule to fit inside the nucleoid. This very rough estimate agrees with earlier studies; Cunha and Odijk (2001 and 2004) repeatedly use a degree of compaction of 1.6×10^3 as compared to the cell volume or 7×10^3 as compared to the nucleoid volume. Bloomfield (1997) estimates a volume reduction of at least 1400.

1.3.b *The sequence of DNA influences its physicochemical properties*

Although this thesis mostly focuses on characteristics that are not very sensitive to the DNA sequence (except for Chapter 2), one effect relating DNA physical properties to DNA sequence is important, namely sequence directed DNA curvature. The CG pair has three hydrogen bridges, which makes its association stronger than the twofold bridge between AT, and the bases bind under slightly different angles. Therefore, the properties of a DNA chain built from CG pairs only are different from one equally long consisting of only AT pairs. In particular, some AT-rich sequences have been shown to lead to a distinct curvature in the axis of the double helix (Hagerman, 1986). Both planar and space curves are possible. The total angle of curvature depends on the sequence itself and environmental factors. Natural curved sequences with length of ~100 bp have been found that lead to angles of curvature of more than 90º (Falconi *et al*., 1998). In bacteria, DNA sequences with high intrinsic curvature appear in regulatory sequences upstream of promoters (Bossi and Smith, 1984) Many bacterial nucleoid proteins, including H-NS, show preferential binding to intrinsically curved DNA sequences such as those in bacterial regulatory sequences. This feature of bacterial nucleoid proteins is thought to be intimately related to their role as global regulators of bacterial gene expression. Prominent examples are the so-called virulence genes of enterobacteria, which are regulated by H-NS. For the particular case of the *virF* promoter, it has been shown that temperature-dependent switching of the virulence genes is controlled by H-NS, which strongly binds to the *virF* promoter at low temperature, when it has a high intrinsic curvature, but does not bind at higher temperatures when the intrinsic curvature of the *virF* promoter is lost (Falconi *et al*., 1998).

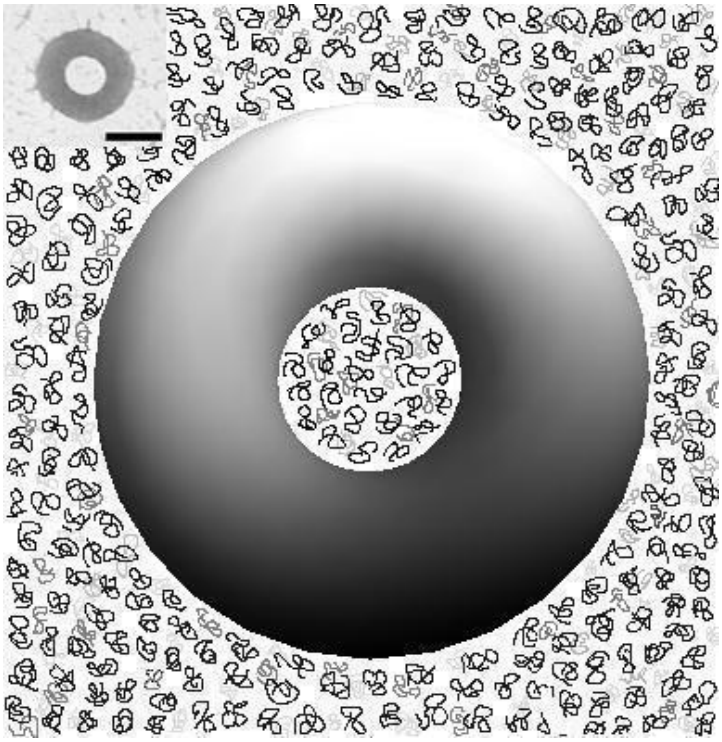

Figure 1.4: Model of DNA under macromolecular crowding conditions
DNA can be condensed into toroids comprising large numbers of individual molecules through depletion by a macromolecular crowding agent. In this picture, the crowding agents are scaled to resemble PEG 20K vs. a toroid of condensed DNA with an outer diameter of 200 nm. Inset: EM picture of collapsed DNA (scale bar 100 nm, courtesy of Sarkar *et al*., 2009).

1.3.c *Macromolecular crowding-induced DNA condensation*

From a physical point of view, DNA is compacted by making the (effective) interaction between DNA segments attractive. One way of achieving this is via excluded volume interactions of the DNA segments with other, non-binding macromolecules that are depleted from the vicinity of the DNA. These non-binding macromolecules induce an effective attraction between the DNA segments that is called the depletion attraction (Asakura and Oosawa, 1958), and this drives compaction of DNA.

The concentrations of macromolecules are generally very high in bacterial cells. They cause strong excluded-volume interactions, and this has various consequences. Together, they are often referred to as effects of macromolecular crowding. Here, we consider DNA condensation induced by macromolecular crowding. Other effects of macromolecular

crowding include changes in reaction rates and protein self-assembly equilibria (Zimmerman and Minton, 1993) compared to dilute solutions.

DNA condensation induced by macromolecular crowding has a simplified model in the so-called Polymer and Salt Induced, or ψ-condensation of DNA. This abrupt transition in DNA configuration can be induced by adding sufficiently large amounts of non-binding polymers and monovalent salt (Lerman, 1971). Polymer-induced ψ-condensation depends on the amount of polymer, its degree of polymerisation (Bessa Ramos *et al*., 2005), and the concentration of monovalent salt (de Vries, 2001). DNA ψ-condensation of single, long DNA molecules has been visualized using fluorescence microscopy (Vasilevskaya *et al*., 1995, Yoshikawa *et al*., 1996). Electron microscopy has shown that individual long DNA molecules often condense into toroids, as illustrated in Fig. 1.4. Consistent with the fact high concentrations of non-binding polymers condense DNA, gently isolated bacterial nucleoids whose volume expanded multiple times during isolation, may be recompacted by the addition of non-binding polymers (Cunha *et al*., 2001).

Not much is known about crowding-induced DNA condensation under circumstances that resemble the *in vivo* situation more closely. Non-binding globular proteins have been shown to be much less effective in condensing DNA than equivalent concentrations of flexible polymers (Castelnovo and Gelbart, 2004; de Vries, 2006; Murphy and Zimmerman, 1995). Only for very low ionic strengths, when the osmotic pressure of the proteins is high enough to drive compaction (de Vries, 2006), mild compaction of dilute linear DNA by globular proteins has been observed experimentally (Krotova *et al*., 2010). The genomic DNA in bacteria is neither linear nor dilute. A more realistic model by Odijk (1998) takes into account both DNA supercoiling, the finite volume of the bacterial cell, and the large amounts of genomic DNA present within this volume. Still neglecting DNA-binding proteins, Odijk (1998) finds that typical concentrations of non-binding globular proteins in bacterial cells should be enough to drive compaction of the genomic DNA into a nucleoid structure.

1.3.d *Charge neutralization causes DNA condensation*

Another way of introducing attractive interactions between DNA segments that ultimately lead to DNA condensation is shielding the large negative charge of DNA. This can be achieved through addition of multivalent cations or polycations (Bloomfield, 1997). Common multivalent cations and polycations that have been shown to condense DNA include polylysine, spermine and spermidine, but also inorganic multivalent cations such as Mg^{2+}.

These compounds collapse DNA into toroidal and rod-like condensates (Chattoray *et al*., 1978, Arscott *et al*., 1990). Attractions between DNA two segments induced by multivalent cations or polycations typically require that the multivalent cations interact with two DNA duplexes at the same time. Many (but not all) prokaryotic nucleoid-associated proteins are highly basic and will neutralize the charge of DNA. However, they typically have only one DNA-binding surface, and may not induce a direct attraction between DNA segments that would drive DNA condensation. In the case of basic nucleoid proteins, the relation between DNA condensation and DNA charge neutralization is not so straightforward.

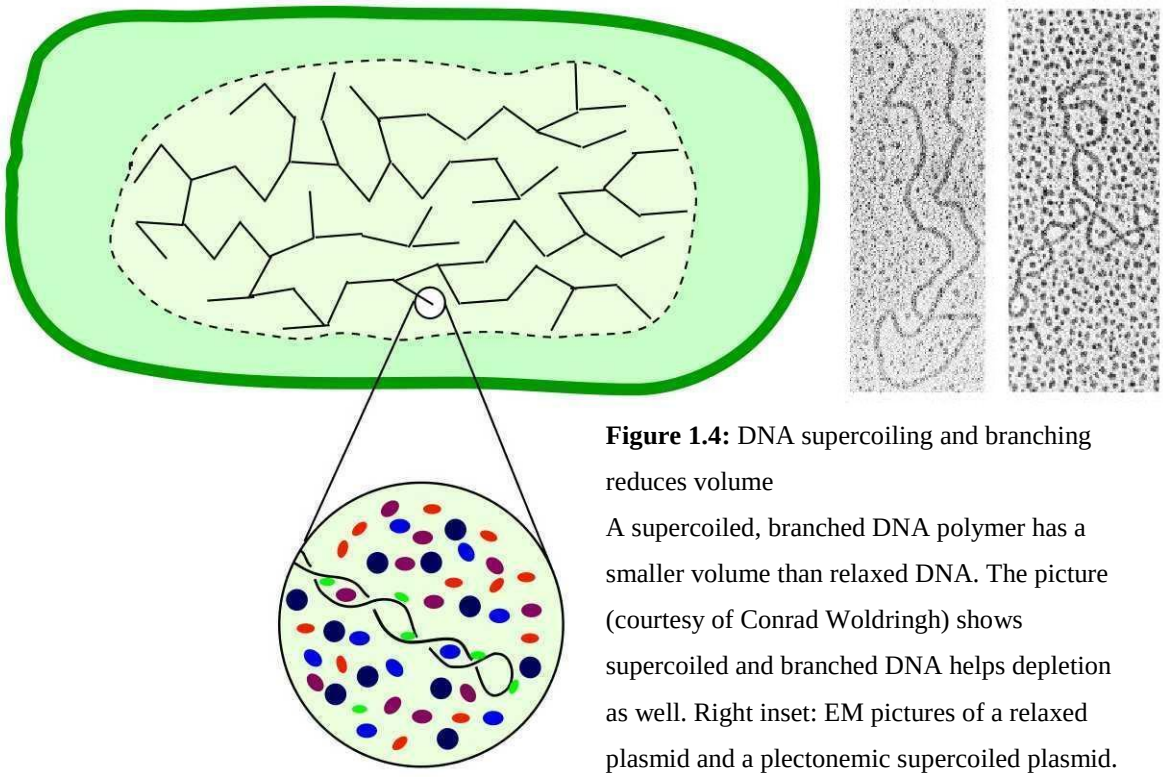

Figure 1.4: DNA supercoiling and branching reduces volume
A supercoiled, branched DNA polymer has a smaller volume than relaxed DNA. The picture (courtesy of Conrad Woldringh) shows supercoiled and branched DNA helps depletion as well. Right inset: EM pictures of a relaxed plasmid and a plectonemic supercoiled plasmid.

1.3.e *Supercoiling also promotes DNA condensation*

DNA supercoiling also contributes to condensation. The circular bacterial chromosome is actively twisted by ATP-consuming enzymes. Twisting leads to global contortions of circular DNA, called writhe. If DNA is writhed, it winds back upon itself and forms a branched plectonemic supercoil, as illustrated in Fig 1.5 (reviewed in Calladine *et al*., 2004). Supercoiling alone is not enough to explain the volume reduction of the genomic DNA by a factor 10^3-10^4. Detailed computations (Cunha, 2001) show that at most, supercoiling

reduces coil volume by one order of magnitude compared to the volume of a linear DNA coil with the same length.

1.4 H-NS and other nucleoid-associated proteins

An important class of proteins associated with the bacterial nucleoid are the so-called nucleoid-associated proteins (NAPs), or nucleoid proteins. These are DNA-binding proteins with high copy numbers. They generally bind DNA independent of sequence, with an affinity lower than most sequence specific regulatory proteins. Although they can bind any DNA sequence, nucleoid proteins often have preferred sequences or DNA configurations to which they bind with increased affinity. Bacterial NAPs are sometimes also called histone-like proteins, though they are not at all homologous to eukaryotic histones. Their function in bacteria is very similar to that of histones in eukaryotes: they modulate the architecture of bacterial chromatin and (thereby) regulate gene expression at a global level. While wrapping by histones is the dominant architectural motif in eukaryotes, various types of NAPs induce various types of structural deformations in DNA such as bending, bridging, or wrapping in bacteria (Luijsterburg *et al*, 2008).

Here we will introduce the nucleoid protein H-NS, and briefly compare it with other major bacterial NAPs: HU, IHF, FIS, Dps and LRP. Finally, some archaeal NAPs are introduced that are relevant for the present thesis, in particular the small basic nucleoid protein Sso7d from the hyperthermophilic archaeon *Sulfolobus Solfataricus.*

1.4.a *H-NS and its oligomerization*

H-NS stands for histone-like (or heat-stable) nucleoid structuring protein. H-NS has a many homologues such as StpA, Ler, SPB, and XrvA. The gene was first mapped by Pon *et al*. (1988). H-NS was shown to be localized in the nucleoid by electron microscopy and immunostaining (Dürrenberger *et al*., 1991). Super-resolution fluorescence microscopy of fusions of H-NS with fluorescent proteins also shows H-NS localizes in the nucleoid, with especially high concentrations in to two compact clusters on the chromosome that account for 60±25% of the total fluorescence (Wang *et al*., 2011), though this cluster formation has not been confirmed independently. Like many other NAPs, H-NS has an increased affinity for DNA sequences known to exhibit intrinsic curvature (Yamada *et al*., 1990). Overproduction

of H-NS is lethal to *E. coli*, and causes nucleoids to condense (Spurio *et al*., 1992). Deletion of H-NS does not impair the cell severely, though deletion mutants have low ploidy and short replication times (Atlung and Hansen, 2002). The small changes in deletion mutants may be due to the presence of many other types of nucleoid proteins, including a range of H-NS homologues that may be (partially) redundant with H-NS (Free *et al*., 2001). H-NS is present at high levels during exponential (~ 20,000 copies/cell) and early stationary (~ 15,000 copies/cell) phase, but decreases in late stationary phase to <10,000 copies/cell (Azam *et al*., 1999a). The *hns* gene is subject to autorepression (Falconi *et al*., 1993).

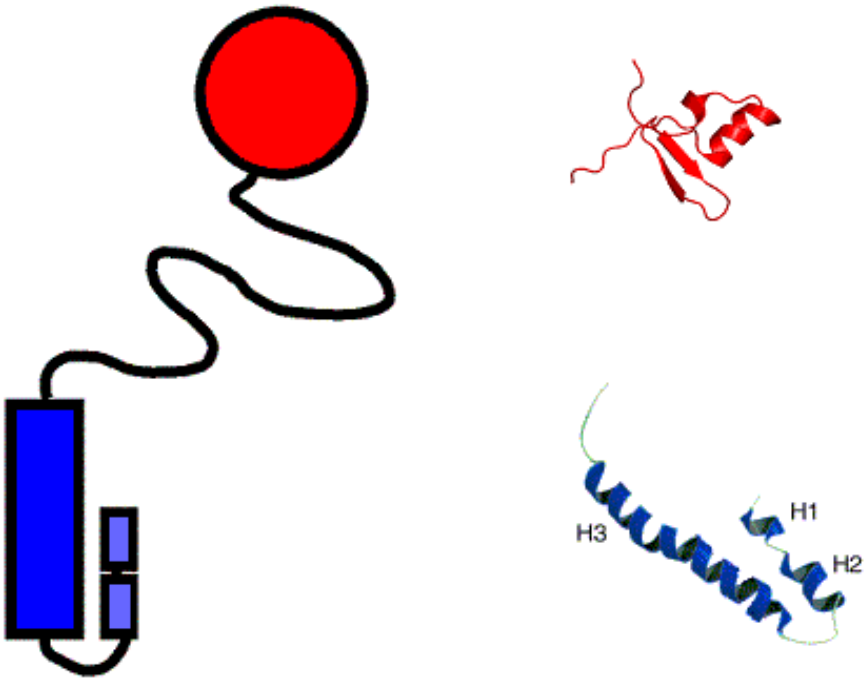

Figure 1.6: The structure of H-NS: the C- and N-domain
A simplified model of H-NS (left) and NMR structures of the domains without the linker (right). The NMR structure of the *E. coli* N-domain (a.a.1-46, blue) is derived from Bloch *et al*. (2002), the NMR structure of the *Salmonella* C-domain (a.a. 91-137, red) is from Gordon *et al*. (2011). The black linker is unstructured, but may still play a role in protein function.

In solution, at low concentrations, H-NS exists predominantly as a very stable dimer (Falconi *et al*., 1988). This dimeric structure is thought to be necessary for recognition of and preferential binding to, curved DNA (Spurio *et al*., 1997). The dimer has two DNA binding domains, so it could bind either to two different DNA duplexes (bridging mode), or bind to two neighbouring sites on the same DNA duplex (non-bridging mode). In the bridging mode, H-NS could form a loop between by binding to two more distant sites on the same DNA

duplex. In fact, this is assumed to be the mechanism by which H-NS preferentially binds in the vicinity of intrinsically curved sequences: these adopt looped configurations more easily (Dame *et al*., 2001: de Vries, 2011). At higher concentrations H-NS dimers self-assemble into large oligomers in solution (Ceschini *et al*., 2000, Stella *et al*., 2005, Smyth *et al*., 2000). Mellies *et al*. (2011) even reports oligomers of between ~800 and ~3000 kDa, corresponding to ~25-100 dimers, depending on protein concentration and buffer composition.

Various groups have investigated the affinity of H-NS for DNA: Friedrich *et al*. (1988) found low association constants for nonspecific DNA of $K_A \approx 10^4\ M^{-1}\ bp^{-1}$, using polyA/T and polyG/C DNA monitored by Trp fluorescence, and a maximum binding of 1 dimer per 12 bp by nitrocellulose filtration. This is quite close to one per helical turn, which is ideal for bridging, though it would be possible for more C-domains to fit on DNA. Dame *et al*. (2006) also measured a maximum DNA occupancy of ~1 dimer per helical turn and found k_{off} to be $1.5 \pm 0.2\ s^{-1}$ pulling two H-NS-bridged strands of DNA apart with optical tweezers. Using an estimated k_{on} of $1.0\times10^5\ M^{-1}\ s^{-1}$ (Eckel *et al*., 2005) they arrive at a K_D of 1.5×10^{-5} M. The rather low affinity of H-NS binding to DNA is generally agreed upon, even though the numbers differ somewhat depending on experimental conditions. But, H-NS binds stronger than most non-specific *E. coli* NAPs (Azam *et al*., 1999b). As mentioned, H-NS preferentially binds to DNA sequences that exhibit intrinsic curvature. More specifically, H-NS preferentially binds to sequences that have a narrow minor groove (Rimsky *et al*., 2001), and/or are enriched in A/T (Navarre *et al*., 2006). It also has an increased affinity for a rather well defined consensus sequence (Lang *et al*., 2007, Sette *et al*., 2009). Like many nucleoid proteins, H-NS constrains DNA supercoils (Tupper *et al*., 1994); if circular DNA coated with H-NS is incubated with enzymes that nick and close DNA, and subsequently is stripped of the H-NS, the resulting DNA remains supercoiled. H-NS is much less effective in constraining supercoils than another prominent bacterial nucleoid protein, HU (Higgins *et al*., 2010).

At high temperatures, both footprinting and gel shift shows that DNA binding is weaker and less cooperative (Bouffartigues *et al*., 2007, Ono *et al*., 2005). Many temperature-dependent bacterial genes are regulated by H-NS (Maurelli *et al*., 1988): various genes that are repressed by H-NS at 30°C are not repressed at 37°C. A well-studied example is the *virF* gene, involved in bacterial virulence (Prosseda *et al*., 1998). For this case, temperature switching has been shown to be a consequence of the temperature-dependent intrinsic curvature of the *virF* promoter, and not due to an intrinsic temperature dependence of the DNA-binding properties of H-NS (Falconi *et al*., 1998).

The H-NS protein consists of a DNA-binding C-domain and a dimerizing N-domain, connected by a flexible, apparently unstructured linker (Figure 1.6). In truncated mutants, the N-domain also trimerizes, and forms oligomers if the linker is also present. Deletion of the C-domain does not abolish oligomerization (Smyth *et al*., 2000) but certain mutations in the C-domain can influence oligomerization (Spurio *et al*., 1997). Mutants lacking part of the C-domain also show enhanced oligomerization (Ueguchi *et al*., 1996). Deletion of the linker completely abolishes oligomerization (Stella *et al*., 2005), yet a 1-77 truncated mutant does show oligomerization (Leonard *et al*., 2009). Similar *wt* oligomerization behaviour was also found in the presence of DNA (Badout *et al*., 2002).

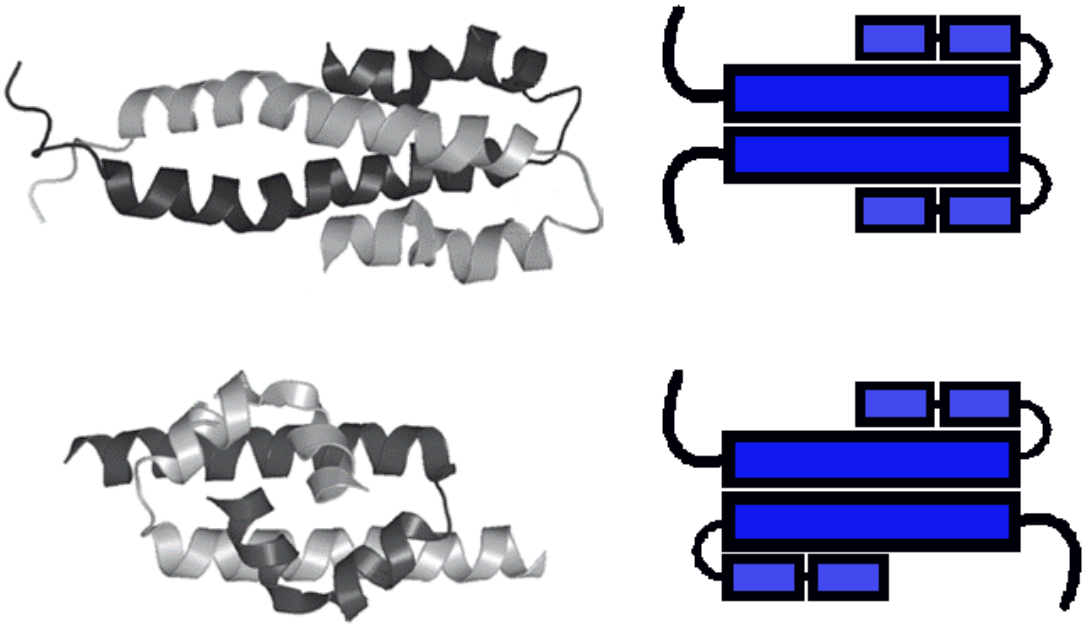

Figure 1.7: The H-NS oligomerization model: parallel and antiparallel modes
Crystal structures of the N-domain in parallel and antiparallel mode. The antiparallel mode above is associated with dimerization at high temperature (Bloch *et al*., 2003). The parallel dimerization shown below is associated with dimerization and higher order oligomerization at temperatures below 30°C (Esposito *et al*., 2003). To the right are simplified models of parallel and antiparallel N-domains.

While crystallization of the whole protein has proven difficult due to the (supposedly) unstructured linker, there are NMR structures of the C-domain (Shindo *et al*., 1995), showing the DNA binding surface (Shindo *et al*., 1999), and the N-domain (Renzoni *et al*., 2001). The N-domain can dimerize in two ways (see Fig. 1.7): either parallel (Esposito *et al*., 2002) or anti-parallel (Bloch *et al*., 2003). A recent structure of the N-domain that includes the linker

shows an antiparallel dimer structure with an extended alpha-helical structure (Arold *et al*., 2010), though older studies argue that the linker is unstructured. It has been hypothesized that H-NS switches between parallel and anti-parallel dimer orientations in a temperature-dependent manner (Ono *et al*., 2005), but so far, this has not been shown in the presence of DNA, and it remains unclear what determines the relative orientation of the N-domains in the H-NS dimer. As shown in AFM pictures (Dame *et al*., 2001) H-NS may connect neighbouring DNA strands by self-assembling stretches of H-NS bridges, forming a zipper-like structure (Figure 1.8 and 9).

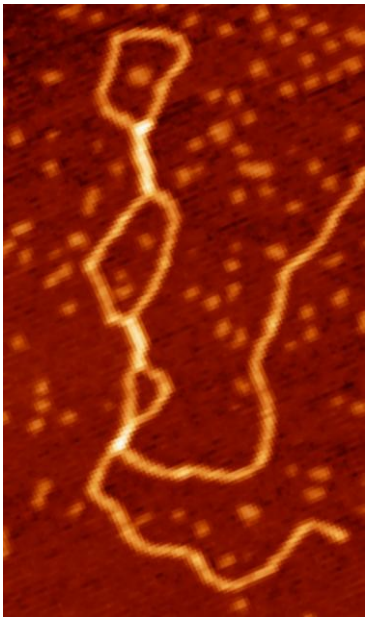

Figure 1.8: H-NS on DNA
H-NS bridges on λ DNA are visualized by AFM. The bridges consist of many H-NS dimers, which may be oligomers. The DNA used has a contour length of 16.1 μm. Copied with permission from Dame *et al*. (2005a).

1.4.b *StpA is a homologue of H-NS*

StpA (suppression of *td*$^-$ phenotype A) is a 133 a.a. DNA-binding protein that is thought to be able compensate for H-NS function in *Δhns* strains (Zhang and Belfort, 1992). StpA is highly homologous to H-NS (58% in *E. coli*, Dorman *et al*., 1999). It constrains supercoils and represses transcription (Zhang *et al*., 1996), especially inhibiting its own and its paralogue's promoter. The homologues have similar domain structure (Cusick and Belfort, 1998) and domain functions (Williams *et al*., 1996). StpA bridges DNA similar to H-NS in AFM studies (Dame *et al*., 2005a). However, the expression patterns of the homologues and some other functions are different. H-NS is always present in large numbers, but StpA is transcribed in short bursts. At its maximal presence, StpA has ~20,000 copies/cell (Azam *et al*., 1999a), though other studies find this homologue always has less copies then H-NS, even

in H-NS knockouts where *stpa* is derepressed (Sonnenfield *et al*., 2001). StpA can suppress various H-NS-dependent genes in H-NS knockouts, but has no effect on those genes in a *wt* background (Free *et al*., 1998). The physiological function of StpA remains unclear, apart from its redundancy with H-NS.

Like H-NS, StpA forms dimers and higher order multimers. StpA dimers are more stable than H-NS dimers and the two proteins form heterodimers that are even more heat-stable (Leonard *et al*., 2009).

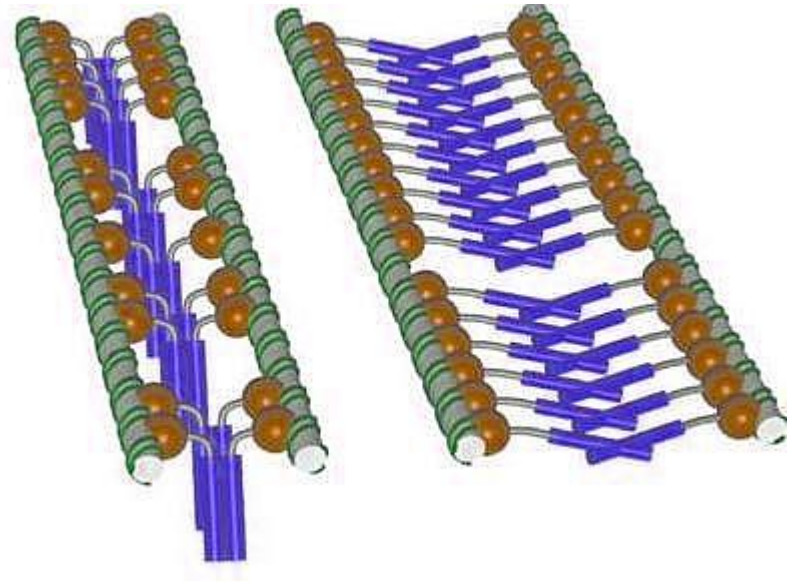

Figure 1.9: H-NS oligomerization/bridging on DNA
This is a hypothetical model for the two modes of H-NS binding to DNA; left the N-domains are parallel, which is thought to be the low temperature dimerization regime, binding the DNA more strongly; right antiparallel N-domains, binding the DNA with less strength at higher temperature, possibly due to loss of cooperative DNA binding. Picture credited to Dame *et al*., 2006.

1.4.c *Other relevant NAPs*

FIS

Factor for Inversion Stimulation (FIS) is a 22 kDa homodimer that bends DNA 50 to 90 º by fitting its DNA-binding helices into two adjacent major grooves (Pan *et al*., 1996). It binds DNA on a degenerate palindromic sequence rich in A/T (Pan *et al*., 1994), but also binds sequence independently, at high concentration. FIS is highly abundant during exponential growth (~60,000 copies/cell), with a much lower concentration in other growth phases (Ball *et al*., 1992; Azam *et al*., 1999a). Its most important physiological function is

thought to be the activation of stable RNA transcription, but FIS is also implicated in spatiotemporal regulation of supercoiling and global gene regulation. FIS binds the *hns* promoter and indirectly counteracts H-NS autorepresssion (Falconi *et al*., 1996). FIS regulation is often antagonistic to H-NS, for example in the regulation of *virF* (Falconi *et al*., 2001). In addition to its indirect architectural functions by the alteration of global superhelical density, FIS contributes to the stabilization of loops and the distribution of topological domain barriers (Hardy and Cozzarelli, 2005, Schneider *et al*., 1997), and increases supercoil branching (Schneider *et al*., 2001). FIS is present at ~60,000 copies/cell during exponential phase in *E. coli*, but not in the other phases (Azam *et al*., 1999a).

HU

HU (histone-like DNA-binding protein or heat unstable protein) is a 20 kDa basic homodimer in most bacteria, though the protein can also form heterodimers with several closely related proteins. In *E coli*, it is always present as a heterodimer. The HU protein bends DNA (over an angle of up to ~140º, Koh *et al*., 2008) and strongly constrains DNA supercoils (Higgins *et al*., 2010): the two kinks induced by HU in the DNA result in 3º underwinding/bp (Swinger *et al*., 2003). HU is homologous to IHF, and also binds the minor groove, but it does so in a sequence-independent way. It is present at >50,000 copies/cell in exponential phase *E. coli* (Azam *et al*., 1999a).

IHF

Integration Host Factor is involved in recombination, replication and translation regulation (Dos Santos and Rodrigues, 2005). This highly abundant heterodimer consists of homologous α and β subunits that are ~10 kDa each (Weisberg *et al*., 1996). IHF is less widespread among bacterial genera than HU. IHF bends DNA the strongest, inducing a very sharp bend of 160-180° in the DNA over approximately 30 bp (Rice *et al*., 1996). It binds in the minor groove, inducing two kinks in the DNA to nearly make a U-turn. This minor groove binder has a highly unusual sequence-specificity. IHF peak concentrations are ~50,000 copies/cell during early stationary phase *E. coli* (Azam *et al*., 1999a).

Dps

Dps (DNA protection during starvation) is mainly known as one of the protein classes that detoxify ROS (reactive oxygen species) and thus protect DNA. It does not appear to be involved in global regulation of bacterial gene expression. The 19 kDa protein forms

dodecamers that results in very stable DNA-bound complexes, consisting of highly ordered crystal-like lattices (Wolf *et al*.,1999), both *in vivo* during starvation and *in vitro*. Its mode of DNA binding cannot be classified clearly, though DNA-binding is known to be mediated by a lysine-rich tail (Ceci et al., 2004). Dps is highly abundant during late stationary phase *E. coli*, in which it reaches concentrations ~ 180,000 copies/cell (Azam *et al*., 1999a). This nucleoid protein has unambiguously shown it can dramatically compact DNA, a property that is of course intimately connected to its function, as suggest by its name, Dps.

LRP

Leucine responsive regulatory protein (LRP) is a transcriptional regulator, in particular of amino acid metabolism. It binds DNA cooperatively and sequence specifically, though the recognition sequence is degenerate. LRP affects the transcription efficiency of the genes it regulates by direct interaction with RNA polymerase. LRP forms homomultimers (dimers, octomers and hexadecamers). Together with its homologues, it has been reported to cause DNA bending, looping, as well as bridging (Tapias *et al*., 2000). Some multimeric LRP homologues apparently even wrap DNA analogous to eukaryotic histones (Beloin *et al*., 2003). LRP affects ~10% of all genes, making it an important regulatory protein. LRP co-regulates various genes together with H-NS. Compared to other NAPs, copy numbers of LRP in *E. coli* are rather low (Azam *et al*., 1999a).

1.4.d *Archaeal NAPs*

While this thesis mainly focuses on the role of the nucleoid protein H-NS in compacting bacterial DNA, it also features research (Chapter 5) on the role of the small archaeal protein Sso7d from the hyperthermophilic *Sulfolobus Solfataricus*, in compacting plasmid DNA *in-vitro*. Whereas most studies on prokaryotic nucleoid-associated proteins have used bacteria, there is also a reasonable number of studies on archaeal nucleoid proteins. We here introduce two archaeal nucleoid proteins that have been particularly well studied: Alba, and Sso7d.

Alba

Alba is a widespread archaeal NAP, occurring in Euryarchaeota and Crenarchaeota, and is also known as Sac10b and Sso10b. Like bacterial NAPs, it is small, basic and highly abundant, present at ~1 dimer per 5 bp, or up to 4% of cellular protein content. Alba binds

DNA strongly and non-specific, with complete decoration at high concentration. At low and intermediate concentration, Alba functions as a DNA bridging protein, which results in DNA compaction (Lurz *et al*., 1986), especially in the case of heterodimers (Jelinska *et al*., 2005).

Sso7d

This archaeal protein is also very abundant (~5% of cell protein), and is even smaller than Alba. Highly conserved among *Sulfolubus*, it is also known as Sul7d and Sac7d, and may be part of a crenarchaeal family of sequence divergent proteins that are still structurally related, which are called Cren7 (Guo *et al*., 2008). It binds DNA non-cooperatively and non-specific with a K_d of 1-5 μM, covering ~4 bp (McAfee *et al*., 1996), inducing a sharp kink (Gao *et al*., 1998) of up to 66°. It also introduces negative supercoiling, and increases DNA thermal stability (Krueger *et al*., 1999).

1.5. Nucleoid proteins and single molecule techniques

In this thesis we mainly use bulk physico-chemical techniques such as light scattering to characterize H-NS oligomerization, and the influence of nucleoid-associated proteins on the large-scale solution structure of (plasmid) DNA. Whereas classic bulk techniques allow for the measurement of physical properties averaged over large numbers of molecules, some current techniques allow us to measure physical properties of single molecules, and to determine distributions for physical properties of ensembles of molecules. Both approaches have advantages and disadvantages that will not be discussed any further here, but single molecule techniques have been very important in studying the interactions between nucleoid-associated proteins and DNA. Here we briefly review some of these techniques and the particular results obtained for nucleoid proteins (especially H-NS) interacting with DNA.

For imaging complexes of single DNA molecules with various nucleoid proteins, Atomic Force Microscopy (AFM) seems to be the preferred method in the more recent literature, presumably because of the ease and accessibility of the method, as compared with Electron Microscopy. AFM has been used for decades on complexes that are adsorbed on a flat solid substrate and dried before imaging (Amrein *et al*., 1988), which allows for very high resolution, but it can also be used on dissolved macromolecules, under conditions more similar to *in vivo* circumstances. AFM pictures of dried H-NS DNA complexes adsorbed on a surface show stretches of H-NS forming bridges two neighbouring DNA duplexes (Figure

1.8, Dame *et al*., 2000). AFM has also been used to measure bending angles induced in DNA due to the binding of nucleoid proteins (Dame *et al*., 2005b).

Force-spectroscopy studies on DNA attached to beads and surfaces are another popular method for single-molecule measurements, where the beads are manipulated with optical or magnetic tweezers. Force extension curves of DNA with and without H-NS were first measured by Amit *et al*. (2003), who concluded that under the conditions of their experiment, H-NS stiffens DNA, but does not form bridges. Using four optical traps to capture two strands of dsDNA, Dame *et al.* (2006) created an assay especially suitable for investigating protein-induced DNA bridging at the single-molecule level. The technique was applied to H-NS, using a different solution than the experiments of Amit *et al*. (2003). In particular, the buffer contained 10 mM Mg^{2+}. Under these conditions, the single molecule assay unequivocally showed bridging, by measuring the forces needed to pull apart two duplexes that had been "zipped" together by H-NS bridges. Later magnetic tweezers studies (Liu *et al*., 2011) suggest that the mode of H-NS binding (bridging or non-bridging mode) sensitively depends on solution conditions, in particular on the concentration of Mg^{2+}.

1.6 Light scattering of DNA and proteins

In this paragraph, we introduce the physicochemical technique of light scattering (LS) that is used in this thesis for characterising H-NS oligomerization, and for characterising the influence of nucleoid proteins on the large-scale solution structure of DNA.

1.5.a *Basic theory of Light Scattering*

For sufficiently dilute solutions of sufficiently small particles or molecules, the absolute intensity of light scattering (the so-called Rayleigh ratio R_θ, which has the dimension of m^{-1}) is given by the Rayleigh equation

$$R_\theta = K_R C M \,, \qquad (1.3)$$

where C is the weight concentration of particles or molecules, M is their molar mass, and K_R is an optical constant called the Rayleigh constant:

$$K_R = \frac{4\pi^2 n_m^2}{\lambda_0{}^4 N_{Av}} \left(\frac{dn}{dc}\right), \qquad (1.4)$$

Where λ_0 is the wavelength of the incident light, n_m is the refractive index of the solvent, N_{Av} is Avogadro's number, and (dn/dC) is the so-called refractive index increment, which is the slope of the refractive index versus concentration curve (n versus C), that determines the contrast of the particles or molecules in light scattering. In practice, count rates I for the sample (subscript s), the solvent (subscript 0) and a reference (usually toluene, subscript t) as determined using the light scattering instrument are converted to the absolute scattering, or Rayleigh ratio, using

$$R_\theta = \frac{I_s - I_0}{I_t} \frac{n_m^2}{n_t^2} R_t . \qquad (1.5)$$

where n_t is the refractive index and R_t is the absolute scattering of the toluene standard (a tabulated quantity). In this thesis, we assume that our (known) sample concentrations C are low enough, and particle sizes are small enough for the Rayleigh equation to hold, so that we can use the scattering intensity as a measure for the solution molar mass M of the particles.

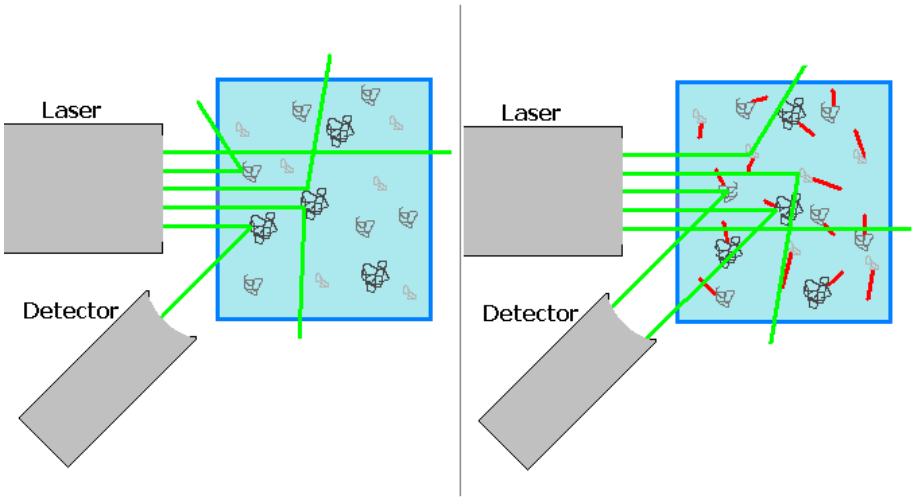

Figure 1.9: DLS graphics

A highly schematic impression of Dynamic light scattering; light falls on particles, and part of it is scattered (I_s). The amount of scattered light changes as particles move in and out of the measurement volume.

But what are the conditions for the Rayleigh equation to hold? The precise formulation of the condition that the molecules or particles are small enough is given in terms of the so-called wavevector (or scattering vector):

$$q = \frac{4\pi n_m}{\lambda_0} \sin\left(\frac{\theta}{2}\right) \qquad (1.6)$$

in which θ is the scattering angle between detector and the transmitted light beam. For the Rayleigh equation to hold, qR_g must be << 1, where R_g is the gyration radius of the particles or molecules. Corrections to the Rayleigh equation at higher concentrations can be formulated in terms of the second virial coefficient B_2, a measure for the interactions between the particles. For small enough particles (qR_g << 1), but at somewhat higher concentrations:

$$R_\theta = \frac{K_R CM}{1 + 2B_2 C / M + ..} \qquad (1.7)$$

Hence, small enough concentrations for the Rayleigh equation to hold, means that we should have B_2C/M << 1.

The way the light scattering intensity fluctuates in time also contains information about the particles. For a small scattering volume, there will be significant fluctuations in the scattered intensity as a consequence of the Brownian or thermal motion of the particles or molecules. The frequency of the fluctuations is related to the speed of motion, or diffusion, of the particles or molecules. The fluctuating scattered intensity $I(t)$ is typically analysed in terms of an autocorrelation function, called the intensity autocorrelation function $g_2(t)$

$$g_2(t) = \frac{\langle I(t) \times I(t+\tau) \rangle}{\langle I(\tau) \rangle^2} \qquad (1.8)$$

The brackets denote an average over the time τ of the experiment. Diffusivity is related to the autocorrelation function $g_1(t)$ of the electric field rather than to the autocorrelation function $g_2(t)$ of the light scattering intensity. The two functions are related by the so-called Siegert relation:

$$g_2(\tau) = 1 + A[g_1(\tau)]^2, \qquad (1.9)$$

where A=0...1 is a constant that depends on the optical set-up. If the dynamic light scattering experiments is performed at a wave vector q, diffusion is probed at length scales q^{-1}. For monodisperse, small particles/molecules (qR_g << 1) the field autocorrelation function decays exponentially with a rate Γ:

$$\begin{aligned} g_1(q,\tau) &= e^{-\Gamma\tau} \\ \Gamma &= q^2 D_t \end{aligned}, \qquad (1.10)$$

where D_t is the translational diffusion constant of the particles or molecules. For spherical particles, hydrodynamic radius may be inferred from the translational diffusion constant, via the Stokes-Einstein relation:

$$D_t = \frac{kT}{6\pi\eta R_H} \qquad (1.11)$$

in which η is the solvent viscosity.

In the absence of detailed information on the actual shape and size of the particles, it is common practice to convert the translational diffusion constant obtained from DLS into an effective hydrodynamic radius $R_{H,eff}$ using the Stokes-Einstein equation. When using this hydrodynamic radius, the assumption that the particle is spherical should be kept in mind. For pure translational diffusion the decay rate Γ should scale as $\Gamma \sim q^2$. Deviations from this behaviour may indicate that other dynamic modes contribute to the dynamic scattering. For example, when considering dynamic scattering at higher values of the wavevector from large polymers such as DNA, rotation and bending modes may contribute to the dynamic scattering. An excellent, more detailed, discussion of DLS can be found in Berne and Pecora (1976).

1.5.b *Light scattering as a method to study proteins and their oligomers*

Modern small-volume DLS equipment is very suitable for routine measurements of the *average* diffusion constants of proteins in solution. A practical point of concern is always that the solution should be free of large aggregates, since the scattering of just a few large aggregates easily overwhelms the scattering of many small proteins. Apart from this, the measurements are very fast and completely non-invasive. This means that it is a very straightforward method to study e.g. how the oligomerization of some protein depends on solution conditions. For polydisperse samples, that includes monomers and various oligomers, in principle it is possible to invert the field autocorrelation function $g_1(t)$ to arrive at the (scattering weighted) distribution of particle sizes, but in practice this is quite complicated and not always reliable (see the review of Gun'ko *et al*., 2003). Therefore, we only use DLS to obtain average hydrodynamic sizes (or translational diffusion constants) of protein oligomers in this thesis.

1.5.c *Light scattering as a method to study DNA*

DLS has been a popular method for studying DNA in solution for a long time, especially because it can measure the large-scale structure and dynamics of DNA in solution non-invasively. While early studies used calf thymus DNA (Schmitz and Schurr, 1973), later

studies often used better defined plasmid DNA. In our studies we also use plasmid DNA, in particular the commonly available pUC18 plasmid, which is 2686 bp long. Whereas at low scattering angles, the dynamical scattering of DNA is determined by the translational motion, at higher scattering angles, or higher values of the wavevector *q*, internal modes such as rotation and bending begin to contribute (Langowski *et al*., 1992). Both the diffusion constant and the internal dynamics of DNA are affected by DNA supercoiling, and this dependence was also investigated using DLS (Langowski *et al*., 1992; Langowski *et al*., 1994). Electrostatic repulsion between DNA double helices has a strong effect on the solution structure of plasmid DNA, and this has also been investigated by considering the salt-dependence of light scattering from plasmid DNA (Langowski *et al*., 1999; Hammermann *et al*., 1997).

1.5.d *Light scattering can be used to study protein-DNA complexes*

Light scattering is not a common method to study protein-DNA complexes. The large volumes required for scattering angle-dependent studies (about 1ml) when using goniometer-based research light scattering equipment may be the cause of this. But modern commercial light scattering equipment often allows for scattering on tiny sample volumes, albeit only for one, or a few scattering angles. In this thesis we mostly use the Malvern Nanosizer SZ, when measuring nucleoid-associated proteins. It has two scattering angles: 173° and 12.8°. The high angle is suitable to study the translational diffusion of proteins and protein oligomers, whereas the low angle is required for studying the translational diffusion of plasmid DNA and complexes of DNA and nucleoid proteins. As we will show, the light scattering experiments straightforwardly give information of both the total molar mass of protein-DNA complexes, and on their solution (hydrodynamic) size.

Previous light scattering studies of protein-DNA complexes include studies on the binding of the *E coli* single strand binding protein to (supercoiled) DNA (Langowski *et al*., 1985). Ramreddy *et al*. (2003) used DLS to measure the increase in flexibility of RecA-nucleoprotein-DNA complexes upon adding ATP. DLS has also been used for the study of RNA-binding proteins from HIV in complex with RNA. It was demonstrated that NCp7 causes the ordered growth of monodisperse large particles that cover polyA RNA (Stoylov *et al*., 1997), and the growth kinetics can also be determined by DLS (Stoylov *et al*., 1999). Recently, there is some use of dsDNA-proteins complexes in DLS. A study by Huffman *et al*.

(2001) showed that dsDNA binds homodimers and -tetramers of ARNT. Arioso *et al*. (2002) demonstrated that only one Ku protein binds a short piece of dsDNA.

1.7. Thesis outline

The core topic of this thesis is the role of the nucleoid-associated protein H-NS in condensing or compacting DNA. As we will show, for the solution conditions we have used (no Mg^{2+}), H-NS can only condense or compact DNA strongly in combination with macromolecular crowding. As a crowding agent we use a simple model system: uncharged flexible polymers. Besides these main topics, we make some excursions to related topics. A first study is concerned with the role of H-NS oligomerization in determining its DNA binding properties. The last study of the thesis concerns the combined role of crowding and nucleoid proteins in condensing DNA for the archaeal nucleoid protein Sso7d. This study shows that the phenomena that we find for H-NS, can also be found for completely different nucleoid proteins, and hence may be more general.

In chapter 2, we study the H-NS self-assembly (or oligomerization) so we may determine its role in DNA binding. We do so by considering the DNA-binding properties for an H-NS mutant (GA-H-NS D68V D71V) that exhibits strongly enhanced self-assembly in solution, and comparing those to *wt* H-NS.

Chapter 3 and 4 form the core of the thesis, and are concerned with the role of H-NS in DNA compaction. In Chapter 2, we investigate the ability of H-NS to compact both linearized and supercoiled plasmid DNA with and without the presence of a macromolecular crowding agent. We do so by determining DNA coil sizes using DLS, and using a simple centrifugal condensation assay for H-NS DNA complexes in the presence of the uncharged flexible polymer PEG. Chapter 4 addresses the effect of H-NS on isolated *E coli* nucleoids: can H-NS compact these nucleoids by itself, or is a combination with macromolecular crowding required, as was found for plasmid DNA in Chapter 3? Finally, in Chapter 5, we study the archaeal protein Sso7d, that strongly bends DNA, and determine its capacity to compact purified DNA both with and without macromolecular crowding, and find very similar effects as we have found for H-NS.

In the general discussion we review our results on the extent of compaction of DNA by NAPs. This review highlights the limited effects of NAPs on DNA compaction and

underscores the importance of additional effects such as the macromolecular crowding that we study in this thesis.

References

Aarsman, M.E.G., Piette, A., Fraipont, C., Vinkenvleugel, T.M.F., Nguyen-Disteche, M. and den Blaauwen, T. 2005. Maturation of the *Escherichia coli* divisome occurs in two steps. Molecular Microbiology 55(6): 1631-1645

Amit, R., Oppenheim, A. B. and Stavans, J. 2003. Increased bending rigidity of single DNA molecules by H-NS, a temperature and osmolarity sensor. Biophysical Journal 84(4): 2467-2473.

Amrein, M., Stasiak, A., Gross, H., Stoll, E. and Travaglini, G. 1988. Scanning tunnelling microscopy of RecA-DNA complexes coated with a conducting film. Science 240(4851): 514-516

Arold, S. T., P. G. Leonard, G. N. Parkinson, and J. E. Ladbury. 2010. H-NS forms a superhelical protein scaffold for DNA condensation. Proc. Natl. Acad. Sci. U. S. A. 107:15728-15732.

Arosio, D., Cui, S., Ortega, C., Chovanec, M., Di Marco, S., Baldini, G., Falaschi, A. and Vindigni, A. 2002. Studies on the mode of Ku interaction with DNA. Journal of Biological Chemistry 277(12): 9741-9748

Arscott, P.G., Li, A.Z. and Bloomfield, V.A. 1990. Condensation of DNA by Trivalent Cations .1. Effects of DNA Length and Topology on the Size and Shape of Condensed Particles. Biopolymers 30(5-6): 619-630

Asakura, S. and Oosawa, F. Interaction between particles suspended in solutions of macromolecules. Journal of Polymer Science 33(126): 183-192

Atlung, T. and Hansen, F.G. 2002. Effect of different concentrations of H-NS protein on chromosome replication and the cell cycle in *Escherichia coli*. Journal of Bacteriology 184(7):1843-1850

Azam, T.A., Iwata, A., Nishimura, A., Ueda, S. and Ishihama, A. 1999a. Growth phase-dependent variation in protein composition of the *Escherichia coli* nucleoid. Journal of Bacteriology 181(20): 6361-6370

Azam, T.A. and Ishihama, A. 1999b. Twelve species of the nucleoid-associated protein from *Escherichia coli* - Sequence recognition specificity and DNA binding affinity. Journal of Biological Chemistry 274(46): 33105-33113

Badaut, C., Williams, R., Arluison, V., Bouffartigues, E., Robert, B., Buc, H. and Rimsky, S. 2002. The degree of oligomerization of the H-NS nucleoid structuring protein is related to specific binding to DNA. Journal of Biological Chemistry 277(44): 41657-41666

Bailey, K. A., and Reeve, J. N. 1999. DNA repeats and archaeal nucleosome positioning. Research in Microbiology 150:701-709

Ball C.A., Osuna R., Ferguson K.C., Johnson R.C. 1992. Dramatic changes in Fis levels upon nutrient upshift in *Escherichia coli*. J Bacteriol 174:8043–8056

Bell, S.D., Botting, C.H., Wardleworth, B.N., Jackson, S.P. and White, M.F. 2002. The interaction of Alba, a conserved archaeal chomatin proteins, with Sir2 and its regulation by acetylation. Science 296: 148-151

Beloin, C., Jeusset, J., Revet, B., Mirambeau, G., Le Hegarat, F. and Le Cam, E. 2003. Contribution of DNA conformation and topology in right-handed DNA wrapping by the *Bacillus subtilis* LrpC protein. Journal of Biological Chemistry 278(7): 5333-5342

Benight, A.S., Wilson, D.H., Budzynski, D.M. and Goldstein, R.F. 1991. Dynamic Light-Scattering Investigations of RecA Self-Assembly and Interactions with Single-Strand DNA. Biochimie 73(2-3): 143-155

Berne, B.J. and Pecora, R. Dynamic Light Scattering: with applications to Chemistry, Biology and Physics. New York: Wiley; 1976.

Bessa Ramos, J.E., de Vries, R. and Neto, J.R. 2005. DNA Psi-condensation and reentrant decondensation: Effect of the PEG degree of polymerization. Journal of Physical Chemistry B 109(49): 23661-23665

Bloch, V., Yang, Y.S., Margeat, E., Chavanieu, A., Auge, M.T., Robert, B., Arold, S., Rimsky, S. and Kochoyan, M. 2003. The H-NS dimerization domain defines a new fold contributing to DNA recognition. Nature Structural Biology 10:212-218.

Bloomfield, V.A. 1997. DNA condensation by multivalent cations. Biopolymers 44(3): 269-282

Borgnia, M.J., Subramaniam, S. and Milne, J.L.S. 2008. Three-dimensional imaging of the highly bent architecture of *Bdellovibrio bacteriovorus* by using cryo-electron tomography. Journal of Bacteriology 190(7): 2588-2596

Bossi, L., and Smith, D. M. 1984. Conformational change in the DNA associated with an unusual promoter mutation in a transfer-RNA operon of *Salmonella*. Cell 39:643-652.

Bouffartigues, E., Buckle, M., Badaut, C., Travers, A. and Rimsky, S. 2007. H-NS cooperative binding to high-affinity sites in a regulatory element results in transcriptional silencing. Nature Structural & Molecular Biology 14(5): 441-448

Calladine, C.R., Drew, H.R., Luisi, B.F. and Travers, A.A. Understanding DNA. 3rd edition Amsterdam: Elsevier Academic Press; 2004

Castelnovo, M., and Gelbart, W. M. 2004. Semiflexible chain condensation by neutral depleting agents: Role of correlations between depletants. Macromolecules 37:3510-3517.

Ceci, P., Cellai, S., Falvo, E., Rivetti, C., Rossi, G. L. and Chiancone, E. 2004. DNA condensation and self-aggregation of *Escherichia coli* Dps are coupled phenomena related to the properties of the N-terminus. Nucleic Acids Research 32:5935-5944.

Ceschini, S., Lupidi, G., Coletta, M., Pon, C.L., Fioretti, E. and Angeletti, M. 2000. Multimeric self-assembly equilibria involving the histone-like protein H-NS - A thermodynamic study. Journal of Biological Chemistry 275(2): 729-734

Chattoraj, D.K., Gosule, L.C. and Schellman, J.A. 1978. DNA condensation with polyamines : II. Electron microscopic studies. Journal of Molecular Biology 121(3): 327-337

Cloutier, T.E. and Widom, J. 2004. Spontaneous sharp bending of double stranded DNA. Molecular Cell 14(3): 355-362

Dame, R. T. and Goosen, N. 2002. HU: promoting or counteracting DNA compaction? FEBS Letters 529(2-3): 151-156

Cunha, S., Woldringh, C.L. and Odijk, T. 2001. Polymer-mediated compaction and internal dynamics of isolated *Escherichia coli* nucleoids. Journal of Structural Biology 136(1): 53-66

Cunha, S. 2004. Experiments on the bacterial nucleoid of *Escherichia coli* viewed as a physical entity. Thesis (PhD).Technische Universiteit Delft.

Cusick, M.E. and Belfort, M. 1998. Domain structure and RNA annealing activity of the *Escherichia coli* regulatory protein StpA. Molecular Microbiology 28(4): 847-857

Dame, R.T., Wyman, C. and Goosen, N. 2000. H-NS mediated compaction of DNA visualized by atomic force microscopy. Nucleic acids research 28(18): 3504-3510

Dame, R.T., Wyman, C. and Goosen, N. 2001. Structural basis for preferential binding of H-NS to curved DNA. Biochimie 83(2): 231-234

Dame, R.T., Luijsterberg, M.S., Krin, E., Bertin, P.N., Wagner, R., and Wuite, G.J.L. 2005a. DNA bridging: a property shared among H-NS-like proteins. Journal of Bacteriology 187(5): 1845-1848

Dame, R. T., J. van Mameren, M. S. Luijsterberg, M. E. Mysiak, A. Janicijevic, G. Pazdzior, P. C. van der Vliet, C. Wyman, and G. Wuite. 2005b. Analysis of scanning force microscopy images of protein-induced DNA bending using simulations. Nucleic Acids Research 33: 2767-2767

Dame, R.T., Noom, M.C., and Wuite, G.J.L. 2006. Bacterial chromatin organization by H-NS protein unravelled using dual DNA manipulation. Nature 444:387-390.

Dorman, C.J., Hinton, J.C.D. and Free, A. 1999. Domain organization and oligomerization among H-NS-like nucleoid-associated proteins in bacteria. Trends in Microbiology 7(3): 124-128

Driessen, R. P. C., and Dame, R. T. 2011. Nucleoid-associated proteins in Crenarchaea. Biochemical Society Transactions 39:116-121.

Dürrenberger, M., La Teana, A., Citro, G., Venanzi, F., Gualerzi, C.O. and Pon, C.L. 1991. *Escherichia coli* DNA-binding protein H-NS is localized in the nucleoid. Research in microbiology 142:373-380.

Dworsky, P. and Schaechter, M. 1973. Effect of Rifampin on Structure and Membrane Attachment of Nucleoid of *Escherichia Coli*. Journal of Bacteriology 116(3): 1364-1374

Eckel, R., Wilking, S. D., Becker, A., Sewald, N., Ros, R. and Anselmetti, D. 2005. Single-molecule experiments in synthetic biology: An approach to the affinity ranking of DNA-binding peptides. Angewandte Chemie-International Edition 44(25): 3921-3924

Edmondson, S.P. and Shriver, J.W. DNA-binding proteins Sac7d and Sso7d from *Sulfolubus*. In: Adams, M.W.W. and Kelly, R. (Eds) Hyperthermophilic enzymes, Part C, Volume 334 (Methods in Enzymology) San Diego: Academic press; 2001. p129-145

Eltsov, M., and Dubochet, J. 2005. Fine structure of the *Deinococcus radiodurans* nucleoid revealed by cryoelectron microscopy of vitreous sections. Journal of Bacteriology 187:8047-8054.

Esposito, D., Petrovic, A., Harris, R., Ono, S., Eccleston, J. F., Mbabaali, A., Haq, I., Higgins, C.F., Hinton, J.C.D., Driscoll, P.C. and Ladbury, J.E. 2002. H-NS oligomerization domain structure reveals the mechanism for higher order self-association of the intact protein. Journal of molecular biology 324:841-850.

Falconi, M., Gualtieri, M.T., La Teana, A., Losso, M.A. and Pon, C.L. 1988. Proteins from the prokaryotic nucleoid: primary and quaternary structure of the 15-kD *Escherichia coli* DNA binding protein H-NS. Molecular Microbiology 2:323-329.

Falconi, M., Higgins, N.P., Spurio, R., Pon, C.L. and Gualerzi, C.O. 1993. Expression of the gene encoding the major bacterial nucleotide protein H-NS is subject to transcriptional auto-repression. Molecular Microbiology 10(2): 273-282

Falconi, M., Brandi, A., La Teana, A., Gualerzi, C.O. and Pon, C.L. 1996. Antagonistic involvement of FIS and H-NS proteins in the transcriptional control of *hns* expression. Molecular Microbiology 19(5): 965-975

Falconi, M., Colonna, B., Prosseda, G., Micheli, G. and Gualerzi, C.O. 1998. Thermoregulation of *Shigella* and *Escherichia coli* EIEC pathogenicity. A temperature-dependent structural transition of DNA modulates accessibility of *virF* promoter to transcriptional repressor H-NS. The EMBO journal 17:7033-7043.

Falconi, M., Prosseda, G., Giangrossi, M., Beghetto, E. and Colonna, B. 2001. Involvement of FIS in the H-NS-mediated regulation of *virF* gene of *Shigella* and enteroinvasive *Escherichia coli*. Molecular Microbiology 42(2): 439-452

Free, A., Williams, R.M. and Dorman, C.J. 1998. The StpA protein functions as a molecular adapter to mediate repression of the *bgl* operon by truncated H-NS in *Escherichia coli*. Journal of Bacteriology 180(4): 994-997

Friedrich, K., Gualerzi, C.O., Lammi, M., Losso, M.A., Pon, C.L. 1988. Proteins from the prokaryotic nucleoid; Interaction of nucleic acids with the 15 kDa *Escherichia coli* histone-like protein H-NS FEBS Letters 229(1), 197-202.

Garcia-Russell, N., Harmon, T.G., Le, T.Q., Amaladas, N.H., Mathewson, R.D. and Segall, A.M. 2004. Unequal access of chromosomal regions to each other in *Salmonella*: probing chromosome structure with phage lambda integrase-mediated long-range rearrangements. Molecular Microbiology 52(2): 329-344

Gao, Y.G., Su, S.Y., Robinson, H., Padmanabhan, S., Lim, L., McCrary, B.S., Edmondson, S.P., Shriver, J.W. and Wang, A.H.J. 1998. The crystal structure of the hyperthermophylic chromosomal protein Sso7d bound to DNA. Nature structural biology 5: 782-786

Gordon, B. R. G., Li, Y. F., Cote, A., Weirauch, M. T., Ding, P. F., Hughes, T. R., Navarre, W. W., Xia, B. and Liu, J. 2011. Structural basis for recognition of AT-rich DNA by unrelated xenogeneic silencing proteins. Proc. Natl. Acad. Sci. U. S. A. 108:10690-10695.

Gun'ko, V.M., Klyueva, A.V., Levchuk, Y.N. and Leboda, R. 2003. Photon correlation spectroscopy investigations of proteins. Advances in Colloid and Interface Science 105: 201-328

Guo, L., Feng, Y.G., Zhang, Z.F., Yao, H.W., Luo, Y.M., Wang, J.F. and Huang, L. 2008. Biochemical and structural characterization of Cren7, a novel chromatin protein conserved among Crenarchaea. Nucleic Acids Research 36(4): 1129-1137

Hagerman, P.J. 1986. Sequence-directed curvature of DNA. Nature 321(6068): 449-450

Hammermann, M., Steinmaier, C., Merlitz, H., Kapp, U., Waldeck, W., Chirico, G. and Langowski, J. 1997. Salt effects on the structure and internal dynamics of superhelical DNAs studied by light scattering and Brownian dynamics. Biophysical Journal 73(5): 2674-2687

Hardy, C.D. and Cozzarelli, N.R. 2005. A genetic selection for supercoiling mutants of *Escherichia coli* reveals proteins implicated in chromosome structure. Molecular Microbiology 57:1636–1652

Higgins, N.P., Booker, B.M. and Manna, D. Molecular Structure and Dynamics of Bacterial Nucleoids. In: Dame, R.T. and Dorman, C.J. (Eds) Bacterial Chromatin. Dordrecht: Springer; 2010. p. 117-148

Huffman, J.L., Mokashi, A., Bachinger, H.P. and Brennan, R.G. 2001. The basic helix-loop-helix domain of the aryl hydrocarbon receptor nuclear transporter (ARNT) can oligomerize and bind E-box DNA specifically. Journal of Biological Chemistry 276(44): 40537-40544

Jelinska, C., Conroy, M.J., Craven, C.J., Hounslow, A.M., Bullough, P.A., Waltho, J.P., Taylor, G.L. and White, M.F. 2005. Obligate hetrodimerization of the archaeal Alba2 protein with Alba1 provides a mechanism for control of DNA packaging. Structure 13: 963-971

Jensen, R. B. 2006. Coordination between chromosome replication, segregation, and cell division in *Caulobacter crescentus*. Journal of Bacteriology 188:2244-2253.

Kavenoff, R. and Bowen, B. C. 1976. Electron-Microscopy of Membrane-Free Folded Chromosomes from *Escherichia-Coli*. Chromosoma 58(2): 89-101

Khokhlov, A.R. and Khachaturian, K.A. 1982. On the Theory of Weakly Charged Poly-Electrolytes. Polymer 23(12): 1742-1750

Koh, J., Saecker, R.M. and Record, M.T. Jr. 2008. DNA Binding Mode Transitions of *Escherichia coli* HU alpha beta: Evidence for Formation of a Bent DNA - Protein Complex on Intact, Linear Duplex DNA. Journal of Molecular Biology 383:324–346

Krawiec, S. and Riley, M. 1990. Organization of the Bacterial Chromosome. Microbiological Reviews 54(4): 502-539

Krotova, M. K., Vasilevskaya, V. V., Makita, N., Yoshikawa, K. and Khokhlov, A. R. 2010. DNA compaction in a crowded environment with negatively charged proteins. Physical Review Letters105:128302.

Krueger, J.K., McCrary, B.S., Wang, A.H.J., Shriver, J.W., Trewhella, J. and Edmondson, S.P. 1999. The solution structure of the Sac7d/DNA complex: a small angle X-ray scattering study. Biochemistry 38: 10247-10255

Lang, B., Blot, N., Bouffartigues, E., Buckle, M., Geertz, M., Gualerzi, C.O., Mavathur, R., Muskhelishvili, G., Pon, C.L., Rimsky, S., Stella, S., Madan Babu, M. and Travers, A. 2007. High-affinity DNA binding sites for H-NS provide a molecular basis for selective silencing within proteobacterial genomes. Nucleic Acids Research 35(18): 6330-6337

Langowski, J., Benight, A. S., Fujimoto, B. S., Schurr, J. M. and Schomburg, U. 1985. Change of Conformation and Internal Dynamics of Supercoiled DNA Upon Binding of *Escherichia-Coli* Single-Strand Binding-Protein. Biochemistry 24(15): 4022-4028

Langowski, J., Kremer, W. and Kapp, U. 1992. Dynamic light scattering for study of solution conformation and dynamics of superhelical DNA. Methods in Enzymology 211: 430-448

Langowski, J., Kapp, U., Klenin, K. and Vologodskii, A. 1994. Solution Structure and Dynamics of DNA Topoisomers - Dynamic Light-Scattering-Studies and Monte-Carlo Simulations. Biopolymers 34(5): 639-646

Langowski, J., Hammermann, M., Klenin, K., May, R. and Toth, K. 1999. Superhelical DNA studied by solution scattering and computer models. Genetica 106(1-2): 49-55

Leonard, P.G., Ono, S., Gor, J., Perkins, S.J. and Ladbury, J.E. 2009. Investigation of the self-association and hetero-association interactions of H-NS and StpA from Enterobacteria. Molecular Microbiology 73(2): 165-179

Lerman, L.S. 1971. A transition to a compact form of DNA in polymer solutions Proc. Natl. Acad. Sci. U. S. A. 68(8): 1886-1890

Liu, Y. J., Chen, H., Kenney, L. J. and Yan, J. 2011. A divalent switch drives H-NS/DNA-binding conformations between stiffening and bridging modes. Genes & Development 24:339-344.

Luijsterburg, M. S., M. F. White, R. van Driel, and R. T. Dame. 2008. The major architects of chromatin: Architectural proteins in Bacteria, Archaea and Eukaryotes. Crit. Rev. Biochem. Mol. Biol. 43:393-418.

Lurz, R., Grote, M., Dijk, J., Reinhardt, R. and Dobrinski, B. 1986. Electron-microscopy study of DNA complexes with proteins from the archaebacterium *Sulfolubus acidocaldarius*. EMBO journal 5: 3715-3721

Maurelli, A.T. and Sansonetti, P.J. 1988. Identification of a Chromosomal Gene Controlling Temperature-Regulated Expression of *Shigella* Virulence. Proceedings of the National Academy of Sciences of the United States of America 85(8): 2820-2824

McAfee, J.G., Edmondson, S.P., Zegar, I. and Shriver, J.W. 1996. Equilibrium DNA binding of Sac7d protein from the hyperthermophilic *Sulfolubus acidocaldarius*: fluorescence and circular dichroism studies. Biochemistry 35: 4034-4045

Mellies, J. L., Benison, G., McNitt, W., Mavor, D., Boniface, C. and Larabee, F. J. 2011. Ler of pathogenic *Escherichia coli* forms toroidal protein-DNA complexes. Microbiology-(UK) 157:1123-1133.

Muñoz A., Valls, M., and de Lorenzo, V. Extreme DNA Bending: Molecular Basis of the Regulatory Breadth of IHF. In: Dame, R.T. and Dorman, C.J. (Eds) Bacterial Chromatin. Dordrecht: Springer; 2010. p. 365-393

Murphy, L.D. and Zimmerman, S.B. 1995. Condensation and Cohesion of Lambda-DNA in Cell-Extracts and Other Media - Implications for the Structure and Function of DNA in Prokaryotes. Biophysical Chemistry 57(1): 71-92

Navarre, W.W., Porwollik, S., Wang, Y.P., McClelland, M., Rosen, H., Libby, S.J. and Fang, F.C. 2006. Selective silencing of foreign DNA with low GC content by the H-NS protein in *Salmonella*. Science 313: 236-238

Niki, H., Imamura, R., Kitaoka, M., Yamanaka, K., Ogura, T. and Hiraga, S. 1992. *E. coli* MukB protein involved in chromosome partition forms a homodimer with a rod-and-hinge structure having DNA binding and ATP/GTP binding activities. EMBO Journal 11: 5101–5109

Odijk, T. 1998. Osmotic compaction of supercoiled DNA into a bacterial nucleoid. Biophysical Chemistry 73(1-2): 23-29

Ono, S., Goldberg, M.D., Olsson, T., Esposito, D., Hinton, J.C.D. and Ladbury, J.E. 2005. H-NS is a part of a thermally controlled mechanism for bacterial gene regulation. The Biochemical journal 391: 203-213

Pan, C.Q., Feng, J.A., Finkel, S.E., Landgraf, R., Sigman, D. and Johnson, R.C. 1994. A Complex Probed by Protein Conjugated with 1,10-Phenanthroline Copper(I) Complex. Proceedings of the National Academy of Sciences of the United States of America 91(5): 1721-1725

Pan, C.Q., Finkel, S.E., Cramton, S.E., Feng, J.A., Sigman, D.S. and Johnson, R.C. 1996. Variable structures of Fis-DNA complexes determined by flanking DNA-protein contacts. Journal of Molecular Biology 264(4): 675-695

Pereira, S. L., Grayling, R. A., Lurz, R. and Reeve., J. N. 1997. Archaeal nucleosomes. Proc. Natl. Acad. Sci. U. S. A. 94:12633-12637.

Pon, C.L., Calogero, R.A. and Gualerzi, C.O. 1988. Identification, cloning, nucleotide sequence and chromosomal map location of *hns*, the structural gene for *Escherichia coli* DNA-binding protein H-NS. Molecular & general genetics 212:199-202

Prosseda, G., Fradiani, P.A., Di Lorenzo, M., Falconi, M., Micheli, G., Casalino, M., Nicoletti, M. and Colonna, B. 1998. A role for H-NS in the regulation of the *virF* gene of *Shigella* and enteroinvasive *Escherichia coli*. Research in Microbiology 149(1): 15-25

Ramreddy, T., Sen, S., Rao, B.J. and Krishnamoorthy, G. 2003. DNA dynamics in RecA-DNA filaments: ATP hydrolysis-related flexibility in DNA. Biochemistry 42(41): 12085-12094

Renzoni, D., Esposito, D., Pfuhl, M., Hinton, J.C.D., Higgins, C.F., Driscoll, P.C. and Ladbury, J.E. 2001. Structural characterization of the N-terminal oligomerization domain of the bacterial chromatin-structuring protein, H-NS. Journal of Molecular Biology 306(5): 1127-1137

Rice, P.A., Yang, S.W., Mizuuchi, K. and Nash, H.A. 1996. Crystal structure of an IHF-DNA complex: A protein-induced DNA U-turn. Cell 87(7): 1295-1306

Rimsky, S., Zuber, F., Buckle, M. and Buc, H. 2001. A molecular mechanism for the repression of transcription by the H-NS protein. Molecular Microbiology 42(5): 1311-1323

dos Santos, M.T. and Rodrigues, P.S. 2005. A genomic-scale search for regulatory binding sites in the integration host factor regulon of *Escherichia coli* K12. Genetics and molecular research 4(4): 783-789

Sarkar, T., Petrov, A.S., Vitko, J.R., Santai, C. T., Harvey, S.C., Mukerji, I. and Hud, N.V. 2009. Integration Host Factor (IHF) Dictates the Structure of Polyamine-DNA Condensates: Implications for the Role of IHF in the Compaction of Bacterial Chromatin. Biochemistry 48(4): 667-675

Schmitz, K.S. and Schurr, J.M. 1973. Rotational Relaxation of Macromolecules Determined by Dynamic Light-Scattering .2. Temperature-Dependence for DNA. Biopolymers 12(7): 1543-1564

Schneider. R., Travers, A.A. and Muskhelishvili, G. 1997. FIS regulates the bacterial growth phase dependent topological transitions in DNA. Molecular Microbiology 26:519–530

Schneider, R., Lurz, R., Luder, G., Tolksdorf, C., Travers, A. and Muskhelishvili, G. 2001. An architectural role of the Escherichia coli chromatin protein FIS in organising DNA. Nucleic Acids Reseach 29:5107-5114

Sette, M., Spurio, R., Trotta, E., Brandizi, C., Brandi, A., Pon, C. ., Barbato, G., Boelens, R. and Gualerzi, C.O. 2009. Sequence-specific Recognition of DNA by the C-terminal Domain of Nucleoid-associated Protein H-NS. Journal of Biological Chemistry 284(44): 30453-30462

Shindo, H., Iwaki, T., Ieda, R., Kurumizaka, H., Ueguchi, C., Mizuno, T., Morikawa, S., Nakamura, H. and Kuboniwa, H. 1995. Solution Structure of the DNA-Binding Domain of a Nucleoid-Associated Protein, H-NS, from *Escherichia-Coli*. FEBS Letters 306(2): 125-131

Shindo, H., Ohnuki, A., Ginba, H., Katoh, E., Ueguchi, C., Mizuno, T. and Yamazaki, T. 1999. Identification of the DNA binding surface of H-NS protein from *Escherichia coli* by heteronuclear NMR spectroscopy. FEBS Letters 455(1-2): 63-69

Smyth, C.P., Lundbäck, T., Renzoni, D., Siligardi, G., Beavil, R., Layton, M., Sidebotham, J.M., Hinton, J.C.D., Driscoll, P.C., Higgins, C.F. and Ladbury, J.E. 2000. Oligomerization of the chromatin-structuring protein H-NS. Molecular Microbiology 36:962-972.

Sonnenfield, J.M., Burns, C.M., Higgins, C.F. and Hinton, J.C.D. (2001) The nucleoid-associated protein StpA binds curved DNA, has a greater DNA-binding affinity than H-NS and is present in significant levels in *hns* mutants. Biochimie 83(2): 243-249

Spurio, R., Dürrenberger, M., Falconi, M., La Teana, A., Pon, C.L. and Gualerzi, C.O. 1992. Lethal overproduction of the *Escherichia coli* nucleoid protein H-NS: ultramicroscopic and molecular autopsy. Molecular & general genetics 231: 201-211

Spurio, R., Falconi, M., Brandi, A., Pon, C.L. and Gualerzi, C.O. 1997. The oligomeric structure of nucleoid protein H-NS is necessary for recognition of intrinsically curved DNA and for DNA bending. EMBO Journal 16 (7): 1795-1805

Staczek, P. and Higgins, N.P. 1998. Gyrase and Topo IV modulate chromosome domain size *in vivo*. Molecular Microbiology 29(6): 1435-1448

Stella, S., Spurio, R., Falconi, M., Pon, C.L. and Gualerzi, C.O. 2005. Nature and mechanism of the in vivo oligomerization of nucleoid protein H-NS. The EMBO journal 24:2896-2905.

Stoylov, S.P., Vuilleumier, C., Stoylova, E., DeRocquigny, H., Roques, B.P., Gerard, D. and Mely, Y. 1997. Ordered aggregation of ribonucleic acids by the human immunodeficiency virus type 1 nucleocapsid protein. Biopolymers 41(3): 301-312

Stoylov, S.P., Stoylova, E., Todorov, R., Schmiedel, P., Thunig, C., Hoffmann, H., Roques, B.P., Le Cam, E., Coulaud, D., Delain, E., Gerard, D. and Mely, Y. 1999. Aggregation of polyA-HIV-1 nucleocapsid protein NCp7 complexes and properties of the aggregates. Colloids and Surfaces a-Physicochemical and Engineering Aspects 152(3): 263-274

Swinger, K.K., Lemberg, K.M., Zhang, Y. and Rice, P.A. 2003. Flexible DNA bending in HU-DNA cocrystal structures. EMBO Journal 22(14): 3749-3760

Tapias, A. Lopez, G. and Ayora, S. 2000. *Bacillus subtilis* LrpC is a sequence-independent DNA-binding and DNA-bending protein which bridges DNA. Nucleic Acids Research 28(2): 552-559

Travers, A.A.. 2005. DNA dynamics: bubble 'n' flip for DNA cyclisation? Current biology 15(10): 377-9

Tupper, A.E., Owen-Hughes, T.A., Ussery, D.W., Santos, D.S., Ferguson, D.J., Sidebotham, J.M., Hinton, J.C. and Higgins, C.F. 1994. The chromatin-associated protein H-NS alters DNA topology in vitro. EMBO Journal 13(1):258-268

Ueguchi, C., Seto, C., Suzuki, T., and Mizuno, T. 1997. Clarification of the dimerization domain and its functional significance for the *Escherichia coli* nucleoid protein H-NS. Journal of Molecular Biology 274:145-151.

Vasilevskaya, V.V., Khokhlov, A.R., Matsuzawa, Y. and Yoshikawa, K. 1995. Collapse of Single DNA Molecule in Poly(Ethylene Glycol) Solutions. Journal of Chemical Physics 102(16): 6595-6602

de Vries, R. 2001. Flexible polymer-induced condensation and bundle formation of DNA and F-Actin filaments. Biophysical Journal 80(3): 1186-1194

de Vries, R. 2006. Depletion-induced instability in protein-DNA mixtures: Influence of protein charge and size. The Journal of Chemical Physics 125: 014905

de Vries, R. 2010 DNA condensation in bacteria: Interplay between macromolecular crowding and nucleoid proteins Biochimie 92 (12):1715-1721

de Vries, R. 2011. Influence of mobile DNA-protein-DNA bridges on DNA configurations: Coarse-grained Monte-Carlo simulations. The Journal of Chemical Physics 135:125104.

Wang, W. Q., Li, G. W., Chen, C. Y., Xie, X. S. and Zhuang., X. W. 2011. Chromosome Organization by a Nucleoid-Associated Protein in Live Bacteria. Science 333:1445-1449.

Watson, J.D. and Crick, F.H.C. 1953. A structure for deoxyribose nucleic acid. Nature 171: 737-738

Weisberg, R.A., Freundlich, M., Friedman, D., Gardner, J., Goosen, N., Nash, H., Oppenheim, A. and RouviereYaniv, J. 1996. Nomenclature of the genes encoding IHF. Molecular Microbiology 19(3): 642

Williams, R.M., Rimsky, S. and Buc, H. 1996. Probing the structure, function, and interactions of the *Escherichia coli* H-NS and StpA proteins by using dominant negative derivatives. Journal of Bacteriology 178(15): 4335-4343

Woldringh, C.L. and Nanninga, N. Structure of nucleoid and cytoplasm in the intact cell. In: N. Nanninga (Ed.) Molecular Cytology of *Escherichia coli.* London: Academic Press; 1985, pp. 161–197.

Woldringh, C.L. 2002. The role of co-transcriptional translation and protein translocation (transertion) in bacterial chromosome segregation. Molecular Microbiology 42(1): 17-29

Wolf, S. G., Frenkiel, D., Arad, T., Finkel, S. E., Kolter, R.and Minsky, A. 1999. DNA protection by stress-induced biocrystallization. Nature 400:83-85.

Yamada, H., Muramatsu, S. and Mizuno, T. 1990. An *Escherichia coli* protein that preferentially binds to sharply curved DNA. Journal of biochemistry (Tokio) 108(3): 420-425

Yamakawa, H. 1971. Modern Theory of Polymer Solutions. Harper & Row, New York.

Yoshikawa, K., Takahashi, M., Vasilevskaya, V.V. and Khokhlov, A.R. 1996. Large discrete transition in a single DNA molecule appears continuous in the ensemble. Physical Review Letters. 76(16): 3029-3031

Zhang, A.X. and Belfort, M. 1992 Nucleotide-Sequence of a Newly-Identified *Escherichia-Coli* Gene, Stpa, Encoding an H-NS-Like Protein. Nucleic Acids Research 20(24): 6735-

Zhang, A.X., Rimsky, S., Reaban, M.E., Buc, H. and Belfort, M. 1996. *Escherichia coli* protein analogs StpA and H-NS: Regulatory loops, similar and disparate effects on nucleic acid. EMBO Journal 15(6): 1340-1349

Zimmerman, S.B. and Minton, A.P. 1993. Macromolecular Crowding - Biochemical, Biophysical, and Physiological Consequences. Annual Review of Biophysics and Biomolecular Structure 22:27-65

Chapter 2

Probing the relation between protein-protein interactions and DNA binding properties of the bacterial nucleoid protein H-NS*

*To be submitted

Abstract

We investigate the relation between oligomerization in solution and DNA binding properties for the bacterial nucleoid protein H-NS by studying oligomerization and DNA binding properties of a D68V-D71V H-NS mutant. By replacing two aspartic acid residues with valines, the H-NS linker region that connects the N-terminal dimerization domain and the C-terminal DNA binding domain is made significantly more hydrophobic. This drives stronger oligomerization in solution and may lead to altered DNA binding properties. Dynamic Light Scattering is used to probe protein oligomerization. Electrophoretic mobility shift assays and DNA footprinting were used to probe the binding of both H-NS and D68V-D71V H-NS to an *hns* promoter fragment.

Using Dynamic Light Scattering we confirm the concentration-dependent oligomerization of H-NS in solution. The oligomerization has a weak and gradual temperature-dependence. Remarkably, the temperature-dependence of H-NS oligomerization was found to be abolished by the addition of two small residues (GA) on the N-terminal side of the protein, a change that has no influence on its DNA-binding properties. The double linker mutation D68V-D71V leads to a dramatically enhanced and strongly temperature-dependent H-NS oligomerization in solution. The DNA binding affinity of D68V-D71V is lower and has stronger temperature dependence than that of H-NS. DNAse I footprinting shows that at high concentrations, regions protected by D68V-D71V H-NS are even larger than for H-NS.

The comparison of H-NS and GA-H-NS demonstrates that the temperature-dependence of H-NS oligomerization need not be related to the temperature-dependence of its DNA binding properties, as has been suggested previously. Results for D68V-D71V demonstrate that even dramatic changes in the oligomerization of H-NS in solution only lead to moderate changes of its DNA binding properties. Both results suggest that it is difficult to draw conclusion about the DNA binding properties of H-NS, from its oligomerization behaviour in solution.

2.1 Introduction

H-NS (Histone-like Nucleoid Structuring protein) is a small 16 kDa protein [1,2] that localizes to the bacterial nucleoid [3,4], where it plays an important role as a global regulator of bacterial gene expression [5]. Control of expression by H-NS is sensitive to environmental conditions, in particular to temperature [6]. The protein consists of a C-terminal domain [7] that binds to DNA, and an N-terminal domain that forms stable dimers, either parallel [8] or antiparallel [9,10]. The two domains are connected by a linker, which is thought to be either unstructured or mainly alpha-helical [10].

H-NS binding to DNA is relatively sequence aspecific, but a consensus sequence has been identified to which H-NS binds with a somewhat increased affinity [11,12]. In addition, H-NS preferentially binds to intrinsically curved DNA, presumably by bridging sites flanking the curved region [13,14]. Electron microscopy [15-17] and AFM images of H-NS/DNA complexes [18-21] show that the protein binds in stretches. Multimerization of H-NS on DNA is also consistent with the observed binding cooperativity and nearly complete protection against DNAse attack observed for promoter sequences such as those of the *proU* [15] and *hns* [13] genes.

At higher concentrations, H-NS dimers in solution (in the absence of DNA) self-assemble into various higher order oligomers [6,9,22-24]. Both the dimerization and the higher order oligomerization are thought to have a crucial influence on the DNA binding properties of H-NS [22,26,27]. It has even been suggested [6] that thermoregulation by H-NS could be mediated by the temperature dependence of H-NS oligomerization [6,24], although there is also strong evidence that the temperature-dependence of DNA intrinsic curvature plays a crucial role [28]. While there may indeed be a direct link between the higher order oligomerization in solution and multimerization on DNA, this need not be the case. Putative protein-protein interactions that drive multimerization on DNA may or may not operate between H-NS molecules in solution. Furthermore, clustering of bound H-NS molecules may also be induced by the DNA template [29,30] rather than by protein-protein interactions.

Here we probe the relation between H-NS oligomerization and DNA binding by studying H-NS with a D68V-D71V double mutation. By replacing two aspartic acid residues D68 and D71 by valines, the H-NS linker region that connects the N-terminal dimerization domain and the C-terminal DNA binding domain is made significantly more hydrophobic, which we expect will drive stronger oligomerization in solution, without affecting H-NS dimerization

by the N-terminal domain or DNA binding by the H-NS C-terminal domain. The expectation of stronger higher order oligomerization is based on the fact that the linker region of H-NS is known to be involved in higher order oligomerization: deletion mutants containing the N-terminal domain plus the linker are capable of higher order oligomerization, but not the N-terminal domain by itself [8]. Other linker mutations have already been shown to lead to certain functional defects: both an E53GT55P double mutation [31], and a R54C mutation [32] have been found to result in proteins that are defective in repressing the H-NS controlled *proU* operon, but these studies did not investigate the relation between oligomerization and DNA binding properties in much detail.

We here perform a more extensive characterization of the solution oligomerization behaviour, both of the wild type H-NS, and the D68V-D71V H-NS. Varying both concentration and temperature, we use Dynamic Light Scattering (DLS), to non-invasively characterize the oligomerization of both full-length proteins. Very little data is available on how the oligomerization of full-length H-NS depends on environmental conditions. For low concentrations, a detailed study was performed by Ceschini *et al.* [25]. We extend this work by also considering higher protein concentrations, for which the higher order oligomerization becomes very strong.

DNA binding properties are investigated for the *hns* promoter sequence, for which H-NS binding has been studied in detail in earlier work [13]. The interaction of both wild type H-NS and H-NS D68V-D71V with *hns* promoter DNA are studied using electrophoretic mobility shift assays, DNAse I footprinting, and an *in-vitro* transcription assay.

2.1 Material and methods

Strains

Overexpression of *wt* H-NS was performed as described previously [12]. The linker mutant H-NS D68V-D71V was produced as a fusion with a Tobacco Etch Virus (TEV) protease cleavage site and a $(His)_6$ tag. Cleavage with TEV protease removes the His tag, but this leaves two additional residues (GA). The final mutant protein is therefore denoted as GA H-NS D68V-D71V. In a similar way we have also produced GA H-NS. Both were overexpressed in *E. coli* UT5600 carrying the plasmids pcI857 and pPLc2833.

Isolation of wt H-NS and mutants

Isolation of *wt* H-NS was done as described before [12]. The GA H-NS and GA H-NS D68V-D71V producing strains were grown, induced and collected as the *wt* H-NS producing strain [12]. Pellets were resuspended in a minimal volume of buffer F (50 mM Na_2HPO_4/NaH_2PO_4 pH 8.0, 100 mM NaCl, 5% glycerol, 0.025% Nonidet P40 detergent) and frozen at -80 ºC. Cells were disrupted and centrifuged as described before [12]. Salt was added to a final concentration of 1 M NaCl, and β-mercaptoethanol to a final concentration of 5 mM. The supernatant after centrifugation was loaded on a NiNTA column, and eluted with a linear imidazole gradient (10 – 250 mM) in Buffer F + 1 M NaCl. Fractions containing the H-NS mutants were dialyzed against Buffer F + 5 mM β-mercaptoethanol and digested by TEV protease (concentration of 30-50:1) overnight at 20 ºC, with 20%

extra TEV protease added for an additional 3-4 h. The reaction mixture was again loaded on the NiNTA column and eluted identical to the previous gradient. Proteins were concentrated and stored identical to *wt* .

Preparation of protein solutions for Dynamic Light Scattering
Frozen protein stock solutions (*wt* H-NS, GA H-NS and GA H-NS D68V-D71V) were slowly thawed on ice. Storage buffer was exchanged for filtered 10 mM Na_2HPO_4/NaH_2PO_4 100 mM NaCl pH 7.0 using Zeba Desalt Spin columns (0.5 ml, Pierce), pre-rinsed with appropriate buffer in a Biofuge Fresco rotor at 14,000 rpm at 4°C. Proteins solutions were concentrated using 0.5 ml Microcon YM-3 3 kDa NMWL centrifugal filters (Millipore Corp.) at room temperature. Concentrations were determined spectrophotometrically, using an absorption coefficient of 0.86 L g^{-1} cm^{-1} at λ=280 nm [2]. Next, protein solutions were diluted to the concentrations required in the experiments, and filtered with 0.5 ml Microcon YM-3 150 kDa NMWL centrifugal filter devices. Finally, concentrations were checked once more using UV spectrometry.

Dynamic Light Scattering
Dynamic Light Scattering experiments were taken with a Malvern Zetasizer Nano ZEN 1600 with a 4 mW He-Ne laser operating at wavelength of λ = 633nm, at a fixed scattering angle of α =173°. DLS measurements were performed in Hellma precision cells type 105.251.005-QS (pathlength 3 mm). Cells were cleaned with 1 M HCl, filtered H_2O, and buffer before being filled with sample. Protein solutions prepared as described above were centrifuged for 1 h at 10,000 g and the cleaned cells were filled with 20-25 µl of protein solution. Samples were left to equilibrate for 30 min. at room temperature prior to the measurements.
Absolute scattering intensities R_θ (Rayleigh ratio) are calculated from

$$R_\theta = \frac{I_s - I_0}{I_t}\frac{n_0^2}{n_t^2}R_t \qquad (2.1)$$

where n_0=1.333 is the solvent refractive index and n_t = 1.496 is the refractive index of the toluene reference. Furthermore, I_s, I_0 and I_t are, respectively, the scattering intensities of the sample, buffer, and toluene reference, and $R_t = 1.35\text{x}10^{-2}$ m^{-1} is the absolute scattering intensity of the toluene reference. Effective hydrodynamic radii $R_{H,eff}$ of protein oligomers reported are taken from a distribution fit of the intensity autocorrelation function. The reported value is the dominant peak reported by the Malvern DTS software, version 5.03.

Electrophoretic mobility shift assay and DNAse I footprinting
Electrophoretic mobility shift assays (EMSA) were performed on –350-0 *hns* promoter labelled with 32P. 10 ng of this DNA was incubated for 10 min at the indicated temperatures with increasing amounts of protein in 15 µl of 10 mM Tris-HCl pH 7.5, 0.5 mM DTT, 10 mM $MgCl_2$, 1 mM Spermidine, 10 mM KCl, 5 % Glycerol and 100 mM NaCl. 1 µl sample buffer (98% glycerol, bromophenol blue and xylene cyanol) was added and samples were loaded on 7% native acrylamide gel and run at the indicated temperatures in TAE buffer (Tris-Acetate-EDTA) pH 7.4. The gel was transferred to 3MM paper, and the bands quantified by a Molecular Imager FX (Bio-Rad) and QuantityOne software. DNAse I footprinting was performed as described previously[12].

In-vitro transcription assay
The *in vitro* transcription was carried out with [α ^{32}P]-UTP as described in Giangrossi *et al*. [34], using as DNA template a 480 bp *hns* fragment. This fragment was amplified by PCR using the oligonucleotides Forward 5'-AGTCCATGCTCTTATTGCGAC and Reverse 5'-TTCTTCTTCGCGACGTTCAGGAACGACAACTTC TAA and plasmid pKK400 as template [35]. The transcription products were loaded on 7% PAGE-UREA gel; the *in vitro* transcribed RNA molecules were detected and quantified by Molecular Imager (Bio-Rad, model FX).

2.3 Results

H-NS linker mutant

The domain structure of H-NS is illustrated in Figure 2.1, as well as the locations of the mutations that are studied here. A plot of the hydropathy index [33] of the H-NS linker is shown in Figure 2.2. The *wt* linker is not very hydrophilic or very hydrophobic. Changing two of the hydrophilic aspartic acid residues at positions 68 and 71 into hydrophobic valines makes the N-terminal side of the linker significantly more hydrophobic. This may drive stronger higher order oligomerization of H-NS dimers, which in turn, may or may not influence DNA binding. H-NS D68V-D71V is produced as a fusion with a His-tag with a TEV protease site. Cleavage leaves two residues (GA), producing a final protein denoted GA H-NS D68V-D71V (Figure 2.1). Possible effects of the addition are checked by comparing the GA H-NS mutant with *wt* H-NS as well.

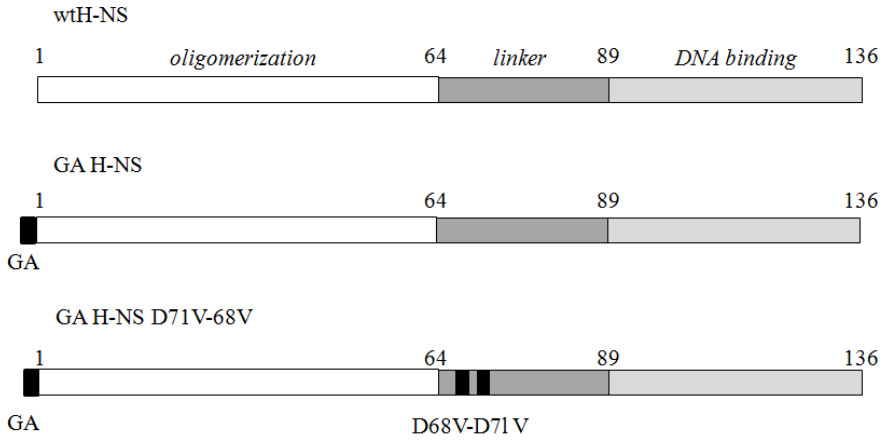

Figure 2.1: Schematic illustration of domain organization in H-NS, and positions of the mutations in GA H-NS and GA H-NS D68V-D71V, which are 138 a.a. long. The N-terminal domain is marked "oligomerization", the C-terminal domain "DNA-binding".

Oligomerization of wt H-NS, GA H-NS and GA H-NS D68V-D71V in the absence of DNA

The concentration-dependence of the effective hydrodynamic radius of oligomers of *wt* H-NS (at room temperature) is shown in Figure 2.3. The oligomers have an effective hydrodynamic radius $R_{H,eff}$ of 6 nm at 0.1 g/L, increasing to about 9 nm at 0.5 g/L. For a hypothetical compact globular protein of 32 kDa (the weight of one H-NS dimer) we expect a radius of 2.6 nm, based on a typical specific density of proteins. This indicates extensive oligomerization of full length H-NS at the rather high protein concentrations considered here. Values for $R_{H,eff}$ of 6 - 9 nm roughly correspond to masses of 200-600 kDa, again assuming globular complexes. The actual shape of the H-NS dimer and its oligomers probably is not compact and spherical;

hence the real molar mass of the oligomers in solution could be lower. In principle the weight-averaged molar mass of the H-NS oligomers in solution can be determined from the static

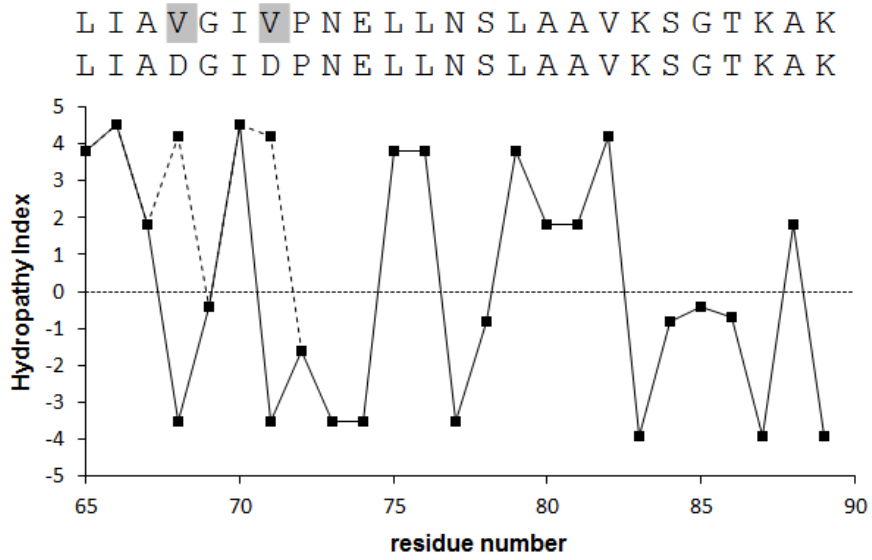

Figure 2.2: Hydropathy index (Kyte and Doolittle scale) of the H-NS linker for the *wt* protein (solid line, lower sequence) and the D68V-D71V mutant (dotted line, upper sequence). The top lines indicate the sequences, with the D→V mutations highlighted in grey.

scattering intensities. Unfortunately this measurement was not possible in the present case due to significant contributions to the scattering intensity of a small fraction of very large contaminants, probably protein aggregates or dust.

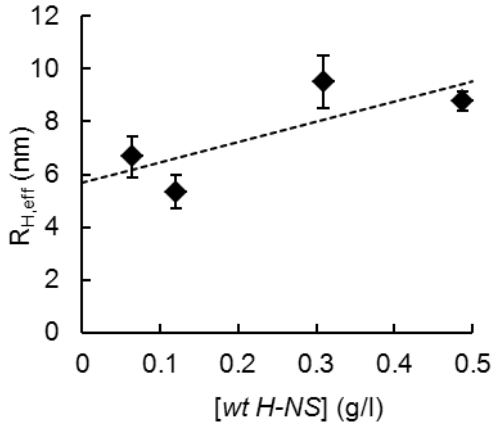

Figure 2.3: Concentration dependence of $R_{H,eff}$ for *wt* H-NS. The dashed line is a guide to the eye.

Results for the temperature-dependence of *wt* H-NS self-assembly are shown in Figure 2.4, for both low (0.064 g/l) and high protein concentration (0.309 g/l). At low concentrations of H-NS, the effective hydrodynamic radius of the oligomers is $R_{H,eff} \approx 6$ nm, which is roughly temperature-independent. At higher H-NS concentration the size of the oligomers becomes

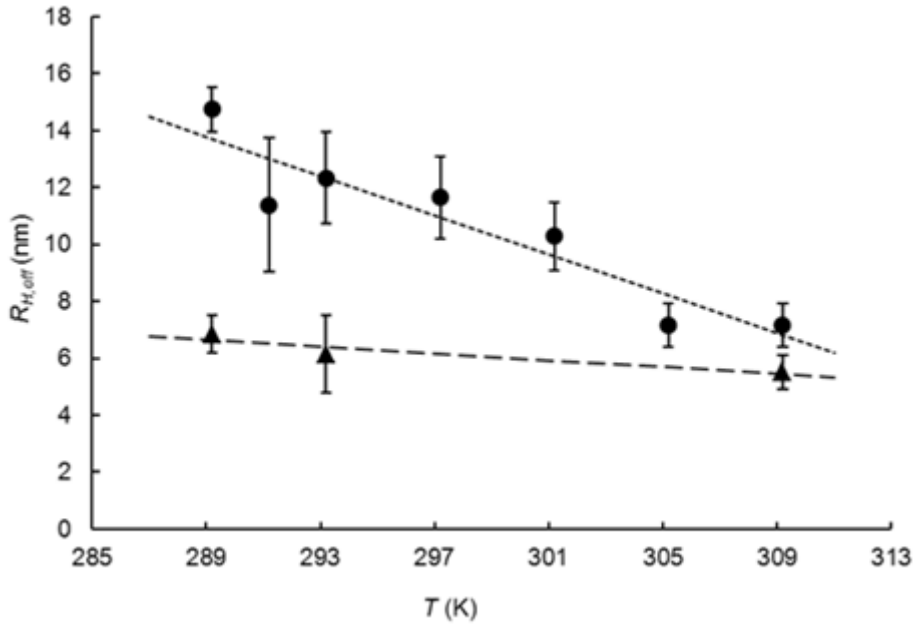

Figure 2.4: Temperature dependence of $R_{H,eff}$ of *wt* H-NS at two concentrations as determined using dynamic light scattering: 0.064 g/l (filled triangles) and 0.309 g/l (filled circles). Lines are guides to the eye.

much larger, and exhibits much stronger temperature dependence. At 0.31 g/l the effective hydrodynamic radius of the H-NS oligomers decreases from 14 nm at 16 °C to about 7 nm at 40 °C.

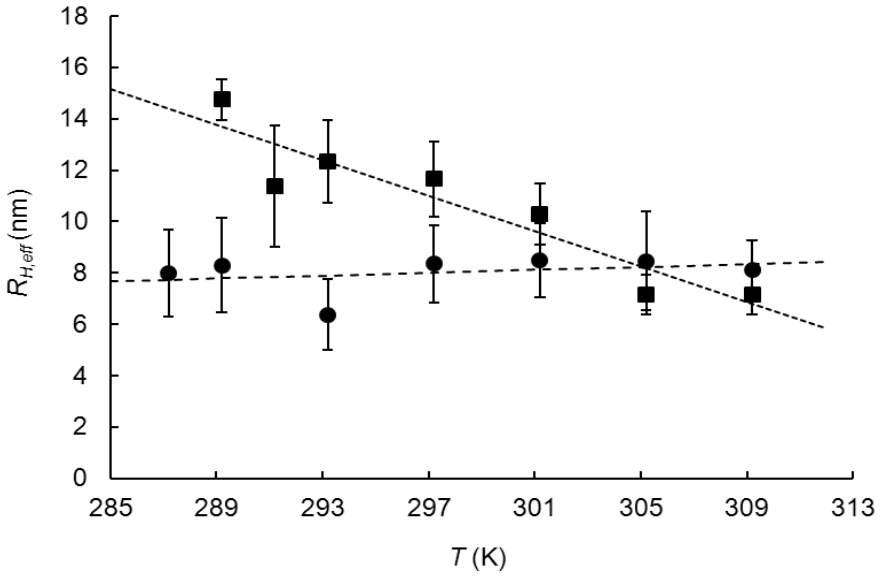

Figure 2.5: Comparison of temperature dependence of $R_{H,eff}$ of *wt* H-NS (0.309 g/L, squares) and GA H-NS (0.488 g/L, circles). Lines are guides to the eye.

Since the method of producing the linker mutation leaves two additional GA residues at the N-terminal side of the protein, it was important to check whether this has any effect on either oligomerization or DNA binding. The results for the effective hydrodynamic radii of oligomers of GA H-NS as a function of temperature are in Figure 2.5. Scattering intensities were found to be of the same order of magnitude as for *wt* H-NS (data not shown) and the effective hydrodynamic radii of oligomers of GA H-NS were also found to be of the same order of magnitude as those for *wt* H-NS. Surprisingly, the temperature dependence of the effective hydrodynamic size of the oligomers that was observed at high concentrations of *wt* H-NS is completely absent for GA H-NS (Fig. 2.5).

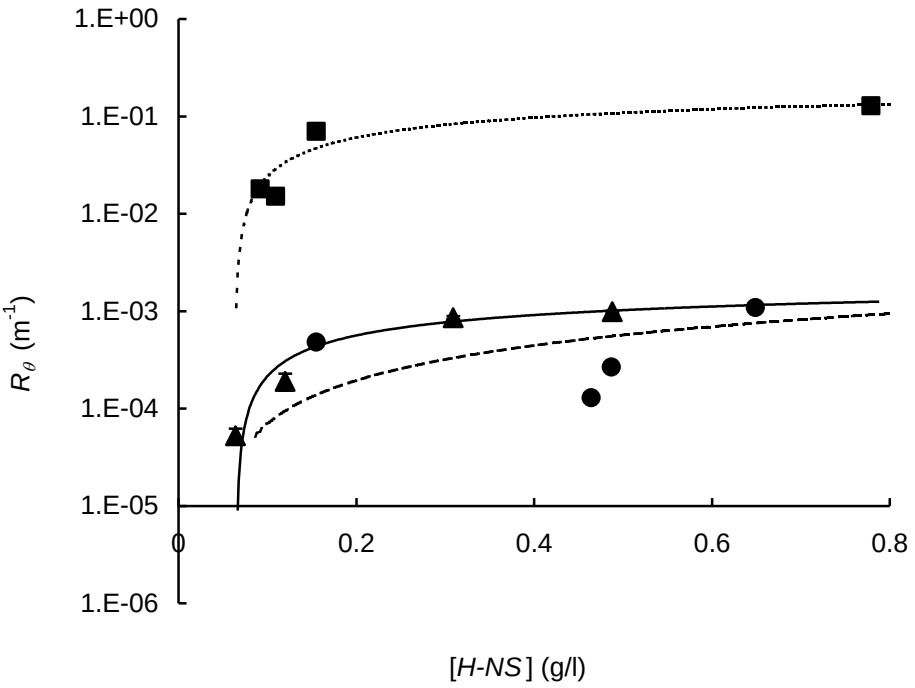

Figure 2.6: Concentration dependence of light scattering intensity of solutions of wt H-NS (triangles, straight line), GA H-NS (circles, dashed line) and GA H-NS D68V-D71V (squares, dotted line) at 20°C. Lines are a guide to the eye.

Oligomerization of the linker mutant GA H-NS D68V-D71V without DNA template is very different from that of *wt* H-NS and GA H-NS. As shown in Figure 2.6, scattering intensities for GA H-NS D68V-D71V are orders of magnitude higher than those for *wt* H-NS and GA H-NS. This indicates a much larger molar mass of the corresponding oligomers. Effective hydrodynamic radii of the GA H-NS D68V-D71V oligomers versus temperature are shown in Figure 2.7, for two protein concentrations. Radii of oligomers of the linker mutant are only weakly dependent on concentration, and are nearly an order of magnitude larger than those

observed for *wt* and GA H-NS. The temperature dependence of the radii is much stronger: $R_{H,eff}$ decreases from around 35 nm at 20°C, to about 20 nm at 40°C.

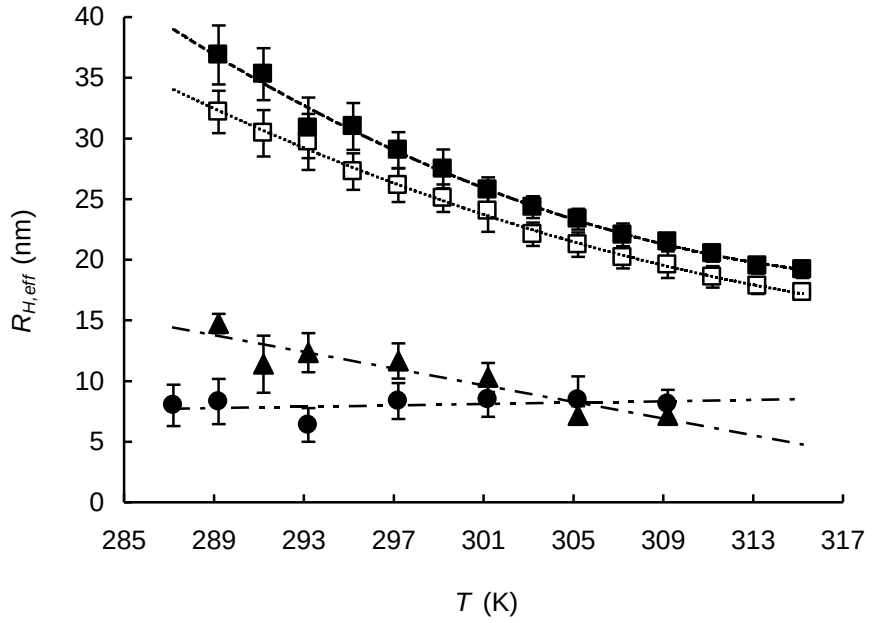

Figure 2.7: The temperature dependence of $R_{H,eff}$ is compared for oligomers of *wt* H-NS (triangles, 0.31 g/L), GA H-NS (circles, 0.49 g/L) and GA H-NS D68V-D71V (open squares, 0.16 g/L and filled squares, 0.78 g/L). Lines are guides to the eye.

Binding of GA H-NS and GA H-NS D68V-D71V to hns promoter DNA

The DNA binding properties of GA H-NS and GA H-NS D68V-D71V were studied for *hns* promoter DNA. Expression of H-NS is autoregulated and the binding of *wt* H-NS to the *hns* promoter is well characterized [13]. Figure 2.8 shows the shifts in electrophoretic mobility of *hns* promoter DNA caused by binding of GA H-NS and GA H-NS D68V-D71V, at 25°C and 37°C. Results for GA H-NS are nearly indistinguishable from published results for *wt* H-NS. Retardation due to binding of GA H-NS D68V-D71V is distinctly different: the linker mutant shows a significantly weaker binding affinity for *hns* promoter DNA, but with larger temperature dependence. DNA footprinting results for GA H-NS and GA H-NS D68V-D71V on *hns* promoter DNA are shown in Figure 2.9, both at 25°C and at 37°C. The pattern of protected sites for GA H-NS at 25°C is similar to that previously described for *wt* H-NS [13]. In fact GA H-NS protects at least three sites localized upstream the *hns* promoter region, and displays a higher binding affinity for two of these sites compared to those located in the -35 and -10 region. For GA H-NS D68V-D71V mutant, higher concentrations of protein are needed to achieve the highest level of protection; however, under these conditions the

protected sites are much more extended than those obtained with GA H-NS, covering more than half of the *hns* promoter DNA sequence, and the DNAse hypersensitivity sites are no longer exposed. This evidence suggests that also the linker mutant binds *hns* gene

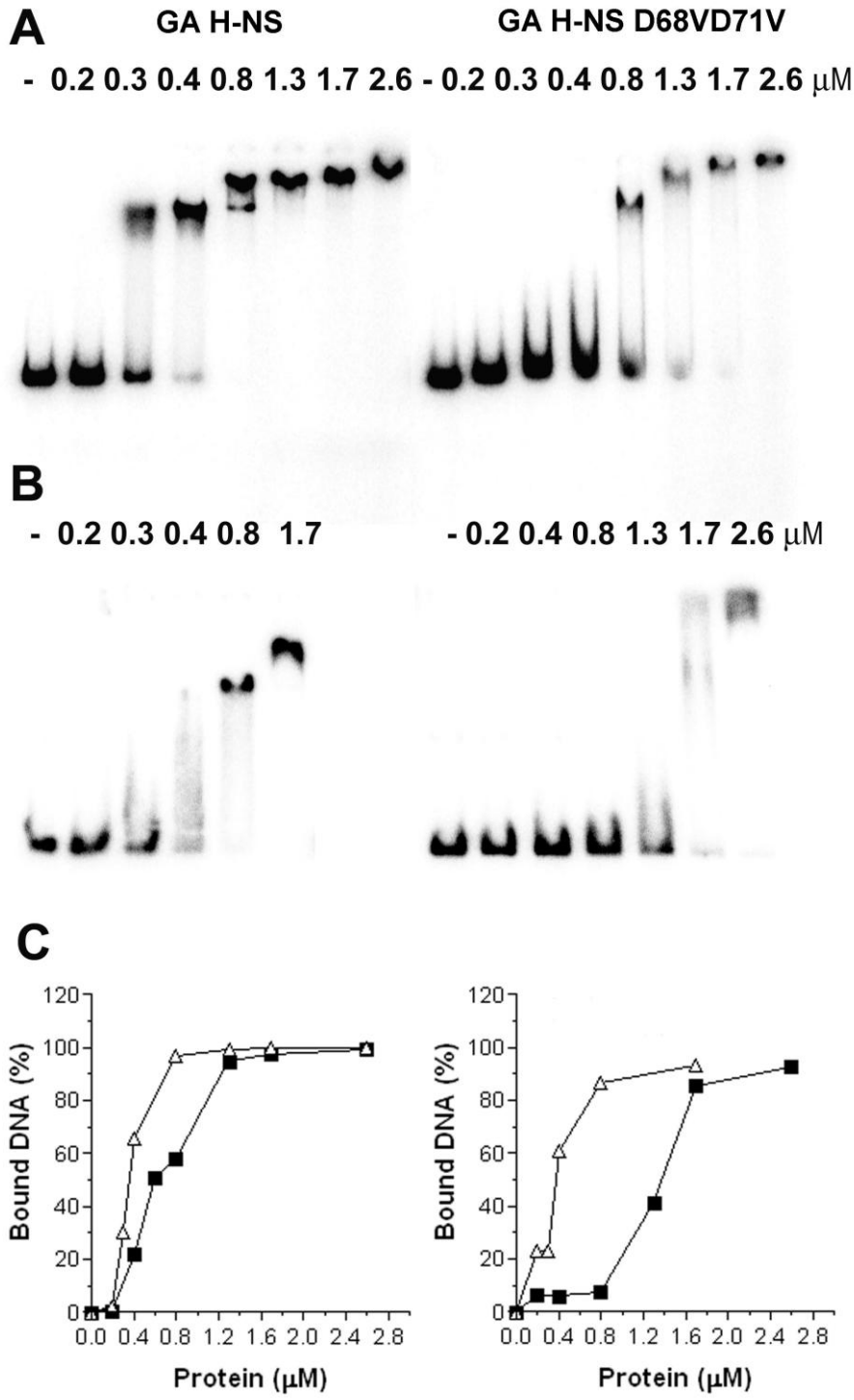

Figure 2.8: Electrophoretic mobility shift assay for GA HNS (left blots) and GA H-NS D68V-D71V (right blots) binding to *hns* promoter. a) EMSA at 25°C. b) EMSA at 37°C. c) Bound DNA (%) against protein concentration at 25°C (left) and 37°C (right) for GA HNS (triangles) and GA H-NS D68V-D71V (squares).

cooperatively because the protection is observed only when a critical concentration of protein (0.64 μM) is provided. At 37°C we observe a very weak protection, only at high concentrations of GA H-NS, in the region that extends from -60 to -200, while the -35 and -10

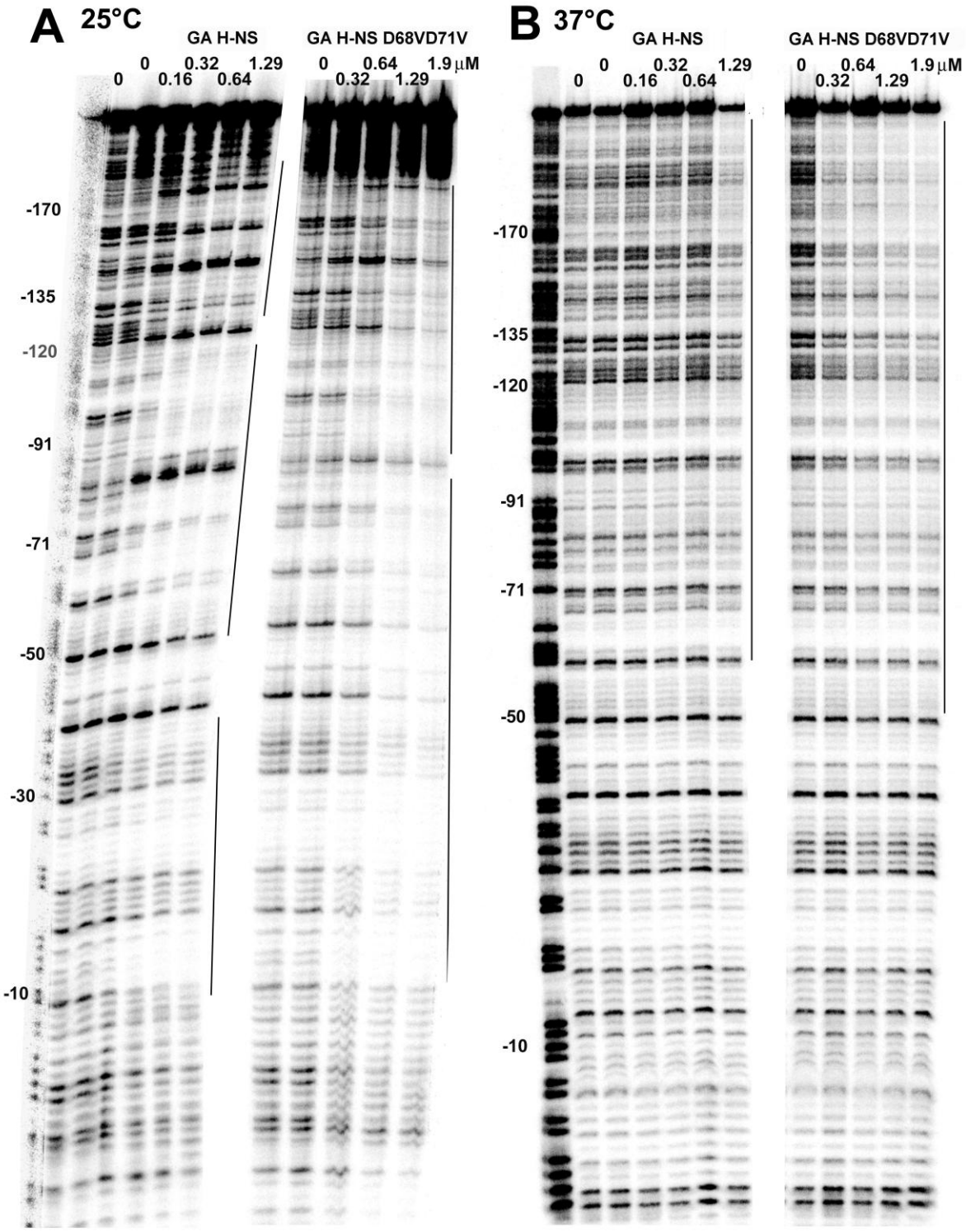

Figure 2.9: DNA footprint assay for GA H-NS (left side of blots) and GA H-NS D68V-D71V (right side of blots) protecting the *hns* promoter from degradation. a) Footprinting at 25°C. b) Footprinting at 37°C.

DNA sequences are no longer protected. A similar result (i.e. absence of protection in the -35 and -10 region) is obtained with the mutant GA H-NS D68V-D71V that gives rise, at 37°C, to a weak and widespread protection starting at the concentration of 0.32 µM. To verify that the observed DNA binding reflects a correct functional activity, an *in vitro* transcription assay was carried out with both proteins. The inhibition of the activity of RNA polymerase at 30°C is shown in Fig. 2.10, where the mutant GA H-NS D68V-D71V displays a stronger transcriptional repression, probably due to the extensive interaction with the DNA promoter as observed in the footprinting experiment.

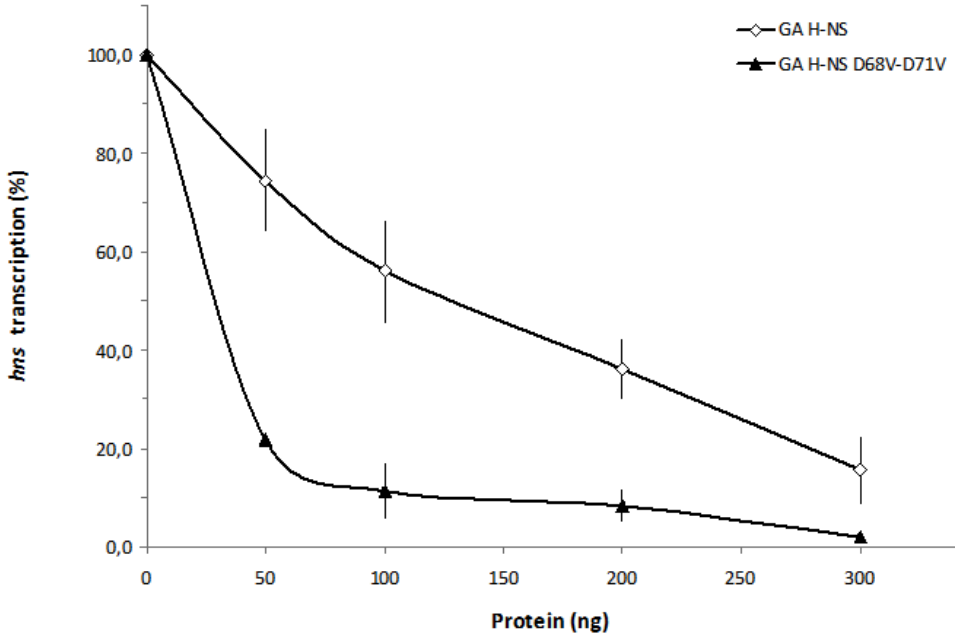

Figure 2.10: *In vitro* transcription carried out at 30°C on *hns* promoter

2.4 Discussion

The addition of two small inert residues (GA) on the N-terminus of H-NS leads to a measurable change in the temperature-dependence of H-NS oligomerization in the absence of DNA. At the same time, DNA binding properties (at least for binding to the *hns* promoter) are essentially unaffected. Previous work has already shown that higher order oligomerization involves the first few residues of the N-terminal region [8], so it should not be surprising that changes to the N-terminal region affect self-assembly. These small, N-terminal changes in protein-protein interactions have a larger effect on H-NS oligomerization in solution than its DNA-binding properties. This discovery highlights that one should be extremely careful in relating H-NS oligomerization in the absence of DNA to its DNA binding properties.

H-NS is thought to be a crucial global regulator of thermosensitive genes, and it has been suggested that the H-NS protein itself is the thermosensor. Specifically, Ono *et al*. [6] have suggested that thermosensing could occur via a switch of the structure of the H-NS dimer from a parallel orientation at low temperature, to an antiparallel orientation at high temperature. Such a drastic change of quaternary structure may be expected to give rise to some rather abrupt changes in the oligomerization behaviour as a function of temperature. Instead, only for some concentrations, we find only a gradual temperature dependence, which is abolished by the addition of GA at the N-terminus of the protein. Therefore we conclude that our dynamic light scattering studies on the self-assembly of GA-H-NS and *wt* H-NS offer no support for the hypothesis that the thermosensor is the H-NS molecule itself under the solution conditions that we have studied.

A further comparison between GA-H-NS and the GA D68V-D71V H-NS linker mutant points in the same direction. Binding of GA H-NS (and *wt* H-NS) to the *hns* promoter sequence is only weakly temperature dependent, especially if it is compared to the very strong temperature dependence when binding to the promoters of certain virulence genes such as *virF* [28]. When introducing the hydrophobic modifications to the linker sequence, H-NS self-assembly in solution is found to be enhanced very strongly, and also becomes strongly temperature dependent. This probably causes the binding of GA D68V-D71V H-NS to the *hns* promoter to also become strongly temperature-dependent. In this case, oligomerization does not compete with binding, but reinforces binding to DNA.

Other studies have also compared oligomerization and DNA binding properties of wild type H-NS with those of H-NS mutants. These studies showed that if H-NS is unable to dimerize [22] or unable to assemble in higher order oligomers [26], its biological function as a transcriptional repressor is compromised. For GA D68V-D71V H-NS, instead of a lack of dimerization or higher-order oligomerization, we find enhanced higher-order oligomerization. The consequences of this enhancement for the proteins' DNA-binding properties indicate to what extent H-NS oligomerization influences the H-NS DNA binding properties.

We tentatively conclude that oligomerizing protein-protein interactions should be rather strong to affect the DNA binding properties of H-NS: modifications that change the self-assembly behaviour in solution mildly (the addition of GA at the N-terminus) have no observable consequences for DNA binding, but modifications that lead to large changes in the protein-protein interactions (the D68V-D71V mutation) and completely different self-assembly in solution, do have a moderate influence on DNA binding.

DNA footprinting and *in-vitro* transcription results confirm the general idea that H-NS cooperative binding is related to H-NS protein-protein interactions: the D68V-D71V mutant, with its increased self-association, leads to significantly larger stretches of protected sites at high protein concentrations. This effect can only be seen if changes to the H-NS self-interactions are made which dramatically affect the proteins' oligomerization in the absence of DNA.

References

1. M. Lammi, M. Paci, C.L. Pon, M.A. Losso, A. Miano, R.T. Pawlik, G. Gianfranceschi, and C.O. Gualerzi, In: U. Hübscher and S. Spadari (Eds) *Proteins Involved in DNA Replication*, Plenum, New York, 1984, pp. 467–477.

2. A. Spassky, S. Rimsky, H. Garreau, and H. Buc. Hla, an E. coli DNA-binding protein which accumulates in stationary phase, strongly compacts DNA in vitro. *Nucl. Acids Res.*, 1984, **12,** 5321-5340.

3. M. Durrenberger, A. La Teana, G. Citro, F. Venanzi, C.O. Gualerzi, and C.L. Pon. Escherichia coli DNA-binding protein H-NS is localized in the nucleoid. *Res. in Microbiol.*, 1991, **142**, 373-380.

4. R. Spurio, M. Dürrenberger, A. La Teana, C.L. Pon, and C.O. Gualerzi. Lethal overproduction of the Escherichia coli nucleoid protein H-NS: ultramicroscopic and molecular autopsy. *Mol. Gen. Genet.*, 1992, **231**, 201-211.

5. C. J. Dorman, H-NS: a universal regulator for a dynamic genome. *Nature Reviews Microbiology* 2004, **2**,391-400.

6. S. Ono, M.D. Goldberg, T. Olsson, D. Esposito, J.C.D. Hinton, and J. E. Ladbury. H-NS is a part of a thermally controlled mechanism for bacterial gene regulation. *Biochem. J.* 2005, **391**, 203-213.

7. H. Shindo, T. Iwaki, R. Ieda, H. Kurumizaka, C. Ueguchi, T. Mizuno, S. Morikawa, H. Nakamura, and H. Kuboniwa, Solution structure of the DNA binding domain of a nucleoid-associated protein, H-NS, from Escherichia coli. *FEBS letters* 1995, **360,** 125-131

8. D. Esposito, A. Petrovic,R. Harris, S. Ono, J.F. Eccleston, A. Mbabaali, I. Haq, C. F. Higgins, J.C.D. Hinton, P.C. Driscoll, and J. E. Ladbury. H-NS oligomerization domain structure reveals the mechanism for higher order self-association of the intact protein. *J. Mol. Biol. 2002*, **324**, 841-850

9. V. Bloch, Y. Yang, E. Margeat, A. Chavanieu, M.T. Augé, B. Robert, S. Arold, S. Rimsky, and M. Kochoyan, The H-NS dimerization domain defines a new fold contributing to DNA recognition. *Nat. Struct. Biol.* 2003, **10**, 212-218.

10. S. T. Arold, P.G. Leonard, G. N. Parkinson, and J. E. Ladbury. H-NS forms a superhelical protein scaffold for DNA condensation. *Proc. Natl. Acad. Sci. USA* 2010, **107**, 15728–15732.

11. B. Lang, N. Blot, E. Bouffartigues, M. Buckle, M. Geertz, C.O. Gualerzi, R. Mavathur, G. Muskhelishvili, C.L. Pon, S. Rimsky, S. Stella, M. Madan Babu, and A. Travers. High-affinity DNA binding sites for H-NS provide a molecular basis for selective silencing within proteobacterial genomes. *Nucl. Acids Res.*, 2007, **35**, 6330-6337.

12. S M. Sette, R. Spurio, E. Trotta, C. Brandizi, A. Brandi, C.L. Pon, G. Barbato, R. Boelens, and C. O. Gualerzi. Sequence-specific Recognition of DNA by the C-terminal Domain of Nucleoid-associated Protein H-NS. *J. Biol. Chem.*, 2009, **284**, 30453-30462.

13. M. Falconi, N. P. Higgins, R. Spurio, C. L. Pon and C.O. Gualerzi. Expression of the gene encoding the major bacterial nucleoid protein H-NS is subject to transcriptional autorepression *Mol. Microbiol.* 1993, 10, 273-282.

14. R. T. Dame, C. Wyman, N. Goosen. Structural basis for preferential binding of H-NS to curved DNA. *Biochimie* 2001, **83**, 231−234.

15. A.E.Tupper, T.A.Owen-Hughes,D.W.Ussery, D. S.Santos,D. J.P.Ferguson, J. M.Sidebotham, J.C.D.Hinton and C.F.Higgins. The chromatin-associated protein H-NS alters DNA topology in vitro, *EMBO J.* 1994, **13**, 258-268.

16. R.Schneider, R. Lurz, G. Luder, C. Tolksdorf, A.Travers, G. Muskhelishvili. An architectural role of the Escherichia coli chromatin protein FIS in organising DNA. *Nucl. Ac. Res.* 2001, **29**, 5107-5114.

17. J. L. Mellies, G. Benison, W. McNitt, D.Mavor, C. Boniface and F. J. Larabee. Ler of pathogenic Escherichia coli forms toroidal protein–DNA complexes. *Microbiology* 2011, **157**, 1123–1133

18. R. T. Dame, C. Wyman, and N. Goosen, N. H-NS mediated compaction of DNA visualised by atomic force microscopy. Nucl. Ac. Res. 2000, **28**, 3504-3510.

19. R.T. Dame and N. Goosen. HU: promoting or counteracting DNA compaction? *FEBS Lett.* 2000, **529,** 151-156.

20. S. Maurer, J. Fritz and G.Muskhelishvili, A Systematic In Vitro Study of nucleoprotein Complexes Formed by Bacterial Nucleoid-Associated Proteins Revealing Novel Types of DNA Organization. *J. Mol. Biol.* 2009, **387**, 1261–1276.

21. Y. Liu, H. Chen, L.J. Kenney, and J.Yan. A divalent switch drives H-NS/DNA-binding conformations between stiffening and bridging modes. Gen. Dev. 2000, **24**, 339–344.

22. R.Spurio, M.Falconi, A.Brandi, C.L.Pon and C. O.Gualerzi, The oligomeric structure of nucleoid protein H-NS is necessary for recognition of intrinsically curved DNA and for DNA bending. EMBO J. 1997,**16,** 1795–1805.

23. C.P. Smyth, T. Lundbäck, D. Renzoni, G. Siligardi, R. Beavil, M. Layton, J.M. Sidebotham, J.C.D. Hinton,P.C. Driscoll,C.F. Higgins, J.E. Ladbury. Oligomerization of the chromatin-structuring protein H-NS. *Mol. Microbiol.* 2000, **36**, 962-972.

24. D. Esposito, A. Petrovic, R. Harris, S. Ono, J.F. Eccleston, A. Mbabaali, I. Haq, C.F. Higgins, J.C.D. Hinton, P.C. Driscoll, J.E. Ladbury. H-NS oligomerization domain structure reveals the mechanism for higher order self-association of the intact protein. *J. Mol. Biol.* 2002, **324**,841-850.

25. S. Ceschini, G.Lupidi, M. Coletta, C. L. Pon, E. Fioretti, and M. Angeletti. Multimeric Self-assembly Equilibria Involving the Histone-like Protein H-NS. A Thermodynamic study. J. Biol. Chem. 2000, **275**,. 729–734.

26. C. Badaut, R.Williams, V. Arluison, E. Bouffartigues, B. Robert, H.Buc, and S. Rimsky. The Degree of Oligomerization of the H-NS Nucleoid Structuring Protein Is Related to Specific Binding to DNA. J. Biol. Chem. 2002, **277**, 41657–41666.

27. S. Stella, R.Spurio, M. Falconi, C.L.Pon, and C.O. Gualerzi, Nature and mechanism of the in vivo oligomerization of nucleoid protein H-NS. *EMBO J.* 2005, **24**, 2896-2905.

28. G. Prosseda, M.Falconi, M. Giangrossi, C. O. Gualerzi, G. Micheli, and B. Colonna. The virF promoter in Shigella: more than just a curved DNA stretch. *Mol. Microbiol.* 2004, 51, 523–537.

29. R.T. Dame, M. C. Noom and G. J. L. Wuite. Bacterial chromatin organization by H-NS protein unravelled using dual DNA manipulation. *Nature*, 2006, **444**, 387-390.

30. R. de Vries. Influence of mobile DNA-protein-DNA bridges on DNA configurations: Coarse-grained Monte-Carlo simulations J. Chem. Phys. 2011, **135**, 125104.

31. R. Williams, S. Rimsky, and H. Buc. Probing the Structure, Function, and Interactions of the Escherichia coli H-NS and StpA Proteins by Using Dominant Negative Derivatives J. Bacteriol. **1996**, 178, 4335–4343.

32. C. Ueguchi, T. Suzuki, T. Yoshida, K. Tanaka and T.Mizuno. Systematic Mutational Analysis Revealing the Functional Domain Organization of Escherichia coli Nucleoid Protein H-NS. *J. Mol. Biol.* **1996**, 263, 149–162.

33. J. Kyte, and R. F. Doolittle, A simple method for displaying the hydropathic character of a protein. J. Mol. Biol. 1982, **157**, 105-132

34. Giangrossi M, Prosseda G, Tran CN, Brandi A, Colonna B, Falconi M. (2010) A novel antisense RNA regulates at transcriptional level the virulence gene *icsA* of *Shigella flexneri. Nucleic Acids Res*. 38: 3362-75.

35. Falconi M, Higgins NP, Spurio R, Pon CL, Gualerzi CO. (1993) Expression of the gene encoding the major bacterial nucleoid protein H-NS is subject to transcriptional auto-repression. *Mol Microbiol.* 10: 273-82.

Chapter 3

Synergetic roles of macromolecular crowding and H-NS in condensing DNA*

*To be submitted

Abstract

Using Dynamic Light Scattering we have investigated the influence of the bacterial nucleoid protein H-NS on coil sizes in solution, for both supercoiled and linear pUC18 DNA. Whereas an increase in the intensity of scattered light upon the addition of H-NS unambiguously indicated that the protein was bound to the DNA, the change in the effective hydrodynamic radius of the coils turned out to be minimal. At the highest concentrations of H-NS, the dynamic scattering data for linear DNA indicated the presence of two populations of complexes; the larger complexes presumably consisting of a number of plasmid DNA molecules linked together by H-NS. It was also found that H-NS has a synergetic effect on polymer-induced condensation of DNA. Facile sedimentation of H-NS/DNA complexes is taken as an indication of condensation of H-NS/DNA complexes in solutions of polyethylene glycol. In the absence of H-NS the critical concentration of polyethylene glycol needed to condense DNA is approximately 15%, whereas the critical concentration is remarkably lower, about 3.5%, at near saturation concentrations of H-NS.

3.1 Introduction

While the role of nucleoid proteins in the global regulation of bacterial gene expression is now firmly established,[1] their contribution to DNA condensation and the formation of the bacterial nucleoid is much less clear. A case in point is H-NS (Histone-like Nucleoid Structuring protein), a small 16 kDa protein[0,3] that localizes to the bacterial nucleoid[4]. Overproduction of H-NS decreases cell viability and leads to compact spherical nucleoids, as observed by electron microscopy[5]. H-NS binding to DNA is relatively non-specific, which is expected for an architectural protein, although H-NS binds with mildly increased affinity to a recently identified consensus sequence[6,7]. Whereas the role of H-NS as a global transcriptional regulator has been well documented[8,9], its influence on the large-scale solution conformations of DNA, or nucleoid architecture, is poorly understood.

Complexes of H-NS with DNA have recently been studied by single molecule techniques such as optical[10] and magnetic[11,12] tweezers. H-NS forms stable dimers in solution, and the two DNA-binding domains of the H-NS dimer can either bind to the same DNA duplex, or form a DNA-protein-DNA bridge. Single molecule studies and AFM imaging on H-NS/DNA complexes have provided evidence for both coating of single DNA duplexes[11,12] and bridging between strands[10,12,13], depending on solution conditions. The concentration of divalent cations appears to play a significant role.[12]

In the single molecule and AFM studies, the H-NS/DNA complexes may be perturbed significantly, either by the forces applied, or by adsorption and subsequent drying. As a consequence, one cannot reliably deduce the impact of H-NS binding on the size of the complexes. Here, we use the non-invasive technique of dynamic light scattering to determine the coil sizes of both linear and supercoiled plasmid DNA, in the absence and presence of bound H-NS, in bulk solutions.

Previously, we have shown[14] that binding of a different, archaeal nucleoid protein, the small and basic Sso7d, has only a minor influence on DNA dimensions in solution (Chapter 5). However, this protein dramatically reduces the critical concentration of PEG (polyethylene glycol, an inert flexible polymer) needed to condense linear DNA even at protein concentrations far below full coverage. DNA condensation by nonbinding polymers (or ψ-condensation; ψ stands for polymer- and salt-induced) is thought to affect the phenomenon of genomic DNA compaction under the influence of "macromolecular crowding" in bacterial cells.[15,16]: namely, the strong excluded volume interactions between DNA and other

nonbinding large molecules, mainly consisting of globular proteins and RNA. Because the bacterial DNA is supercoiled, the nucleoid is not condensed though it is subject to compaction. In addition to studying the direct effect of H-NS on the DNA dimensions, we will also investigate synergetic effects, particularly the possible cooperation between the H-NS binding and polymer depletion in reducing DNA volume even further.

The pUC18 DNA that we use (either supercoiled or linearized) is 2686 bp long, which corresponds to a contour length of $L \approx 900$ nm. Assuming a traditional value of 50 nm for the DNA persistence length l_p, the molecule measures about 20 persistence lengths, or about $N = 10$ Kuhn segments (each of Kuhn length $l_K = 2\, l_p = 100$ nm). Hence, the estimated gyration radius of the linear molecule is

$$R_g = \frac{1}{\sqrt{6}} N^{1/2} l_K \approx 130nm \qquad (3.1)$$

In this study we start with the case of isolated DNA coils, as the interpretation of their dynamic light scattering is reasonably straightforward. This requires that the DNA concentration is much lower than the overlap concentration:

$$C^* \approx M / N_A R_g^3 \approx 1.4mg/ml \qquad (3.2)$$

where N_A is Avogadro's number and $M = 1.8$ MDa is the pUC18 molar mass. Our light scattering experiments were carried out at a concentration of 50 µg/ml, sufficient to get an acceptable light scattering signal for bare DNA, yet well below the estimated overlap concentration.

Association constants of nucleoid proteins for non-specific DNA are lower than those of sequence-dependent DNA binding proteins. For H-NS, the association constant for non-specific DNA is estimated[17] to be $K_a \approx 10^4$ M^{-1} calculated per DNA basepair. At low DNA coverage, the ratio of bound to free H-NS approximately equals $K_a \cdot [\mathrm{DNA(bp)}]$, or about 0.75 at a DNA concentration of 50 µg/ml. Hence, for the conditions we impose, most of the H-NS molecules will be bound rather than free, even at low coverage, despite the low DNA concentration. The estimated size of the binding site is about 12bp per H-NS dimer.[17] By varying the concentration from 0 to 1 H-NS per 3 bp of DNA, we study the entire range from low coverage to complete saturation.

Implications of our results for the role of H-NS and other nucleoid proteins in the formation of a nucleoid structures in bacteria and archaea will be discussed at the end of the paper.

3.2 Experimental and methods

Isolation and purification of DNA
E. coli strain LMC899 containing pUC18 plasmid was grown overnight in 100 ml TY medium supplemented with 50 µg/ml ampicillin (Sigma Aldrich). Plasmid DNA was isolated using High Pure Plasmid Isolation Kit (Roche Applied Science) according to the instructions of the manufacturer. Linearized pUC18 DNA was obtained by digestion with *Xba*I (Fermentas) for 2 hours at 37ºC. Following digestion, DNA was ethanol precipitated and resuspended in 10 mM NaH_2PO_4/Na_2HPO_4 100 mM NaCl (for DLS) or 150 mM NaCl (for sedimentation assays). DNA concentrations were determined spectrophotometrically.

Isolation and purification of H-NS
Overexpression of H-NS in *E. coli* and purification were essentially as described previously.[7] After the last purification step, H-NS was dialysed against a buffer consisting of 20 mM Tris-HCl, 0.1 mM EDTA, 10% Glycerol, 200 mM NH_4Cl, 0.5 mM DTT, pH7.7, and aliquots were stored frozen at -80C.

Buffer exchange and concentration protocol
Directly before use an appropriate amount of H-NS was taken from the -80°C freezer. Samples were thawed on ice, and the storage buffer was exchanged for a 10 mM NaH_2PO_4/Na_2HPO_4 buffer with 100 mM NaCl (light scattering experiments) or 150 mM NaCl (sedimentation assay) using 0.5ml Zeba Desalt Spin columns (Pierce). H-NS was concentrated using 0.5 ml Microcon YM-3 3 kDa NMWL centrifugal filter devices. H-NS concentrations were measured by UV absorption, using an absorption coefficient[3] of 0.86 L g^{-1} cm^{-1} at 280 nm.

Angle-dependent dynamic light scattering on supercoiled pUC18 plasmid DNA
Dynamic light scattering measurements were performed on an ALV light scattering instrument equipped with an ALV-5000/60X0 external digital correlator and a 300 mW solid state laser (Cobolt Samba-300 DPSS laser) operating at a wavelength of 532 nm. A refractive index matching bath of filtered cis-decalin surrounded the cylindrical quartz scattering cell, filled with approximately1 ml of sample. Temperature was controlled at 20 ± 0.1°C using a Haake F8-C35 thermostat. The scattering angle was varied between 30° and 90°, in steps of 10°. For each scattering angle, 5-10 measurements of 60-250s were performed. These were averaged to give a single intensity autocorrelation function $g_2(t)$. Distributions of relaxation rates Γ were extracted from the intensity autocorrelation functions $g_2(t)$ using a CONTIN analysis.[18] For all angles between 30° and 90° there was a clear dominant peak at some relaxation rate $\Gamma_{peak}(q)$ Effective diffusion constants were calculated from $D_{eff}(q) = q^2\Gamma_{peak}(q)$.

Fixed angle light scattering on H-NS / DNA complexes
All measurements were done using Hellma precision cells type 105.251.005-QS. Cells were cleaned with 1 M HCL, rinsed with MilliQ H_2O and 96% ethanol, followed by drying with N_2 and pre-rinsing with the appropriate buffer. Samples were centrifuged at 10,000g for 20 minutes to reduce scattering by dust, and the cells were filled with typically 20µl of sample. Light scattering experiments on DNA H-NS complexes were done using a Malvern Zetasizer Nano ZEN 1600 with a 4mW He-Ne laser operating at wavelength of λ = 633nm, at a fixed scattering angle of θ=12.8°. This gives a fixed scattering wavevector of $q = 4\pi n_0 \sin(\theta/2)/\lambda = 3.0 \cdot 10^6$ m^{-1}, where n_0=1.333 is the solvent refractive index. Absolute scattering intensities R_θ (Rayleigh ratio) are calculated from

$$R_\theta = \frac{I_s - I_0}{I_t}\frac{n_0^2}{n_t^2}R_t \qquad (3.3)$$

where I_s, I_0 and I_t are, respectively, the scattering intensities of the sample, buffer, and toluene reference, and R_t = 1.35×10^{-2} m^{-1} is the absolute scattering intensity of the toluene reference. For each sample, 50 measurements of 2 minutes were performed. A small number of these showed a scattering intensity that was much higher than the average, and these were discarded. The remaining measurements were averaged to give the final values for the scattering intensity, and the scattering intensity autocorrelation function $g_2(t)$. Distributions of relaxation rates Γ of the autocorrelation functions were determined using a CONTIN analysis.[18] From the peak positions Γ_{peak},

effective diffusion constants D_{eff} were calculated from $D_{eff} = q^2\Gamma_{peak}$. Effective hydrodynamic radii $R_{H,eff}$ were calculated from D_{eff} using the Stokes-Einstein relation.

Condensation assay

Poly(ethylene glycol), or PEG, with a molar mass of 20 kg/mol (Sigma Aldrich) was dissolved in 10 mM NaH_2PO_4/Na_2HPO_4 buffer with 150 mM NaCl. H-NS/DNA complexes were prepared in the same buffer, and equilibrated for at least 30 minutes. Next, 50 µl of H-NS/DNA complexes and 50 µl of PEG solution were mixed to give a final DNA concentration of 12 ng/µl. Samples mixed thoroughly, incubated for 1h at room temperature, and centrifuged at 10,000 *g* for 1 h at 20ºC. After centrifugation, 5 µl of the supernatant was electrophoresed on a 1% agarose gel, using ethidium bromide to stain the DNA.

3.3 Results

First, we compare the results of dynamic light scattering of one solution at small volumes and fixed scattering angle (12.8°), with that obtained with the help of a traditional goniometer based set-up in which the scattering angle was varied continuously, namely, for a 50 µg/ml solution of bare supercoiled pUC18. We used the fixed angle scattering instrument because the amounts of available H-NS necessitated small sample volumes.

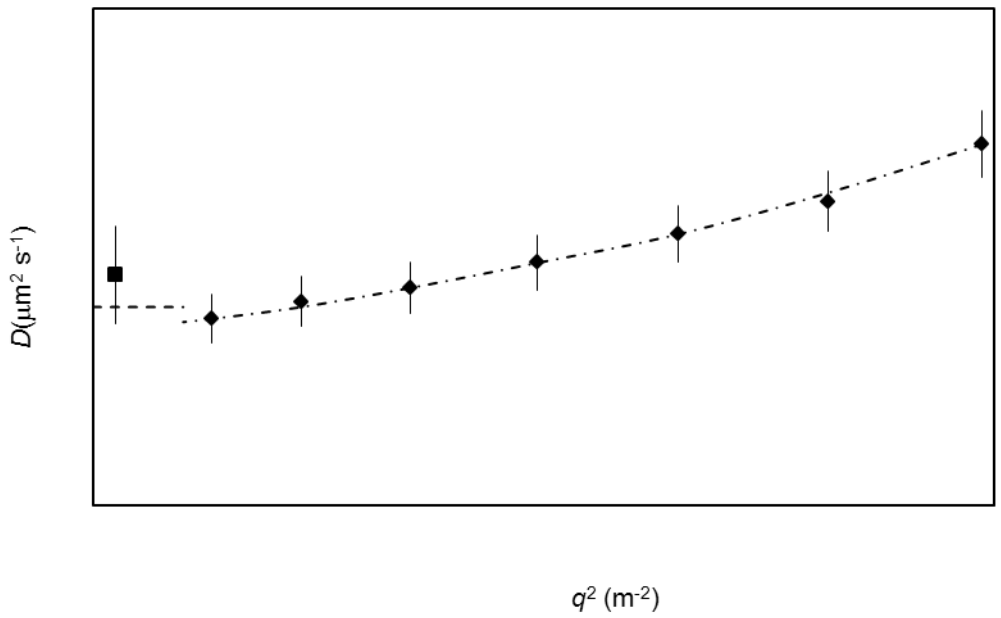

Figure 3.1: Effective diffusion constants D_{eff} (µm^2 s^{-1}) of 50 µg/ml supercoiled pUC18 as a function of the squared wavevector q^2 (m^{-2}), in the low wavevectors regime. The square symbol indicates the fixed angle instrument (scattering angle $\theta = 12.8°$). Diamonds indicate a traditional large cell set up with goniometer. The dashed line at $q \rightarrow 0$ is the value $D = 5.0$ µm^2 s^{-1} reported by Langowski *et al.*[19]

At the low scattering angles considered here, we found the decay of the time correlation functions to be nearly monoexponential. Effective diffusion constants $D_{eff}(q)$

depending on the magnitude q of the wavevector were obtained from the dominant peaks in a CONTIN analysis of the autocorrelation functions $g_2(t)$, and are shown in Figure 3.1. The diffusion constant at q=0 extrapolated from the angle-dependent measurements is equal to that determined by the fixed angle apparatus. Thus, we were able to get a convenient estimate of true diffusion constants with the latter instrument despite the small sample volumes used. Both measurements for the diffusion constant at q = 0 also agree with the value of D = 5 μm^2 s^{-1} for bare supercoiled pUC18 reported by Langowski *et al.*[19].

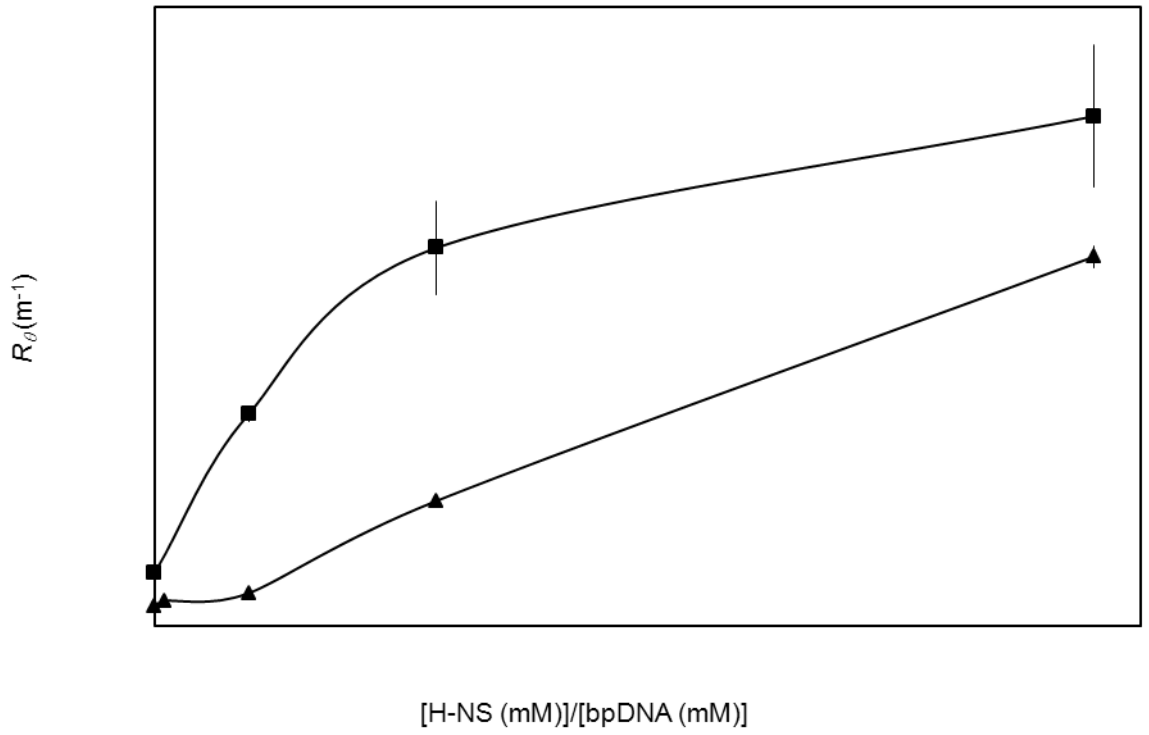

Figure 3.2: Intensities of scattered light (in terms of the Rayleigh ratio R_θ in m^{-1}) for supercoiled (triangles) and XbaI linearised (squares) pUC18 (50 μg/ml) with increasing amounts of H-NS.

Upon the addition of H-NS, the intensity of light scattered at 12.8° increases for both the supercoiled and the linearized plasmid DNA (Fig. 3.2). However, as shown in Fig. 3.3, the corresponding changes in the effective hydrodynamic radius $R_{H,eff}$ of the complexes are insignificant, remaining almost within the margin of error. At all H-NS concentrations, the effective hydrodynamic radius of the linearized plasmid is larger than that of the supercoiled plasmid. The observed increase in scattering is a factor of 7 for the linearized plasmid DNA, and 10 times for the supercoiled plasmid at the highest H-NS concentrations (see Fig. 3.2).

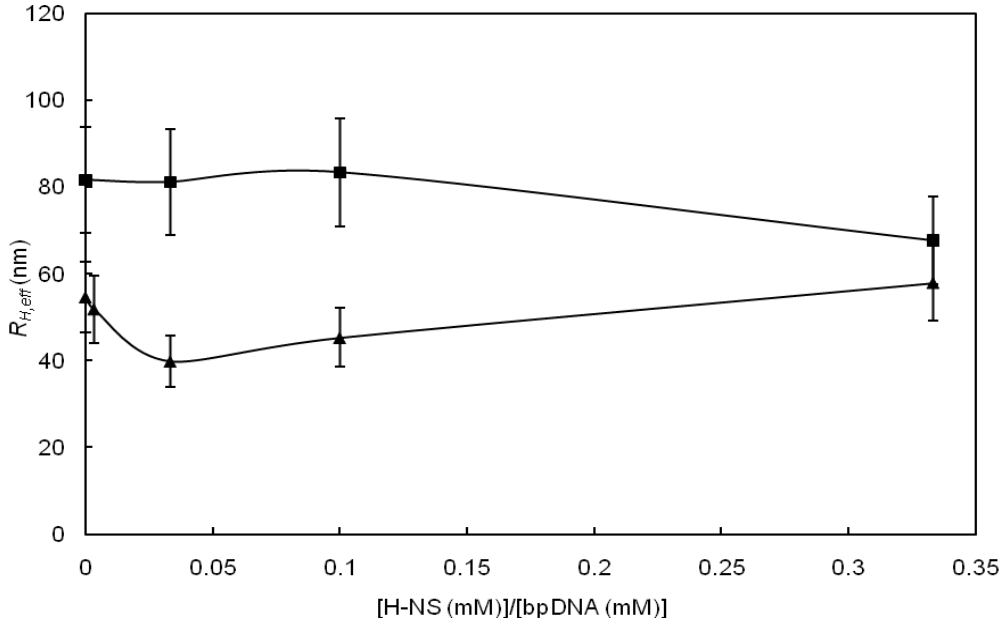

Figure 3.3: Effective hydrodynamic radii of supercoiled (triangles) and XbaI linearized (squares) pUC18 DNA (50 μg/ml) with increasing amounts of H-NS. Effective hydrodynamic radii are derived from the relaxation rates corresponding to the dominant peak in a CONTIN analysis of the dynamic light scattering autocorrelation functions. For linearized DNA at the highest concentration of H-NS, a second peak at a slower relaxation rate is found, which is not included in this figure.

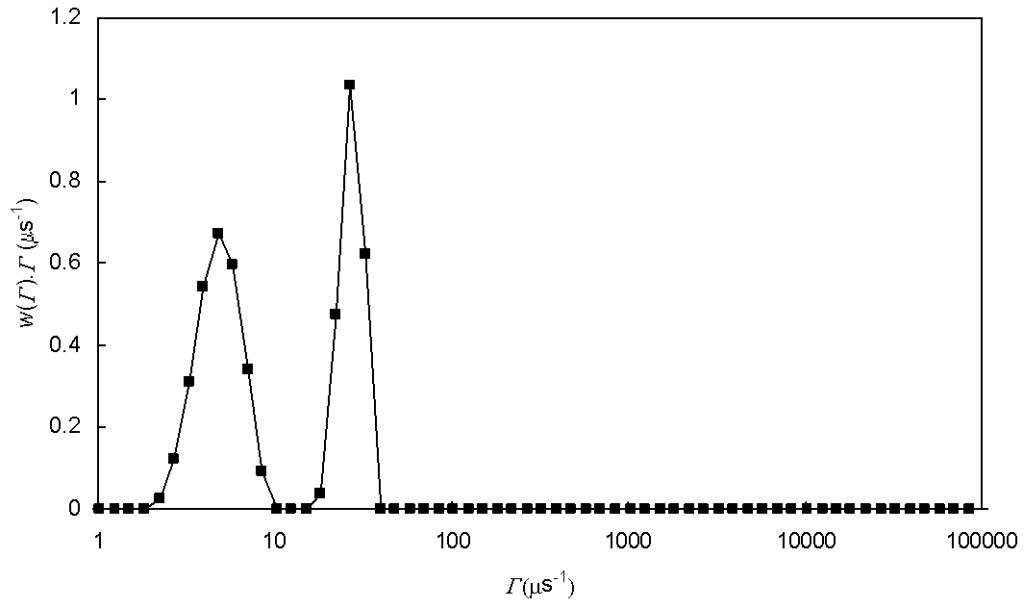

Figure 3.4: Distribution of relaxation rates from a CONTIN analysis of the correlation function for complexes of linearized pUC18 (50μg/mL) with H-NS in a molar ratio of 1 H-NS per 3 bp. The first peak at $\Gamma \approx 5\ \mu s^{-1}$ has a relative area of 0.44 and corresponds to an effective hydrodynamic radius of $R_{H,eff}$ = 384 nm. The second peak, at $\Gamma \approx 27\ \mu s^{-1}$ has a relative area of 0.37 and corresponds to an effective hydrodynamic radius of $R_{H,eff}$ = 68 nm. The size shown in Fig. 3 is the size corresponding to this second peak.

Effective hydrodynamic radii $R_{H,eff}$ in Fig. 3.3 were calculated from the dominant peak of a CONTIN fit of the autocorrelation data. In most cases we found the decay of the correlation curves was indeed nearly single exponential. A notable exception to this general scenario was the measurement at the ratio of 1 H-NS per 3 bp of linear pUC18. In this case, we show the full CONTIN fit (amplitude versus relaxation rate Γ) in Fig 3.4. One peak corresponds to an effective hydrodynamic radius of 68 nm, and a second peak to a much larger effective hydrodynamic radius of 384 nm.

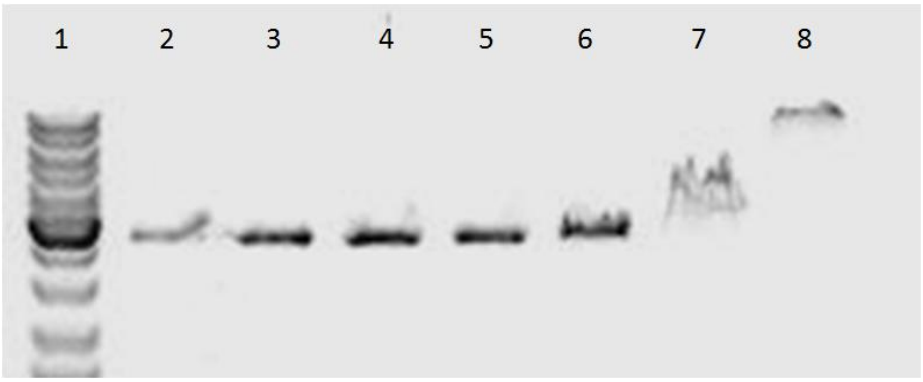

Figure 3.5: Agarose gel electrophoresis of complexes consisting of linearized pUC18 and H-NS. Lane 1: Mw ladder, lane 2: control = linear pUC18, lanes 3-8: linear pUC18 plus increasing concentrations of H-NS, [H-NS]/[DNA(bp)] = 0, 1/300, 1/100, 1/30, 1/10 and 1/3.

Having established that H-NS does not significantly compact DNA coils by itself under our the solution conditions, we next investigated the combined effect of nonbinding flexible polymers (PEG20K; polyethylene glycol with molar mass 20,000 g/mol) and H-NS on DNA condensation. First, an electrophoretic mobility shift assay was used to assess the binding of H-NS to DNA under the conditions of the sedimentation assay. As can be seen in Fig. 3.5, retardation starts to be significant at 1 H-NS per 10 bp DNA whereas at 1 H-NS per 3bp of DNA, retardation becomes very strong.

The sedimentation assay is based on the increased susceptibility of DNA condensates induced by flexible polymers and H-NS to sedimentation, so they can be spun down in a centrifuge. The DNA present in the supernatant is analysed by agarose gel electrophoresis. If sedimentable DNA condensates are formed, the corresponding DNA bands on the gel should vanish. Results for condensation in the absence of H-NS are shown in Figure 3.6. The DNA band starts to fade at 14% and has completely disappeared at 16% of PEG, such that we estimate a critical concentration of 15±2%, consistent with previously reported data.[20]

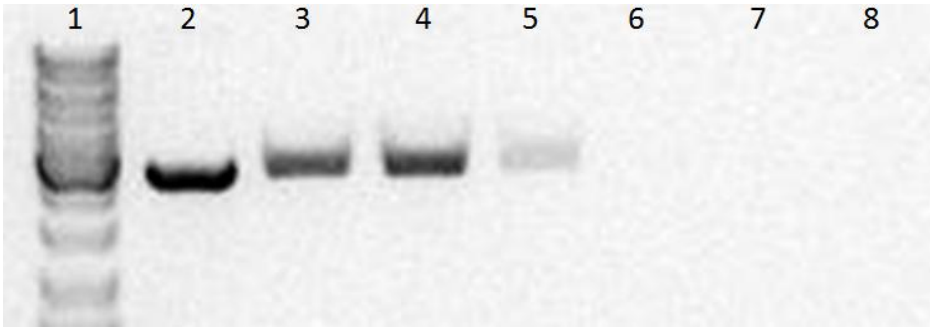

Figure 3.6: Agarose gel electrophoresis of the supernatant resulting from centrifugation of mixtures of linearized pUC18 with different concentrations of PEG20K at 0.15M NaCl. Lane 1: Mw ladder, lane 2: control = linear pUC18, lanes 3-8: linear pUC18 plus increasing concentrations (%w/w) of PEG20K: 10, 12, 14, 16, 18 and 20.

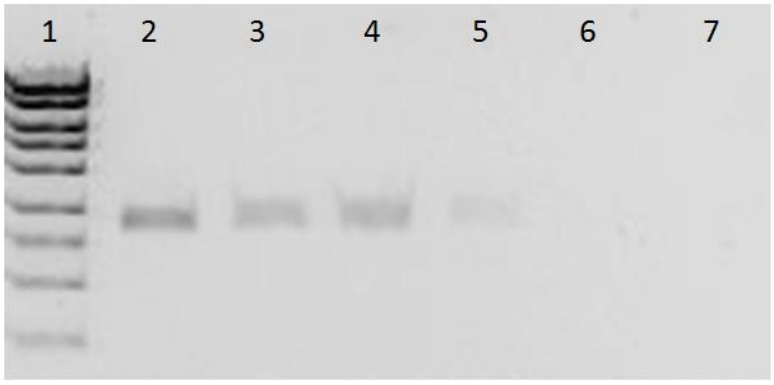

Figure 3.7: Agarose gel electrophoresis of the supernatant resulting from the centrifugation of complexes of linearized pUC18 with H-NS at a molar ratio of 1/30 bp, and various concentrations of PEG20K at 0.15 M NaCl. Lane 1: Mw ladder. Lanes 2-7: increasing concentrations of PEG 20K: 5, 6, 7, 8, 9 and 10 %w/w.

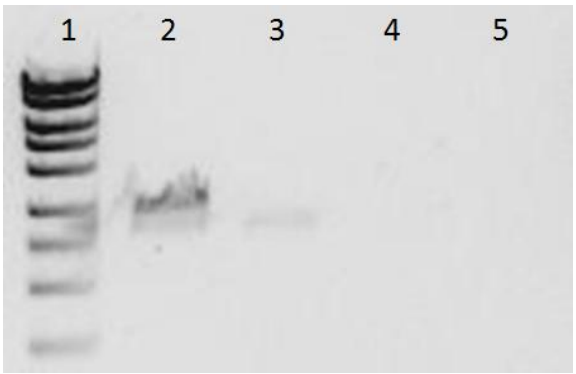

Figure 3.8: Agarose gel electrophoresis of the supernatant resulting from centrifugation of complexes of linearized pUC18 with H-NS at a molar ratio of 1:10 and various concentrations of PEG20K at 0.15M NaCl. Lane 1: Mw ladder. Lanes 2-5: increasing concentrations of PEG 20K: 2, 3, 4 and 5 %w/w.

Results for the polymer-induced condensation of H-NS/DNA complexes are shown in Figures 3.7 and 3.8 for [H-NS]/[DNA] molar ratios of 1 H-NS per 30bp and 1 H-NS per 10bp, respectively. At the lower concentration, the critical polymer concentration decreases to 8.5±1

% w/w (Figure 3.7). At the higher concentration of 1 H-NS per 10 bp, the transition occurs at 3.5±1 % (w/w) of polymer (Figure 3.8).

3.4 Discussion

First, we discuss the results for the increase in the static intensity on the addition of H-NS to the DNA solutions, as shown in Fig. 3.2. The observed increase in scattering is a substantial factor of 7 for the linearized DNA, and increases to 10 times for the supercoiled DNA at the highest H-NS concentrations. If we assume the simplification that the scattering contrast for DNA and H-NS are roughly equal, the scattering intensity should be proportional to the mass of the complexes when the scattering angle and the concentration are zero (the scattering contrast is given in terms of the refractive index increment, but this is hard to determine at present). However, we know that the mass of DNA fully saturated by H-NS is about 6 times that of bare DNA[17]. Our estimates may overestimate the actual value somewhat, but they cannot be significantly improved until the refractive index increment of H-NS is established.

Although the static scattering convincingly demonstrates that there is significant binding of H-NS to DNA, it comes as a surprise that the corresponding changes in the effective hydrodynamic radii $R_{H,eff}$ are minimal (see Fig. 3.3). If H-NS were to bind to DNA mainly in a bridging mode, one would have expected at least some degree of compaction, especially for linear chains. The fact that no compaction is observed strongly indicates that under the conditions of our experiments, bridging cannot be extensive. It is well to note that according to Liu *et al.*[12], H-NS only binds in a bridging mode above a certain concentration of divalent ions. Below this concentration, H-NS is thought merely to coat single DNA duplexes. Our measurements have been indeed been carried out in the absence of any divalent ions. On the other hand, the CONTIN analysis for linear DNA at the highest concentration of added H-NS (Fig. 4) suggests that complexes could be formed consisting of multiple DNA duplexes. This may imply a small degree of intermolecular bridging, but it is difficult to assess this in a quantitative fashion.

Conditions in bacterial cells are quite different from those in our *in-vitro* experiments. Hence we cannot conclude that H-NS does not directly cause DNA compaction *in-vivo*. Our results do suggest that H-NS may contribute to DNA condensation via a synergetic effect. High concentrations of nonbinding macromolecules such as RNA and globular proteins may

drive DNA compaction via depletion interactions[15,16], an effect that we here mimic using polymer. The dramatic effect of H-NS binding on DNA condensation by polymer depletion that we find here is in agreement with our previous conclusion[14] and the earlier work of Murphy and Zimmerman.[25] Protein binding leads to more efficient DNA condensation by polymers, and hence may also enhance crowding induced DNA condensation by cytosolic macromolecules such as nonbinding proteins and RNA.

As we have argued before[14] (Chapter 5 of this thesis), two effects of NAP binding are the most likely contributors to enhanced condensation: charge neutralization of the DNA by the typically basic nucleoid proteins, and an increased effective diameter of the DNA. On a more speculative note, DNA-bridging proteins such as H-NS may have an additional effect. It has already been argued that a switch to the bridging mode of DNA binding for H-NS is triggered by multivalent cations[12]. We would like to add that the local concentration of DNA segments should also play an important role. Since crowding-induced condensation leads to a dramatic enhancement of the local concentration of DNA segments, this should also strongly enhance the probability of bridging. Hence, DNA condensation and the DNA-binding mode (bridging or non-bridging) may be coupled for H-NS.

Finally, we would like to remark on the wavevector dependence of the effective diffusion constant $D_{eff}(q)$ of bare supercoiled pUC18 (Fig. 3.1). This is very similar to that obtained previously by other workers for pUC18[19] and other plasmids.[21] A general theory for the initial decay rate of the correlation function of dilute polymer solutions was derived by Akcasu and Gurol[22]. This theory was elaborated by Stockmayer and co-workers in addressing the effects of chain architecture and stiffness on the dynamic scattering of polymers.[23,24] This approach does not seem to have been applied to supercoiled DNA. The initial decay rate Γ of the electric field autocorrelation function $g_1(t)$ determined by dynamic light scattering experiment is

$$\Gamma = -\frac{d \ln g_1(t)}{dt}\bigg|_{t=0} \tag{5}$$

At the low scattering angles that we have used, the decay of the correlation function was found to be dominated by a single relaxation peak in the CONTIN analysis of $g_1(t)$. To a good approximation, this peak therefore corresponds to the initial relaxation rate Γ, which is related to the effective diffusion constant by $\Gamma = q^2 D_{eff}(q)$ (see Fig. 1). The general form of Γ for a dilute polymer solution in the limit of low q is:

$$\Gamma(q) = q^2 D(1 + Cq^2 R_g^2 + ...) \tag{6}$$

where C is a convenient dimensionless constant that depends on the chain architecture and flexibility[23,24,] and R_g is the radius of gyration. Radii of gyration for supercoiled plasmids of various lengths have been compiled by Fishmann and Patterson[21]. From their data, the expected radius of gyration for our 2.7 kb supercoiled plasmid is $R_g \approx 73$ nm, which gives $C = 0.16 \pm 0.02$ from the slope in Fig. 1. A similar value of $C = 0.13$ can be deduced via the data of Fishman and Patterson for a somewhat longer 3.7 kb plasmid.

For semiflexible chains, the C parameter depends on the contour length L scaled by the Kuhn length l_K, and on the chain topology. Theoretical predictions are available for linear[23] and untwisted circular semiflexible chains[24], but not for semiflexible chains that are supercoiled (i.e. twisted and circular). A qualitative interpretation of the parameter C is that it is a measure of the relative strength of low frequency internal modes (rotation, bending), as compared to those due to translation. Supercoiling may be expected to reduce the extent of internal motion as compared to that of linear chains, and circular untwisted chains; supercoiling should thus lead to a lower value of C. At $L/l_K \approx 10$, predicted values are $C = 0.18$ for untwisted circular chains[24], and $C = 0.23$ for linear chains[23]. We conclude that our low value of C is consistent with supercoiling restraining the chain dynamics.

3.5 Concluding Remarks

The dramatic enhancement of ψ condensation of DNA by bound nucleoid proteins has now been demonstrated for three completely different nucleoid proteins: bacterial HU[25], archaeal Sso7d[14], and, in this work, for bacterial H-NS. We emphasize that these proteins by themselves do not condense DNA. In fact, we have shown here that the global dimensions of DNA are essentially not perturbed at all by H-NS.

The work of Sarkar *et al.*[26] addresses another interesting aspect of this interplay: whereas polymer-induced condensates have a predominantly toroidal shape when DNA is bare, complexes of DNA with HU condense into shapes that are distinctly different, such as cylindrical.

The theoretical arguments that we have put forward suggest that the enhancement of DNA condensation could be generic, and should also occur for other types of nonbinding depletive macromolecules that have large excluded-volume interactions with DNA. In bacterial cells, these would be nonbinding globular proteins, and also RNA. Indeed, Murphy and Zimmerman have shown[25] that serum albumin at weight concentrations of up to 25% did

not condense bare linear DNA, whereas concentrations much lower than this did condense HU/DNA complexes. In other words, effects observed for inert PEG of the appropriate size may also be expected for biologically relevant crowding agents such as globular proteins and RNA, at least qualitatively.

Nevertheless, quantitative differences could show up. One example is that linear bare DNA requires high salt to be condensed by inert flexible polymer[20], but low salt to be condensed by nonbinding globular proteins.[27] In the former, the salt dependence is due to the screening of electrostatic repulsion between DNA needed to condense the DNA more readily.[28] In the latter case, the salt dependence stems from the electrostatic protein-protein repulsion.[29] Condensation requires high protein osmotic pressures, and hence a low ionic strength.

We have here referred to the DNA complexes induced by PEG and H-NS as condensates. The term DNA condensation has been in use for a very long time[30,31]: it connotes a state of close packing with an attendant high probability that a phase transition has taken place (even though the DNA is of finite size). Often DNA condensates that have been studied in the pas stringently fall in this category. Without an in-depth study of the DNA configuration within our "condensates", we do not know at present how strict the terminology is.

Compaction of DNA has to be distinguished from condensation, even though DNA may sometimes also condense when it is compacted by external forces. For instance, the isolated *E. coli* nucleoid may be gradually compressed by increasing the PEG concentration in the surrounding buffer.[32,33] The DNA is then compacted as a continuous process in the absence of any transition. The DNA in the compressed state is, furthermore, of a low volume fraction so the term "condensation" would make little sense. Such a type of compaction was predicted some time ago.[15] Of course, DNA condensation may still be related to DNA compaction. In this respect, the experiments outlined here have been carried out simultaneously by us on *E. coli* nucleoids. These experiments are described in Chapter 4.

References

1. S. C. Dillon and C. J. Dorman, *Nature Rev. Microbiol.*, 2010, **8**, 185-195.

2. M. Lammi, M. Paci, C.L. Pon, M.A. Losso, A. Miano, R.T. Pawlik, G. Gianfranceschi, and C.O. Gualerzi, In: U. Hübscher and S. Spadari (Eds) *Proteins Involved in DNA Replication*, Plenum, New York, 1984, pp. 467–477.

3. A. Spassky, S. Rimsky, H. Garreau, and H. Buc, *Nucl. Acids Res.*, 1984, **12,** 5321-5340.
4. M. Durrenberger, A. La Teana, G. Citro, F. Venanzi, C.O. Gualerzi, and C.L. Pon, *Res. in Microbiol.*, 1991, **142**, 373-380.
5. R. Spurio, M. Dürrenberger, A. La Teana, C.L. Pon, and C.O. Gualerzi, *Mol. Gen. Genet.*, 1992, **231**, 201-211.
6. B. Lang, N. Blot, E. Bouffartigues, M. Buckle, M. Geertz, C.O. Gualerzi, R. Mavathur, G. Muskhelishvili, C.L. Pon, S. Rimsky, S. Stella, M. Madan Babu, and A. Travers, *Nucl. Acids Res.*, 2007, **35**, 6330-6337.
7. S M. Sette, R. Spurio, E. Trotta, C. Brandizi, A. Brandi, C.L. Pon, G. Barbato, R. Boelens, and C. O. Gualerzi, *J. Biol. Chem.*, 2009, **284**, 30453-30462.
8. T. Atlung, and H. Ingmer, *Mol. Microbiol.*, 1997, **24**, 7-17.
9. F. Hommais, E. Krin,C. Laurent-Winter, O. Soutourina,A.Malpertuy, J.-P. Le Caer, A. Danchin, and P. Bertin, *Mol. Microbiol.*, 2001, **40**, 20-36.
10. R. T. Dame, M. C. Noom, and G. J. L. Wuite, *Nature*, 2006, **444**, 387-390.
11. R. Amit, A.B. Oppenheim, and J. Stavans, *Biophys. J.*, 2003, **84**, 2467–2473
12. Y. Liu, H.Chen, L. J. Kenney, and J.Yan, *Genes Dev.*, 2010, **24**, 339-344.
13. R. T. Dame, C. Wyman, and N. Goosen, *Nucl. Acids Res.*, 2000, **28**, 3504-3510.
14. E. Bessa, K. Wintraecken, A. Geerling, and R. de Vries, *Biophys. Rev. Lett.*, 2007, **2**, 259–265.
15. T. Odijk, *Biophysical Chemistry*, 1998, **73**, 23-29.
16. R. de Vries, *Biochimie*, 2010, **92**, 1715-1721.
17. K. Friedrich, C.O. Gualerzi, M. Lammi, M.A. Losso, C.L.Pon, *FEBS Lett*. 1988, **229**, 197-202.
18. S.W. Provencher, *Comp. Phys. Comm.*, 1982, **27**, 229-242.
19. J. Langowski, U. Kapp, K. Klenin, and A. Vologodskii, *Biopolymers*, 1994, **34**, 639-646.
20. V. V. Vasilevskaya, A. R. Khokhlov, Y. Matsuzawa, and K. Yoshikawa, *J. Chem. Phys.*, 1995, **102**, 6595-6602.
21. D. M. Fishman and G. D. Patterson, *Biopolymers*, 1996, **38**, 535-552.
22. Z. Akcasu and H. Gurol, *J. Polym. Sci. Polym. Phys. Ed.*, 1976, **14**, 1-10.
23. W. H. Stockmayer and M. Schmidt, *Pure Appl. Chem.*, 1982, **54**, 407—414.
24. K. Hubert, W.H. Stockmayer, and K. Soda, *Polymer*, 1990, **31**, 1811-1815.
25. L.D. Murphy and S.B. Zimmerman, *Biophys. Chem.* 1995, **57**, 71-92.
26. T. Sarkar, I. Vitoc, I. Mukerji and N. V. Hud, *Nucl. Acids Res.*, 2007, **35**, 951–961.
27. M.K. Krotova, V.V. Vasilevskaya, N. Makita, K. Yoshikawa, and A.R. Khokhlov, *Phys. Rev. Lett.* 2010, **105**, 128302.
28. R. de Vries, *Biophys. J.*, 2001, **80**, 1186–1194.
29. R. de Vries, *J. Chem. Phys.*, 2006, **125**, 014905
30. V.A. Bloomfield, *Biopolymers*, 1991, **31,** 1471-1481.
31. L.S. Lerman, *Proc. Natl. Acad. Sci. USA*, 1971, **68**, 1886-1890.
32. S. Cunha, T. Odijk, E. Suleymanoglu, C.L.Woldringh, *Biochimie*, 2001, **83**, 149-154.
33. S. Cunha, C.L. Woldringh, T. Odij*k, J. Struct. Biol.*, 2001**, 136**, 53-66.

Chapter 4

The effect of DNA binding protein H-NS on nucleoid compaction*.

*To be submitted

Abstract

Escherichia coli nucleoids were isolated with a new osmotic shock method using ampicillin to disrupt the peptidoglycan layer. The DAPI-stained isolated nucleoids were photographed using confocal microscopy. The addition of a low concentration of the nucleoid-associated protein H-NS enhanced the compaction originally due to macromolecular crowding induced by PEG. Remarkably, in the absence of PEG, H-NS did not affect the compaction of the nucleoids even at high concentrations. Our results confirm a general synergetic enhancement of macromolecular crowding by the cytoplasm together with the binding of protein to the nucleoid DNA.

4.1 Introduction

The chromosomal DNA of *Escherichia coli* is compacted into a tiny, separate structure called the nucleoid (Mason & Powelson, 1956). The compaction of the nucleoid is believed to be maintained by three effects: supercoiling of the DNA, macromolecular crowding owing to the cytoplasm and binding of multivalent ions and certain proteins to the DNA (Zimmerman, 2006). It is noteworthy that none of these factors by themselves can collapse the chromosome to the degree observed *in vivo*. Gyrase is responsible for supercoiling the DNA (Gellert *et al*., 1976) but its inhibition merely leads to slightly larger nucleoids *in vivo* (Stuger *et al*., 2002). Supercoiling by itself of the chromosomal DNA *in vitro* cannot account for the size of the nucleoid *in vivo* (Boles *et al*., 1996; Cunha *et al*., 2001b). However, it is generally thought that a synergy of all these effects could achieve the desired compaction (de Vries, 2010).
The *E. coli* cytoplasm contains a high concentration of protein and RNA molecules (up to 340 mg/ml). It has been known for some time that the cytoplasm induces macromolecular crowding (Zimmerman and Trach, 1991). Polyethylene glycol (PEG) with a molar mass of 20 kg/mol consists of linear polymer coils whose size is of the order of magnitude of the typical dimensions of cytoplasmic proteins. It is a reasonably inert agent and its crowding properties are thought to mimic those of cytoplasm. In a previous study, the volumes of isolated *E. coli* nucleoids were measured as a function of increasing concentrations of PEG, resulting in a continuous decrease in volume up to 70 times (Cunha *et al*., 2001b). Here we take this investigation one step further and study the synergetic effect of the H-NS protein with crowding.
In view of the very small size of the bacterial nucleoid *in vivo*, it is very difficult to quantitatively visualize by light microscopy. Many attempts have been made to visualize its detailed structure by electron microscopy (Robinow and Kellenberger, 1994). Fixation procedures are required in that case but that is a drastic and suspect procedure. It causes a marked change of the solution properties of the biopolymers involved (Woldringh and Odijk, 1999). On the other hand, it is reasonable to assume that the topological properties of the nucleoid are not altered after a mild liberation from a cell, so it then makes sense to study its properties *in vitro* by light microscopy. Therefore, a variety of isolation protocols were developed over several decades (Sloot *et al*., 1983; Worcel and Burgi, 1972; Murphy and Zimmerman, 1997, Cunha *et al*., 2001b, Wegner *et al*., submitted for publication). All of them involve a step where the cell wall is first disrupted before lysis. In all our experiments we use

a new gentle method of isolating the nucleoid by osmotic shock, which is described in detail in Wegner *et al*. (2012). The nucleoids are stained by using DAPI, a very selective DNA dye. They are then directly visualized using fluorescence microscopy.

There are studies that already indicate that the binding of proteins to DNA combined with the crowding interaction by PEG results in a relatively more severe compaction of plasmid or linear DNA (Murphy and Zimmerman, 1993; Ramos *et al*., 2007). Here we focus on the nucleoid-associated protein H-NS. This protein is involved in the regulation of a broad range of genes as well as in the perturbation of the DNA structure (Atlung and Igmer, 1997, Dame *et al*., 2006). In Chapter 3, we described a set of experiments concerning the synergetic compaction of plasmid DNA. Here, we carried out complementary experiments on isolated nucleoids which come much closer to mimicking the compaction of the highly branched *E. coli* chromosome *in vivo*. Our results suggest that incubation of isolated nucleoids with a high concentration of H-NS does not change their volume. By contrast, combining H-NS binding with PEG-induced crowding leads to a dramatic compaction of the chromosomal DNA.

4.2 Materials and methods

Strain and growth conditions

E. coli wild type strain LMC500 (K-12 MC4100 LysA) was grown for several days in glucose minimal medium (6.33 g $K_2HPO_4 \times 3H_2O$, 2.95 g KH_2PO_4, 1.05 g $(NH_4)_2SO_4$, 0.10 g $MgSO_4 \times 7H_2O$, 0.28 mg $FeSO_4 \times 7H_2O$, 7.1 mg $Ca(NO_3)_2 \times 4H_2O$, 4 g glucose, 50 mg lysine, 4 mg vitamin B_1 per 1 liter) at 28°C. Overnight culture of 5 ml of well-grown cells was centrifuged at 2500 rpm at room temperature. The pellet was resuspended in 20 ml of glucose minimal medium supplemented with 0.25 % of TY (20 g/l bacto-tryptone, 5 g/l yeast extract, 5.9 g/l MgSO4*7 H2O, 0.58 g/l NaCl) and 20 % sucrose. The culture was grown for a few hours until OD_{450}=0.4.

Nucleoid isolation

Nucleoids were isolated according to the ampicillin-method (Wegner *et al*., 2012). A 5 ml LMC500 culture was grown in glucose minimal medium with 0.25% TY and 20% sucrose supplemented with 400 µl of 100 mg/ml ampicillin (final concentration 2 mg/ml). At this juncture it is important to mix the culture while shaking the cuvette at the same time to avoid cell lysis. After the addition of ampicillin, the culture was grown for an additional 2 hours at 30°C. Subsequently, the culture was divided into 1.5 ml aliquots and spun down at 5000 rpm for 15 min at room temperature. The pellets were resuspended in 250 µl of sucrose buffer (0.58 M sucrose, 10 mM NaPi pH 7.0, 10 mM EDTA and 100 mM NaCl).

Cover slip coating

Cover slips were cleaned and coated with BSA protein (Sigma) prior to microscopy experiments in order to prevent attachment of the sedimenting nucleoids to the glass surface. First, the coverslips were dipped into 37 % HCl, washed in 3 successive 500 ml beakers filled with demi water and blow-dried. A drop of 200 µl of 200 mg/ml BSA solution was placed on a parafilm. An acid-cleaned cover slip put on a metal holder and immobilized with stickers was placed on the drop. After 30 minutes of incubation at room temperature, the cover slip was rinsed with demi water and blow-dried.

Incubation with wt H-NS

wt H-NS was purified, stored and buffer exchanged as described in Chapter 1 of this thesis. To check for consistent binding to DNA, we regularly performed electrophoretic mobility shift assays using pUC18 as a non-specific H-NS binding template. Ampicillin-isolated nucleoids (1.16 µl) were mixed with 4 µl of *wt* H-NS (final concentration of 100 µg/ml) in 10 mM phosphate buffer at pH=7 with 150 mM NaCl and incubated for 30 min at room temperature (in this thesis, this means around 22ºC). As a control, 4 µl of 10 mM phosphate buffer at 150 mM NaCl was used.

Polymer-mediated compaction

Polyethylene glycol (PEG, 20 kg/mol (Sigma)) was dissolved overnight at 65°C in 10 mM phosphate buffer at pH=7 with 150 mM NaCl to a concentration of 25 % (w/v). First, 6 µl of a suspension of isolated nucleoids was incubated with wild type H-NS (final concentrations 0, 12 and 24 µg/ml) for 30 min at room temperature. Then it was gently mixed by pipetting with 30 µl of a solution containing PEG (final conc. 0-5 % w/v), DAPI (final concentration of 500 ng/ml) and NaCl (150 mM) and incubated for another 30 minutes. 10 µl of the solution was applied to an acid-cleaned, BSA treated cover slip placed on a metal holder. Another cover slip was placed on top to protect the sample from evaporation while photos were being taken.

Microscopy and image analysis

All images were acquired using the A1 confocal laser scanning microscope (Nikon) with a 100x lens at room temperature (about 22°C). DAPI-stained nucleoids were illuminated at 405 nm wavelength with a scanning speed of 1 frame/sec. The detector was equipped with an emission longpass filter. The confocal pinhole was open during the experiments. Only free-floating nucleoids were photographed. Image analysis was performed using the public domain software ObjectImage (Visscher *et al.* 1994). Volume distributions were estimated by analyzing a large number of nucleoids. Typically we measured at least 80 nucleoids per sample and repeated this three times, per solution condition.

4.3 Results

Representative images for nucleoids in the absence of PEG and H-NS are shown in Fig. 4.1A. Representative images of nucleoids after adding H-NS at a concentration of 100 µg/ml H-NS are shown in Fig. 4.1B. A visual inspection immediately indicates that H-NS has little to no effect on nucleoid volume.

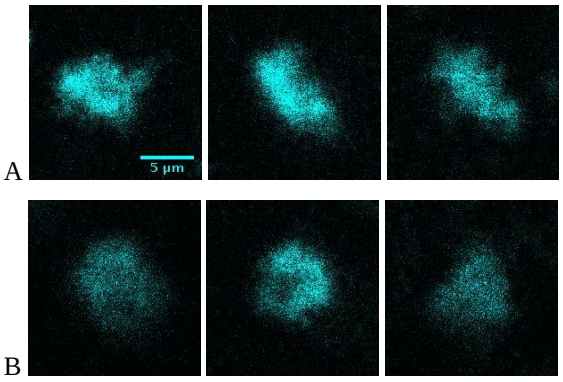

Figure 4.1. Fluorescent images of representative isolated nucleoids without (A) and with the addition of 100 µg/ml H-NS (B).

Volume distributions obtained by analyzing a large number of images of nucleoids are shown in Fig 4.2A. The nucleoid volume distributions are broad, spanning values between 20 and 100 μm^3. This is caused, at least in part, by the variation in DNA content of individual bacteria, which can vary by a factor of at least 2 depending on the cell cycle. The nucleoid volume distribution after adding H-NS at a concentration of 100 μg/ml H-NS is shown in Fig. 4.2B. Remarkably, the images and the resulting nucleoid volume distributions are very similar for nucleoids incubated with or without 100 μg/ml H-NS. The average nucleoid volumes V_n calculated from the distributions are V_n = 43±14μm^3 without H-NS, and V_n =44±17μm^3 after incubation with 100 μg/ml H-NS, a difference much smaller than the margin of error.

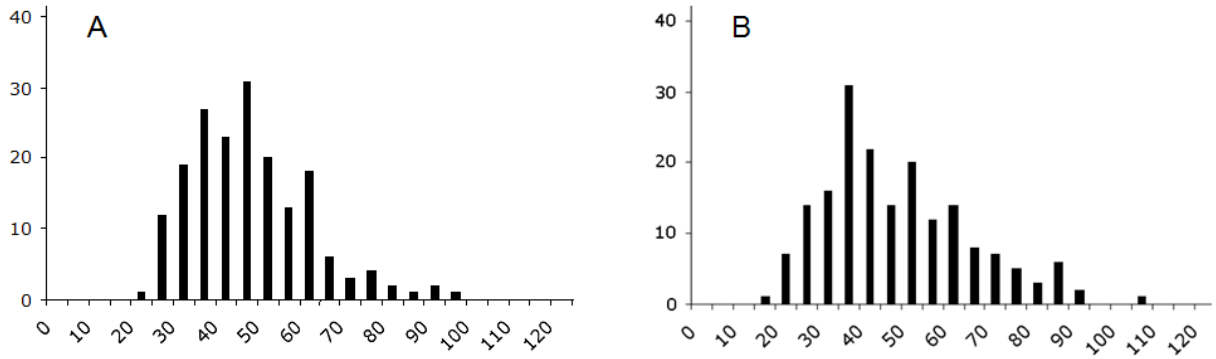

Figure 4.2. Volume distributions of isolated nucleoids incubated without (A) and with 100 μg/ml *wt* H-NS (B). The x-axis indicates the nucleoid volume measured in μm^3 and the y-axis denotes the frequency. The total number of observations was n =183 for the nucleoids without and n = 191 for the nucleoids with H-NS.

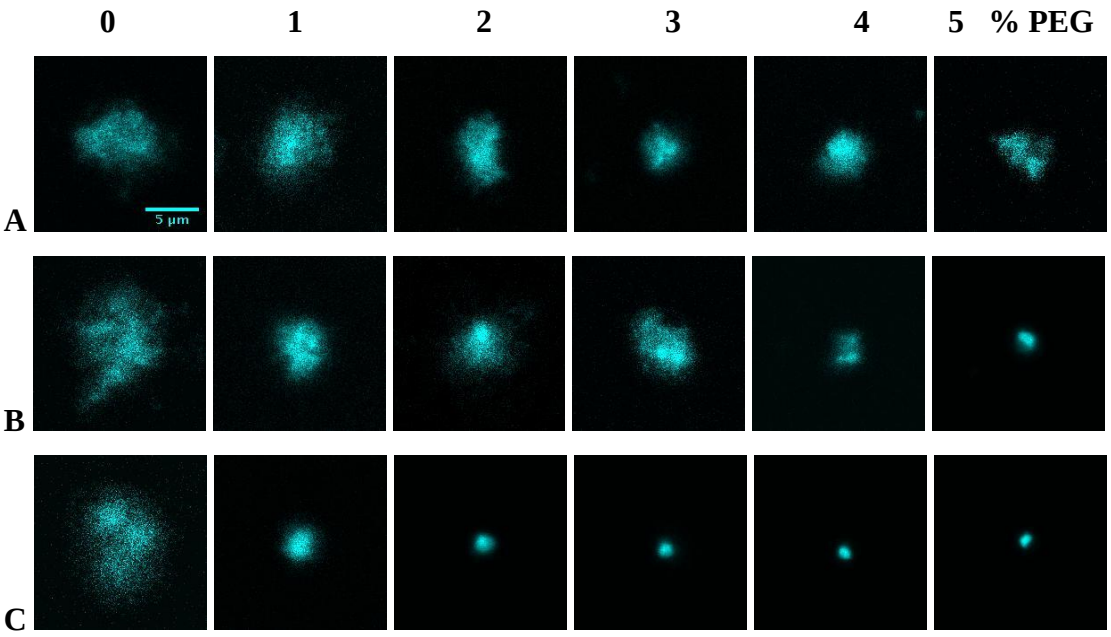

Figure 4.3. Fluorescent images of representative isolated nucleoids without (A) and with addition of 12 μg/ml (B) and 24 μg/ml H-NS (C) as a function of increasing concentrations of PEG.

In Figure 4.3, we show representative pictures of isolated *E. coli* nucleoids at various concentrations of PEG at 0, 12, and 24 µg/ml H-NS . They clearly show enhanced compaction with increasing PEG concentration. The average volume of a population consisting of typically 50 to 60 nucleoids is represented by each entry in Table 4.1. The addition of 24 µg/ml H-NS causes a drastic reduction in the concentration of PEG necessary for appreciable compaction to 1 % (Fig. 3 C). A three-dimensional plot (Fig. 4.4) summarizes the entries from Table 4.1.

% PEG	*Control* Volume [µm^3]	St. dev.	*12 µg/ml H-NS* Volume [µm^3]	St. dev.	*24 µg/ml H-NS* Volume [µm^3]	St. dev.
0	39.73	19.51	59.15	27.71	39.55	19.8
1	32.22	19.48	27.07	15.35	5.86	7.36
2	19.23	11.47	22.02	11.67	1.38	1.26
3	11.38	6.06	17.29	7.41	1.03	1.11
4	13.81	7.68	6.24	7.87	0.79	0.65
5	8.06	4.25	1.55	2.43	0.65	0.52

Table 4.1. Average index volumes of isolated nucleoids incubated at various concentrations of H-NS.

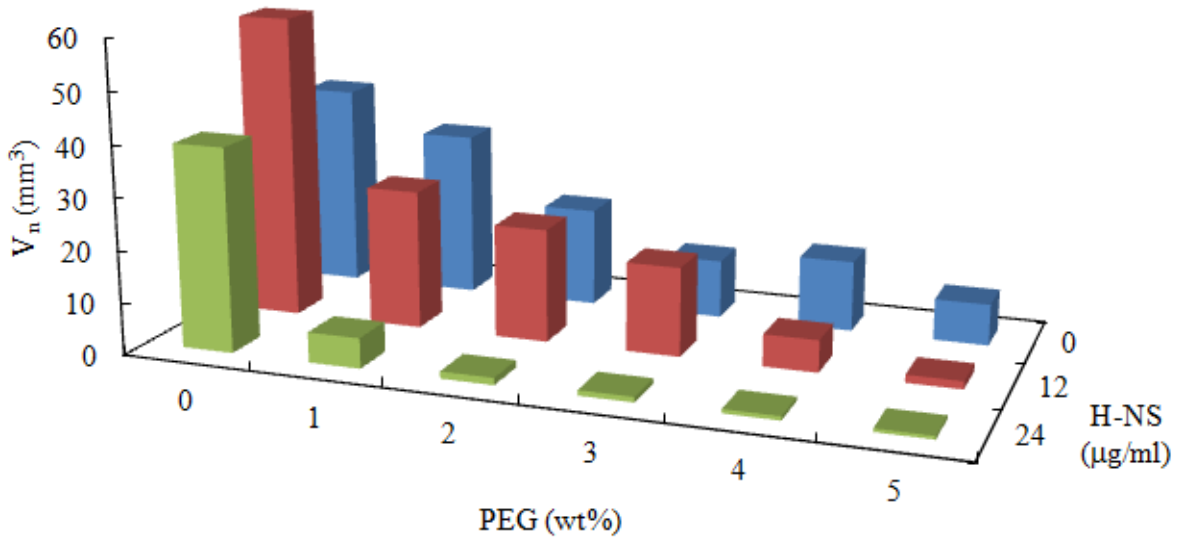

Figure 4.4. Average index volumes of isolated nucleoids as a function of both the weight fraction of PEG and the concentration of H-NS.

Because it was often difficult to distinguish via imaging between a compact nucleoid and a remnant spheroplast ("ghost cell"), we always determined by visual inspection, whether the DAPI-stained object was one of the two prior to scanning. One characteristic property of a ghost cell is its obvious round shape (Fig. 4.5B), whereas compact nucleoids adopt a more irregular structure (Fig. 4.5A).

A **B**

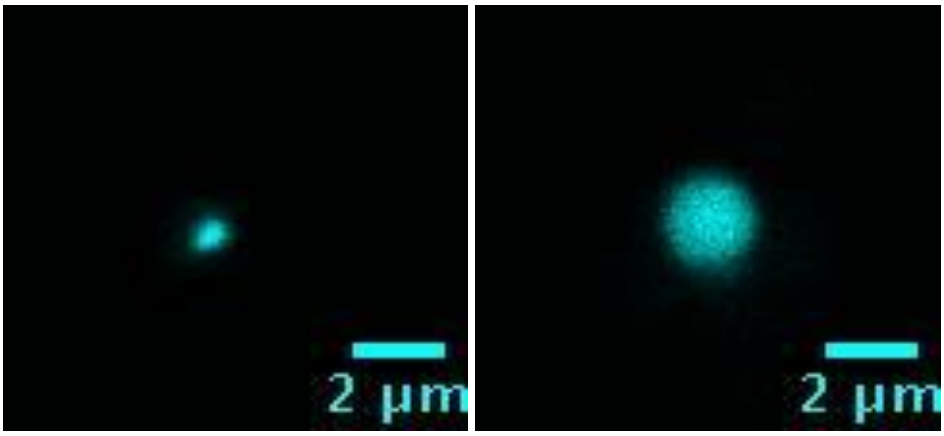

Figure 4.5. Images showing the difference between a compact nucleoid after incubation with 24 µg/ml H-NS (A) and a spheroplast (B), both in solutions containing 5 % PEG.

4.4 Discussion

It is qualitatively obvious from Table 4.1 and Fig. 4.4 that H-NS has a dramatic effect on the PEG-induced compaction of the *E. coli* nucleoid. We attempt to interpret the synergetic effect of H-NS and PEG within the framework of the thermodynamic coexistence equations introduced previously (Cunha 2001b). We first need to assess the degree of binding of the H-NS protein to the chromosomal DNA.

We estimate the DNA concentration in the lysate which is the end product of our ampicillin protocol (Wegner *et al*., 2012). From the optical density of the cell culture, the fact that typically 80% of the cells are actually lysed and a nucleoid consists of 1.58 chromosomal equivalents, we know that the concentration of DNA in the ultimate lysate must be about 5×10^{-8} M bp DNA. At these low concentrations, we may express the binding of H-NS to double-stranded DNA to a first approximation as (Friedrich *et al*., 1988)

$$\frac{C_B}{C_F[DNA]} = K_a \approx 1.1\times10^4 M^{-1} \qquad (4.1)$$

where C_B is the effective concentration of bound H-NS, C_F is the concentration of free H-NS and the molarity M is given in terms of bp DNA. For instance, in Fig. 1B the concentration of H-NS is 6.4×10^{-6} M so that we have $C_B/[DNA] \approx 7\times10^{-2}$ i.e. the DNA is halfway covered by H-NS dimers. We suppose one dimer binds about 12bp of DNA (Friedrich *et al*., 1988). Nevertheless, there is clearly a certain degree of uncertainty in these numbers.

w_0 (g/ml)	w_i (g/ml)	V_n (μm^3)	G
0.01	0.0099056	27.1	799
0.02	0.0198106	22.0	1846
0.03	0.02967158	17.3	4507
0.04	0.038895	6.24	18604
0.05	0.045027	1.55	92980

Table 4.II. Measure of the free energy G of the isolated nucleoids at 12μg/ml H-NS and at various PEG concentrations w_0 in the bulk.

The DNA helix forms complexes with H-NS dimers in a rather complicated fashion (Shindo *et al*., 1995; Bloch *et al*., 2003; Arold *et al*., 2010). In previous work we argued that the depletion interaction between PEG chains and the DNA helix (de Vries, 2001) is the primary cause of the compaction of the *E. coli* nucleoid immersed in a PEG reservoir (Cunha *et al*., 2001). In the H-NS experiments at hand, the major effect of H-NS appears to be an increase in the thickness of the nucleoidal DNA, which in turn enhances the depletion interaction (i.e. the H-NS/DNA complex repels the PEG coils by entropic depletion). Moreover, we know from *in vitro* studies that bound H-NS at not too high concentrations does not influence the configurational statistics of the DNA chains (this thesis, Chapter 3). Here, we tentatively introduce an enhancement h of the DNA radius a of 1 nm and 2nm, as a result of H-NS associated at 12 μg/ml and 24 μg/ml concentrations, respectively (a = 1 nm).

w_0 (g/ml)	w_i (g/ml)	V_n (μm^3)	G
0.01	0.0094181	5.9	6675
0.02	0.0159543	1.38	60348
0.03	0.0225864	1.03	141098
0.04	0.0281827	0.79	269213
0.05	0.033317	0.65	440862

Table 4.III. Measure of the free energy G of the isolated nucleoids at 24μg/ml H-NS and at various PEG concentrations w_0 in the bulk.

We next compute the size of a nucleoid as a function of PEG weight fraction in the manner outlined by Cunha *et al*. (2001b). The PEG-(H-NS/DNA) interaction per nm of the DNA helical contour is given by

$$\frac{f_{dep}}{k_B T} = E_1\left(1+\frac{h}{a}\right)^{1/3} w + E_2\left(1+\frac{h}{a}\right)^{9/4} w^{9/4} \qquad (4.2)$$

Here, the previous expression valid for pure PEG is amended by geometric factors on the basis of the theory developed by de Vries (2001) (k_B is Boltzmann's constant, T is the temperature, the constants $E_1 = 4$ and $E_2 = 50$, and f_{dep} is expressed in units k_BT/nm when w is in g/ml). A PEG coil which has a radius of gyration of merely 6.9 nm is easily able to enter the nucleoid and may even wrap itself around the H-NS/DNA complex locally. The depletion interaction causes a difference in the concentration of PEG coils inside and outside the globular chromosome; thermodynamic equilibrium demands equality of the respective PEG chemical potentials as well as the osmotic pressure. We let the nucleoid have a free energy F_n of compression balancing the depletion interaction; the quantity ultimately obtained is

$$G \equiv -\frac{V_n}{k_B T}\frac{\partial F_n}{\partial V_n} \qquad (4.3)$$

in terms of the nucleoid volume $\underline{V_n}$ from Table 4.1. We have summarized the numerical outcome of the coexistence equations in Tables 4.II and 4.III; w_i is the weight fraction of PEG inside nucleoids. As in the work of Cunha (2001b), we have plotted G versus $\ln V_n$ in Fig. 4.6. The data points may be fitted to linear least-squares plots within the experimental margin of error (we have not plotted the data at zero H-NS. This baseline conflicts with the data of Cunha (2001b) and is obviously wrong. Unfortunately, the entire experiment could not be repeated for logistic reasons. This is one of the reasons the present results must be viewed as only preliminary). Eq. (4.3) then yields the free energies of the respective nucleoids

$$F_n = 2.58\left(\frac{V_0}{V_n}\right)^{1.56} \qquad \text{at } 12\mu\text{g/ml H - NS} \qquad (4.4)$$

$$F_n = 92\left(\frac{V_0}{V_n}\right)^{1.86} \qquad \text{at } 24\mu\text{g/ml H - NS} \qquad (4.5)$$

Where V_0 is the volume of the nucleoid at zero PEG (See Table 4.I).

On the one hand it is gratifying that the procedure adopted for nucleoids in pure PEG can be translated to the case with H-NS. Indeed, Fig. 4.6 proves that scaling relations of the free energy versus the nucleoid volume remain viable. On the other hand, the two expressions

given by Eqs. 4.4 and 4.5 are in effect indistinguishable given the margin of error so it is not possible at present to draw any more significant conclusions. We hope more accurate work by us in the near future will lead to a higher accuracy.

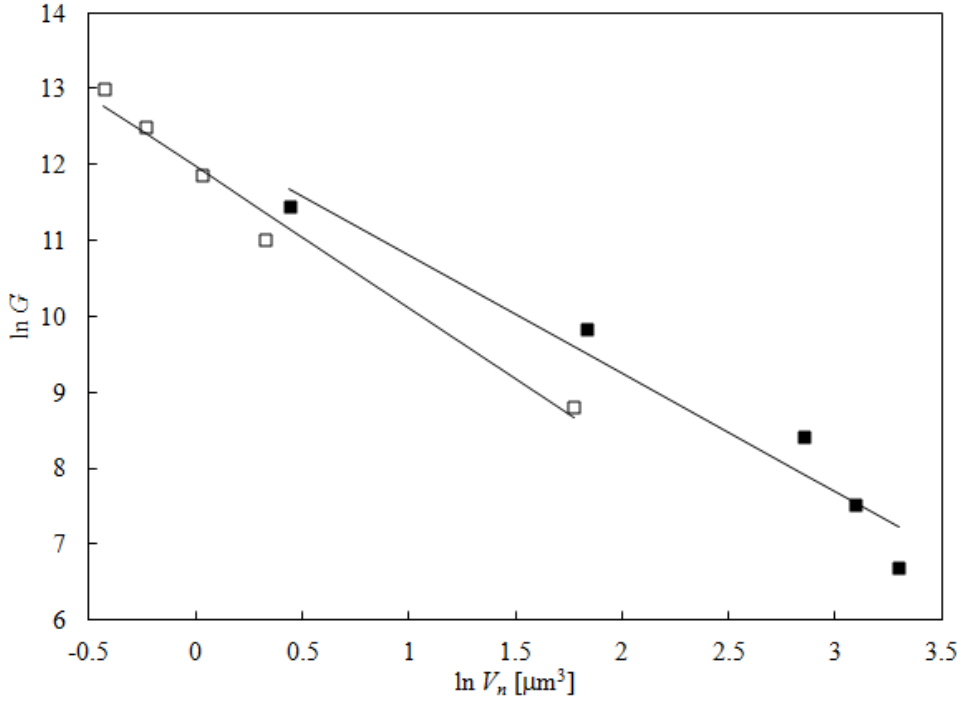

Figure 4.6. Relation between G and the index volume Vn for isolated nucleoids immersed in various PEG solutions at two H-NS concentrations. The data in Tables II and III are plotted in a double-logarithmic format. Linear least-squares fits yield ln$G$ = 12.4(±0.5)-1.56(±0.20)lnV_n at 12 μg/ml and ln$G$ = 12.0(±0.13)-1.86(±0.15)lnV_n at 24 μg/ml H-NS.

References

Arnold, S.T.; Leonard, P.G.; Parkinson, G.N.; Ladbury, J.E. (2010) H-NS forms a superhelical protein scaffold for DNA condensation, Proc. Natl. Acad. Sci. USA 107: 15728-15732

Atlung, T. & H. Ingmer, (1997) H-NS: a modulator of environmentally regulated gene expression. Mol Microbiol 24: 7-17.

Bloch, V.; Yang, Y.; Margeat, E.; Chavanieu, A.; Augé, M.T.; Robert, B.; Arold, S.; Rimsky, S.; Kochoyan, M. (2003) The H-NS dimerization domain defines a new fold contributing to H-NS recognition. Nat. Struct. Biol. 101: 212-218

Boles, T. C., J. H. White & N. R. Cozzarelli, (1990) Structure of plectonemically supercoiled DNA. J Mol Biol 213: 931-951.

Brunetti, R., G. Prosseda, E. Beghetto, B. Colonna & G. Micheli, (2001) The looped domain organization of the nucleoid in histone-like protein defective Escherichia coli strains. Biochimie 83: 873-882.

Cunha, S., T. Odijk, E. Suleymanoglu & C. L. Woldringh, (2001a) Isolation of the Escherichia coli nucleoid. Biochimie 83: 149-154.

Cunha, S., C. L. Woldringh & T. Odijk, (2001b) Polymer-mediated compaction and internal dynamics of isolated Escherichia coli nucleoids. J Struct Biol 136: 53-66.

Dame, R. T., M. C. Noom & G. J. Wuite, (2006) Bacterial chromatin organization by H-NS protein unravelled using dual DNA manipulation. Nature 444: 387-390.

de Vries, R. (2001) Flexible polymer-induced condensation and bundle formation of DNA and F-actin filaments. Biophys. J. 80:1186-1194

de Vries, R., (2010) DNA condensation in bacteria: Interplay between macromolecular crowding and nucleoid proteins. Biochimie.

Friedrich, K.; Gualerzi, C.O.; Lammi, M.; Losso,M.A.; Pon, C.L. (1988) Proteins from the prokaryotic nucleoid: interaction of nucleic acids with 15kDa *Escherichia coli* histone-like protein H-NS, FEBS Lett. 229: 197-202

Gellert, M., K. Mizuuchi, M. H. O'Dea & H. A. Nash, (1976) DNA gyrase: an enzyme that introduces superhelical turns into DNA. Proc Natl Acad Sci U S A 73: 3872-3876.

Mason, D. J. & D. M. Powelson, (1956) Nuclear division as observed in live bacteria by a new technique. J Bacteriol 71: 474-479.

Murphy, L. D. & S. B. Zimmerman, (1995) Condensation and cohesion of lambda DNA in cell extracts and other media: implications for the structure and function of DNA in prokaryotes. Biophys Chem 57: 71-92.

Murphy, L. D. & S. B. Zimmerman, (1997) Isolation and characterization of spermidine nucleoids from Escherichia coli. J Struct Biol 119: 321-335.

Odijk T., (1998) Osmotic compaction of supercoiled DNA into a bacterial nucleoid. Biophysical Chemistry 73: 23-29.

Ramos, E. B., K. Wintraecken, A. Geerling & R. de Vries, (2007) Synergy of DNA-binding nucleoid proteins and macromolecular crowding in condensing DNA. Biophysical Reviews and Letters 2: 259-265.

Robinow, C. & E. Kellenberger, (1994) The bacterial nucleoid revisited. Microbiol Rev 58: 211-232.

Shindo, H.; Iwaki, T.; Ieda, R.; Kuwimizaka, H.; Ueguchi, C.; Mizuno, T.; Morikawa, S.; Nakamura, H.; Kuboniwa, H. (1995) Solution structure of the DNA-binding domain of the nucleoid-associated protein H-NS from *Escherichia coli*, FEBS Lett. 360: 125-131

Sloof, P., A. Maagdelijn & E. Boswinkel, (1983) Folding of prokaryotic DNA. Isolation and characterization of nucleoids from Bacillus licheniformis. J Mol Biol 163: 277-297.

Spassky, A., S. Rimsky, H. Garreau & H. Buc, (1984) H1a, an E. coli DNA-binding protein which accumulates in stationary phase, strongly compacts DNA in vitro. Nucleic Acids Res 12: 5321-5340.

Stuger, R., C. L. Woldringh, C. C. van der Weijden, N. O. Vischer, B. M. Bakker, R. J. van Spanning, J. L. Snoep & H. V. Westerhoff, (2002) DNA supercoiling by gyrase is linked to nucleoid compaction. Mol Biol Rep 29: 79-82.

Valkenburg, J. A. & C. L. Woldringh, (1984) Phase separation between nucleoid and cytoplasm in Escherichia coli as defined by immersive refractometry. J Bacteriol 160: 1151-1157.

van Noort, J., S. Verbrugge, N. Goosen, C. Dekker & R. T. Dame, (2004) Dual architectural roles of HU: formation of flexible hinges and rigid filaments. Proc Natl Acad Sci U S A 101: 6969-6974.

Vischer, N. O. E., P. G. Huls, and C. L. Woldringh. 1994. OBJECT-IMAGE - an interactive image- analysis program using structured point collection Binary-Comput. Microbiol. 6:160-166.

Wegner, A.S.; Alexeeva, S.; Odijk, T.; Woldringh, C.L. (2012) Characterization of *Eschericia coli* nucleoids released by osmotic shock, J. Struct. Biol. In press.

Woldringh, C.L. & T. Odijk, (1999) Structure of DNA within the bacterial cell: Physics and physiology; In Charlebois, R.L. (Ed.), Organization of the Prokaryotic Genome, Chap. 10 pp. 171-187, Am. Soc. of Microbiology, Washington DC

Worcel, A. & E. Burgi, (1972) On the structure of the folded chromosome of Escherichia coli. J Mol Biol 71: 127-147.

Zimmerman, S. B., (2006) Shape and compaction of Escherichia coli nucleoids. J Struct Biol 156: 255-261.

Zimmerman, S. B. & S. O. Trach, (1991) Estimation of macromolecule concentrations and excluded volume effects for the cytoplasm of Escherichia coli. J Mol Biol 222: 599-620.

Supplementary Material

Volume distributions of isolated nucleoids incubated with various concentrations of H-NS and PEG.

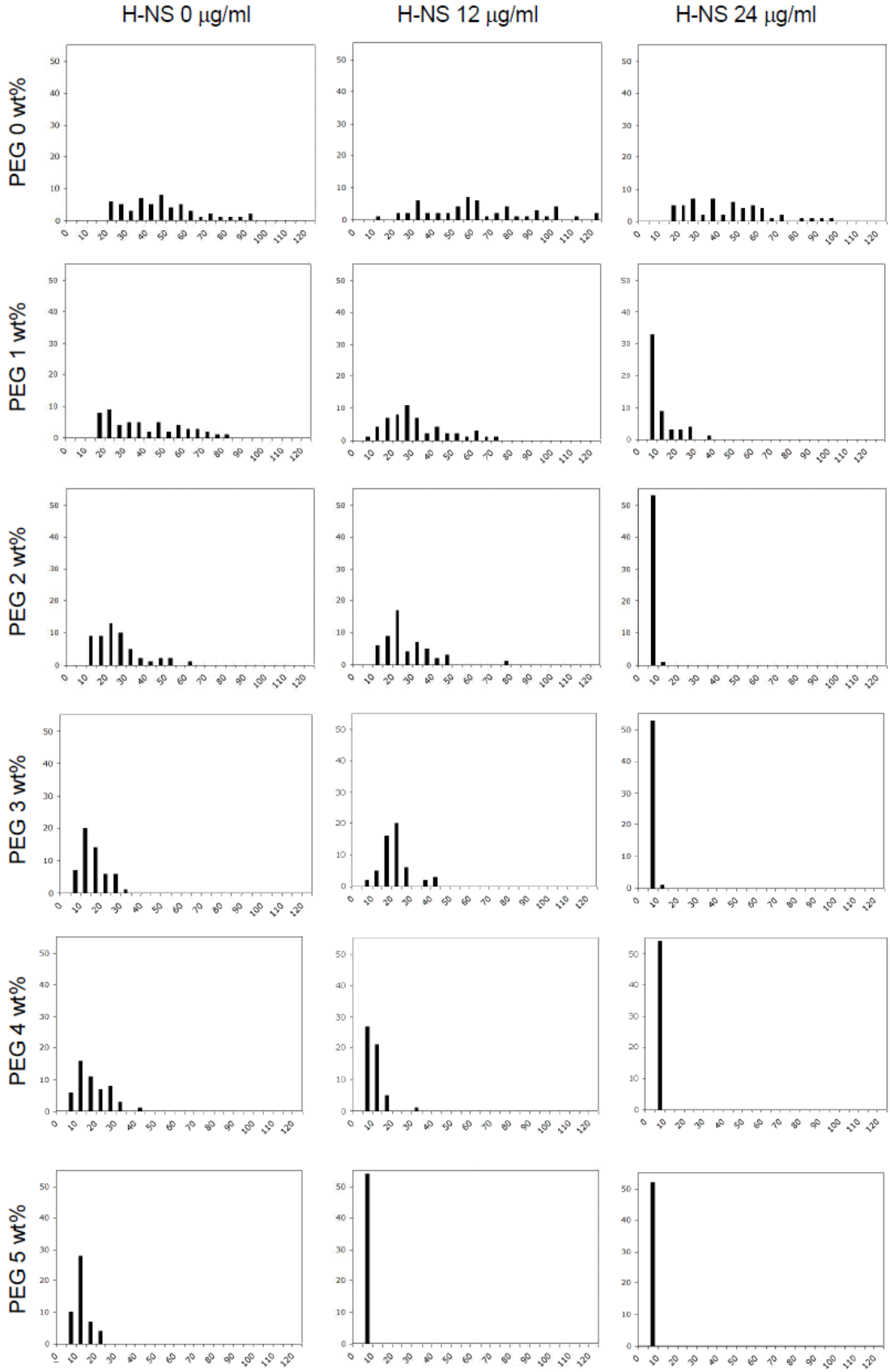

Chapter 5

Synergy of DNA-bending nucleoid proteins and macromolecular crowding in condensing DNA*

*Published as J. E. Bessa Ramos, Jr., K. Wintraecken, A. Geerling, and R. de Vries. 2007. Synergy of DNA-bending nucleoid proteins and macromolecular crowding in condensing DNA. Biophysical Reviews and Letters (BRL) 2:259-265.

Abstract

Many prokaryotic nucleoid proteins bend DNA and form extended helical protein-DNA fibers rather than condensed structures. On the other hand it is known that such proteins (such as bacterial HU) strongly promote DNA condensation by macromolecular crowding. Using theoretical arguments, we show that this synergy is a simple consequence of the larger diameter and lower net charge density of the protein-DNA filaments as compared to naked DNA, and hence, should be quite general. To illustrate this generality, we use light-scattering to show that the 7kDa basic archaeal nucleoid protein Sso7d from *Sulfolobus Solfataricus* (known to sharply bend DNA) likewise does not significantly condense DNA by itself. However, the resulting protein-DNA fibers are again highly susceptible to crowding-induced condensation. Clearly, if DNA-bending nucleoid proteins fail to condense DNA in dilute solution, this does not mean that they do not contribute to DNA condensation in the context of the crowded living cell.

5.1 Introduction

The effect of nucleoid proteins on the global gene expression in prokaryotic cells is now well established (Dorman and Deighan, 2003) but their role in nucleoid compaction is less clear. For example, many of the most abundant prokaryotic nucleoid proteins introduce bends in DNA. When complexed with DNA at appreciable coverage, helical protein-DNA filaments are formed that are typically extended rather than condensed. This has been shown, for example, for bacterial HU from *E coli* using AFM and single-molecule force measurements (Dame and Goosen, 2002; van Noort *et al*., 2004) and for archaeal Sac7d from *Sulfolobus acidolaricus* using small angle X-ray scattering (Krueger *et al*., 1999). On the other hand Murphy and Zimmerman (1995) find that *E. coli* HU strongly promotes crowding induced DNA condensation (induced by adding flexible polymers or non-binding proteins such as serum albumin or bacterial cytoplasmic proteins). This effect is especially strong at the high HU concentrations for which it has been suggested (Dame and Goosen, 2002; van Noort *et al*., 2004) that HU should counteract DNA compaction.

Why are extended helical HU-DNA filaments so much more susceptible to crowding induced condensation? Here we wish to explain the molecular basis for this somewhat unexpected synergy in terms of a simple theory that we previously developed for polymer-induced condensation of semiflexible polyelectrolytes (de Vries, 2001). We also briefly comment on the relation between this phenomenon and the formation and stability of prokaryotic nucleoids.

To complement the previous results on *E. coli* HU, and to illustrate the generality of the phenomenon, we also study crowding-induced condensation of extended protein-DNA filaments for another well characterized DNA bending nucleoid protein: archaeal Sso7d from *Sulfolobus solfataricus*. This protein, and the nearly identical Sac7d from *Sulfolobus acidolaricus* have been shown to non-specifically introduce sharp bends into double stranded DNA. At higher concentrations, they fully cover DNA at about one protein per 4bp, and form extended helical filaments (Krueger *et al*., 1999).

5.2 Materials and Methods

Protein expression and purification

The protein Sso7d was overexpressed in *E. coli* (DE3)pLysS, harboring the plasmid pET-3b/*sso7d*, described before (McAfee *et al*., 1995). Pelleted cells from 1.5 l culture were suspended in 15ml of suspension buffer: 30 mM Na_2HPO_4-HCl, 500 mM NaCl, pH 6.5. Cells were lysed using a French press (3 times at 1000 psi) and

centrifuged for 50 min at 12,000 g, 4 °C. To remove the majority of *E. coli* proteins, the supernatant was heated to 80°C for 40 min, centrifuged for 2 hours at 45,000 g at 4° C, and filtered using a 0.45 µm pore size syringe filter. After a concentration step, we exchanged buffer using disposable PD10 columns, to buffer A: 30 mM Na_2HPO_4-HCl, pH 6.5. The suspension was loaded onto a MonoS column, equilibrated with buffer A, and eluted with a linear NaCl gradient (0 to 0.6 M). Sso7d eluted at around 0.35 M. No other bands were detected on SDS-PAGE for fractions in the peak center, but some minor contaminations of around 15 kDa were detected for the fractions further away from the peak center. These fractions were pooled and concentrated, applied to a Superdex 75 column, and eluted with buffer A, after which SDS-PAGE showed only a single band corresponding to Sso7d. Purified protein was exchanged to storage buffer (20 mM Tris-HCl pH 7.7, 1 mM EDTA, 20% glycerol, 200 mM NH_4Cl, 200 ppm NaN_3, 200 ppm β-mercaptoethanol) by PD10 columns, concentrated to about 3 mg/ml and stored at -4°C. Protein concentrations were determined by UV spectrophotometry using (Krueger *et al*., 1999) λ_{278} = 1.1 ml/(mg•cm).

DNA purification
Plasmid pUC18 (2686 bp) was isolated from *E. coli* using Qiagen Kits according to the instructions of the manufacturer, and linearized using EcoRI.

Light scattering
Light-scattering was measured at 25°C using a Malvern NanoS, operating at a wavelength of 633 nm and a scattering angle of 173°. The effective hydrodynamic radius reported is the peak position of the monomodal distribution fit as reported by the Malvern DTS software, version 5.0. Absolute scattering intensities were calculated using toluene as a standard. For all of the experiments, concentrated stock DNA was diluted in 10 mM Tris-HCl buffer, pH 7.0, 150 mM NaCl. The final DNA concentration in the experiments was 12 µg/ml, as determined by UV spectrophotometry. Protein concentrations ranged from 0 to 1 protein per basepair.

Condensation assay
The condensation assay that was used is similar to that of Murphy and Zimmerman (1995). Protein-DNA complexes are equilibrated with flexible polymer solutions (final DNA concentration and buffer conditions as in the light-scattering experiment), centrifuged at 13000 g for 1 h and the supernatant is analyzed using agarose gel-electrophoresis. Condensation is observed as a decreased, and ultimately vanishing intensity for the DNA bands in the agarose gels.

5.3 Results and discussion

To demonstrate that Sso7d indeed does not condense DNA in free solution at physiological ionic strength, as was shown previously for the nearly identical Sac7d using small angle X-ray scattering, we have performed static and dynamic light-scattering measurements on complexes with 2686 bp long pUC18 DNA, linearized with EcoRI. The effective hydrodynamic radius and scattered intensity as a function of protein/DNA molar ratio are shown in Figure 5.1. The static scattering closely follows the extent of binding since free proteins hardly contribute to the scattering. It clearly shows the expected saturation above 1 protein per 4 bp. The reported effective hydrodynamic radius should only be considered as a rough estimate of the size of the complexes, but it clearly shows the same trends as observed in the single molecule force measurements for HU: a substantial but not drastic compaction at low protein concentrations followed by a slight expansion for over-saturated protein-DNA

fibers (Dame and Goosen, 2002). The main conclusion however, is that the protein clearly does not condense linear DNA fragments from dilute solutions.

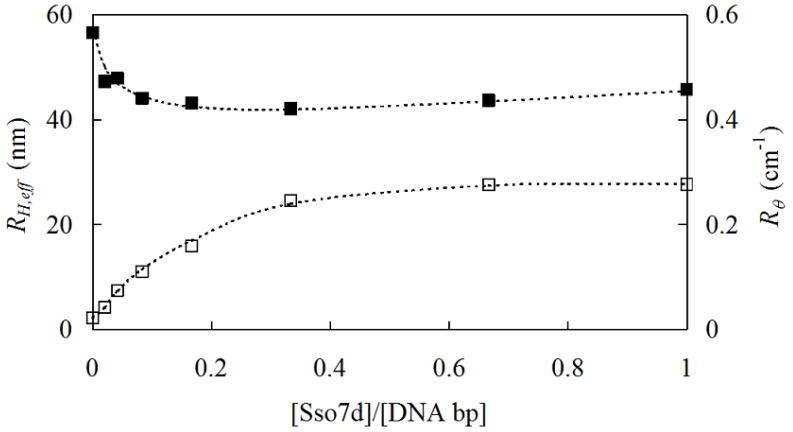

Figure 5.1: Light Scattering

Effective hydrodynamic radius (left y-axis, top curve) and scattered intensity or Rayleigh ratio R_θ (right axis, bottom curve) of complexes of EcoRI linearized pUC18 DNA with Sso7d, as a function of protein/DNA molar ratio, at a fixed DNA concentration of 12 µg/ml, in a 30mM Tris-HCl buffer, pH 7, 150 mM NaCl.

Next consider crowding-induced condensation of Sso7d-DNA fibers. To connect with previous experimental and theoretical work we have used poly(ethylene oxide) with a molar mass of 20 kg/mol as a crowding agent. DNA-Sso7d complexes were equilibrated in buffers containing increasing amounts of PEO and centrifuged. Crowding induced condensates are centrifuged down, and the supernatant is analyzed for the amount of complex remaining in solution using agarose gel-electrophoresis. Figure 5.2 shows a typical gel for the condensation assay. At a first critical concentration of PEO, the concentration of DNA-Sso7d complexes in the supernatant (after centrifugation) starts decreasing, after a second critical concentration of PEO, no more DNA-Sso7d complexes are detected anymore.

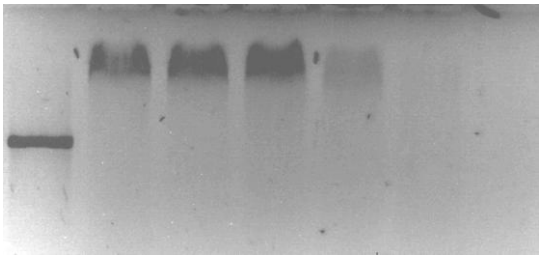

Figure 5.2: Agarose gel electrophoresis as used in the condensation assay

Lane 1: DNA (pUC18 linearized with EcoRI). All other lanes are at a fixed concentration of Sso7d of 1 protein per 12bp, and increasing concentrations of PEO: Lane 2: 0 w%, Lane 3 : 1 w%, Lane 4: 2 w%, Lane 5: 3 w%, Lane 6: 4 w% and Lane 7: 5 w%.

Figure 5.3 shows our estimates for the two critical PEO concentrations as a function of the protein/DNA ratio. Condensation of EcoRI linearized pUC18 without Sso7d occurs in a rather narrow window around 8% (w/v) of PEO. Increasing the Sso7d/DNA ratio, the amount of PEO needed for condensation decreases rapidly. At low protein concentrations, the transition regime is rather broad, but beyond saturation the transition becomes very sharp again and occurs at around 3% of PEO.

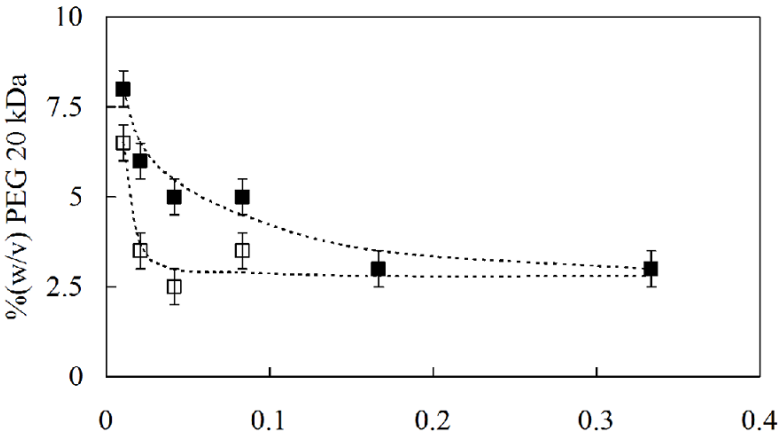

Figure 5.3: Condensation assay

Estimated concentration of polymer (PEG 20 kg/mol) at which DNA concentration in the supernatant (after centrifuging for 1 h at 13,000 g) starts decreasing (open squares), resp. concentration of polymer beyond which no DNA is detected anymore in the supernatant (closed squares) using agarose gel electrophoresis.

Previously, we have developed simple analytical estimates for the (ionic strength-dependent) amount of flexible polymer needed to condense semiflexible polyelectrolytes such as DNA and F-actin filaments (de Vries, 2001). These estimates, which assume all polymer is excluded from the condensates, can also be applied to the protein-DNA filaments that we study here. The idea is to compare the free energies (or chemical potentials) of inserting semiflexible polyelectrolytes in solutions of flexible polymers in resp. the free and condensed form. Insertion of free (i.e uncondensed or extended) semiflexible polyelectrolytes can be dealt with using polymer scaling theory. Per unit length of semiflexible polymer:

$$f_{ins,\,free} \approx \mu_1 w + \mu_2 w^{9/4} \qquad \text{(eq. 5.1)}$$

where w is the polymer weight concentration (%w/v), and μ_1 and μ_2 are numerical prefactors that depend on the radius a of the semiflexible polyelectrolyte. When inserting a condensate,

one has to first push away the flexible polymers (osmotic work) to create space for the condensate and then to assemble the condensate inside this space (packing energy):

$$f_{ins,cond} \approx f_{osm} + f_{pack} \qquad \text{(eq. 5.2)}$$

The packing energy is dominated by the electrostatic repulsion between neighbouring semiflexible polyelectrolytes in liquid-crystalline condensates, and possibly enhanced by thermal undulations (Odijk, 1993; Strey *et al*., 1999). It can be estimated using theoretical equations of state for liquid crystalline semiflexible polyelectrolytes (Odijk, 1993; Strey *et al*., 1999), or computed from experimentally determined osmotic pressures of polyelectrolyte liquid crystals (Strey *et al*., 1999). To estimate the amount of polymer need to condense semiflexible polyelectrolytes we use the fact that the chemical potentials, or insertion free energies, should be equal at the transition point:

$$f_{ins,free} \approx f_{ins,cond} \qquad \text{(eq. 5.3)}$$

To change the critical concentration of depletion agent needed for condensation (without changing the depletion agent itself) requires changing either the insertion energy for free semiflexible polyelectrolytes, or the insertion free energy of condensed semiflexible polyelectrolytes. The former is especially sensitive to the radius *a* of the semiflexible polyelectrolyte, the latter especially to the polyelectrolyte linear charge density *ν*.

Polyelectrolyte	*a* (nm)	*ν* (*e*/nm)	w_c (%)
DNA	1.0 (Krueger *et al*., 1999)	0.17	8
Sso7d-coated DNA	2.5 (Krueger *et al*., 1999)		3
F-actin (Tang *et al*., 1997)	4.0	0.25	3

Table 5.1: Critical polymer concentrations needed to condense semiflexible polyelectrolytes at ns = 0.15M

This is illustrated in Table 5.1 where we compare typical condensation thresholds for resp. naked DNA, Sso7d-coated DNA (saturated filaments), and F-actin filaments. The Sso7d protein is basic with an estimated charge at pH 7 of +4…+6 (extrapolated from Tang *et al*., 1997). This means that the net electrostatic repulsion between saturated Sso7d-DNA filaments will certainly be less than that between naked DNA, but it is not clear by exactly how much. Comparing this to naked DNA and F-actin it is clear that the increased effective polyelectrolyte radius induced by protein binding cannot fully explain the decrease of the condensation threshold. Therefore, it is very likely that in the present case the decreased

effective charge of the protein-DNA filaments also plays a significant role in reducing the condensation threshold.

Although we here assume flexible polymers as the depletion agent, the conclusions may be expected to hold more generally: thick protein-DNA filaments with a low net charge density are much more susceptible to depletion condensation, be it by flexible polymers, or by cytoplasmic, non-DNA binding proteins.

What is the role of this synergy in the formation and stabilization of nucleoids in prokaryotic cells? Odijk (1998) has convincingly shown that for the supercoiled genomic DNA of bacteria, confined by the bacterial cell wall, depletion interactions of the DNA with non-binding proteins are sufficiently strong to drive a phase separation into a nucleoid phase rich in DNA (but not as concentrated as DNA condensates obtained from dilute solutions) and a cytoplasm phase rich in non-binding globular proteins. Our results suggest that the effect of nucleoid proteins could be included in such a theory (to lowest order) by allowing for a somewhat larger thickness and a lower charge density of the DNA.
In any case, it is clear that if some particular nucleoid protein-DNA filament is extended and/or rigid in dilute solution, this clearly does not mean that the protein does not contribute to DNA compaction in the crowded environment of the living cell

Acknowledgements
We thank Stephen Edmondson for providing the E. coli strain overexpressing Sso7d, and John van der Oost for useful discussions. EB was supported by a CAPES grant.

References

Dame, R. T. and Goosen, N. 2002. HU: promoting or counteracting DNA compaction? FEBS Letters 529:151-156.

Dorman, C. J. and Deighan, P. 2003. Regulation of gene expression by histone-like proteins in bacteria. Current Opinion in Genetics & Development 13:179-184.

Krueger, J. K., B. S. McCrary, A. H. J. Wang, J. W. Shriver, J. Trewhella, and S. P. Edmondson. 1999. The solution structure of the Sac7d/DNA complex: A small-angle X-ray scattering study. Biochemistry 38:10247-10255.

McAfee, J. G., S. P. Edmondson, P. K. Datta, J. W. Shriver, and R. Gupta. 1995. Gene cloning, expression and characterization of the Sac7 proteins from the hyperthermophile *Sulfolubus acidocaldarius*. Biochemistry 4:10063-10077.

Murphy, L. D., and S. B. Zimmerman. 1995. Condensation and cohesion of λ DNA in cell extracts and other media: Implications for the structure and function of DNA in prokaryotes. Biophys. Chem. 57:71-92.

van Noort, J., S. Verbrugge, N. Goosen, C. Dekker, and R. T. Dame. 2004. Dual architectural roles of HU: Formation of flexible hinges and rigid filaments. Proc. Natl. Acad. Sci. U. S. A. 101:6969-6974.

Odijk, T. 1998. Osmotic compaction of supercoiled DNA into a bacterial nucleoid. Biophysical Chemistr 73:23-29.

Odijk, T. 1993. Undulation-enhanced electrostatic forces in hexagonal polyelectrolyte gels. Biophys. Chem. 46:69-75.

Strey, H. H., V. A. Parsegian, and R. Podgornik. 1999. Equation of state for polymer liquid crystals: Theory and experiment. Physical Review E 59:999-1008.

Tang, J. X., T. Ito, T. Tao, P. Traub, and P. A. Janmey. 1997. Opposite effects of electrostatics and steric exclusion on bundle formation by F-actin and other filamentous polyelectrolytes. Biochemistry 36:12600-12607.

Todorova, R., and B. Atanasov. 2004. The role of the salt concentration, proton, and phosphate binding on the thermal stability of wild and cloned DNA-binding protein Sso7d from *Sulfolobus solfataricus*. International Journal of Biological Macromolecules 34:135-147.

de Vries, R. 2001. Flexible polymer-induced condensation and bundle formation of DNA and F-actin filaments. Biophys. J. 80:1186-1194.

Chapter 6

General Discussion:

the extent of DNA compaction by nucleoid proteins

6.1 Introduction

The main topic of this thesis is the interplay between H-NS and macromolecular crowding in compacting DNA. Our broader motivation for this study is to better understand the formation of nucleoid structures in prokaryotes. More generally, DNA condensation or compaction *in vivo* is thought to occur by at least four mechanisms: the association of nucleoid proteins with DNA, macromolecular crowding, neutralization of the charges on DNA and DNA supercoiling. Whether these mechanisms can be considered the main driving force for the formation of the prokaryotic nucleoid is a matter of on-going debate. An important problem is that many questions on DNA compaction in bacteria are asked on a qualitative (yes or no) level. As explained in the introduction, compared to a freely coiling, linear DNA with the length of the bacterial genome, the required degree of (volume) compaction is 10^3-10^4, or 3 to 4 orders of magnitude. Another way of specifying the required degree of compaction is in terms of the DNA weight concentration in the bacterial nucleoid. For the 4.7 Mbp long *E coli* genomic DNA, in a nucleoid with a typical volume of 0.1-0.3 μm^3 (Woldringh and Nanninga, 1985), this weight concentration is around 100 g/L (Bohrmann *et al*., 1993).

To make progress, it is crucial to establish the quantitative contribution of the various mechanisms to the overall degree of DNA compaction. As an example, the direct contribution of supercoiling to the compaction of the genomic bacterial DNA has been shown to be only about 1 order of magnitude by detailed numerical estimates (Cuhna *et al*., 2001). Many papers on NAPs state that nucleoid proteins are very important for compacting DNA without much proof. In this discussion we critically analyse the existing data on DNA compaction by nucleoid proteins by reviewing the methods used, and the results obtained by previous studies to underpin the importance additional mechanisms such as macromolecular crowding. The degree of volume reduction of DNA coils by nucleoid proteins is the crucial quantity that we wanted to extract from aforementioned papers. We can conclude that nucleoid proteins typically reduce the volume of large DNA coils by one order of magnitude or less, with a few notable exceptions (Dps in particular). Hence, the extent of the NAPs' direct contribution to compaction is similar to that of supercoiling, but even the combined effect of supercoiling and nucleoid proteins (about 2 orders of magnitude in volume reduction) is not sufficient. Other mechanisms such as macromolecular crowding must contribute too.

6.2 Nucleoid-associated proteins and DNA compaction

Nucleoid-associated proteins or NAPs bind to - and often deform - DNA. They are present in high copy numbers compared to other DNA binding proteins, like DNA replication proteins and transcription factors. NAPs have an established role in the regulation of bacterial gene expression. These same proteins are also thought to play a major role in establishing the architecture of the nucleoid. In this discussion we ask the question: do NAPs also contribute to compaction into a dense nucleoid structure? Many previous studies have answered this question affirmatively, but did not check the actual *degree* of DNA volume reduction caused by nucleoid proteins compared to the typical degree of compaction required for nucleoid formation (the volume of a freely coiling linear DNA molecule with the length of the genomic DNA must be reduced by 3 or 4 orders of magnitude). We first briefly review the techniques commonly used to assess DNA compaction by nucleoid proteins, and discuss their relative strengths and limitations. Next, we review results that have been obtained for a range of bacterial nucleoid proteins.

A very simple assay for DNA condensation is based on sedimentation (Figure 6.1a). The method relies on highly condensed DNA sedimenting at increased gravitational fields. The assay measures the fraction of condensed DNA, deduced from the DNA concentration in the supernatant, as a function of the buffer composition (which may include crowding agents, NAPs, etc.). It cannot determine the actual degree of compaction. An example of this approach is the work of Murphy and Zimmerman (1995). We have used this simple assay for both H-NS and Sso7d, in Chapters 3 and 5 of this thesis.

Next, static and dynamic light scattering are classical physical techniques for determining solution sizes that can be applied to a very wide range of systems. As mentioned in the introduction, many light scattering studies have been performed on linear and supercoiled DNA, but very few studies have extended this approach to the effect of NAPs on DNA coil sizes in solution, as we do here. However, for the cases that we have studied (the bacterial nucleoid protein H-NS from *E. coli*, and the archaeal nucleoid protein Sso7d from *Sulfolobus Solfataricus*) we found that the binding of the nucleoid proteins hardly influenced the solution coil size of plasmid DNA.

For very large DNA coils, coil sizes can be determined directly by fluorescence microscopy (Yoshikawa *et al*., 1995). The method requires DNA labelling, which can influence DNA behaviour, but carefully chosen dyes and dye concentrations resolve that

problem. Coil sizes should be larger than a micron to be able to give accurate volume estimates. Therefore, the method is best at measuring moderate degrees of compaction, and cannot (quantitatively) determine compaction factors as large as 10^3 to 10^4. Those condensates have sizes below the optical resolution. For example, if we were to compact 48.5 kDa λ DNA (commonly used in these studies) to a final (internal) concentration of around 100 g/L, comparable to the DNA concentration in the nucleoid, this would correspond to a radius of the compacted coil of around 60 nm.

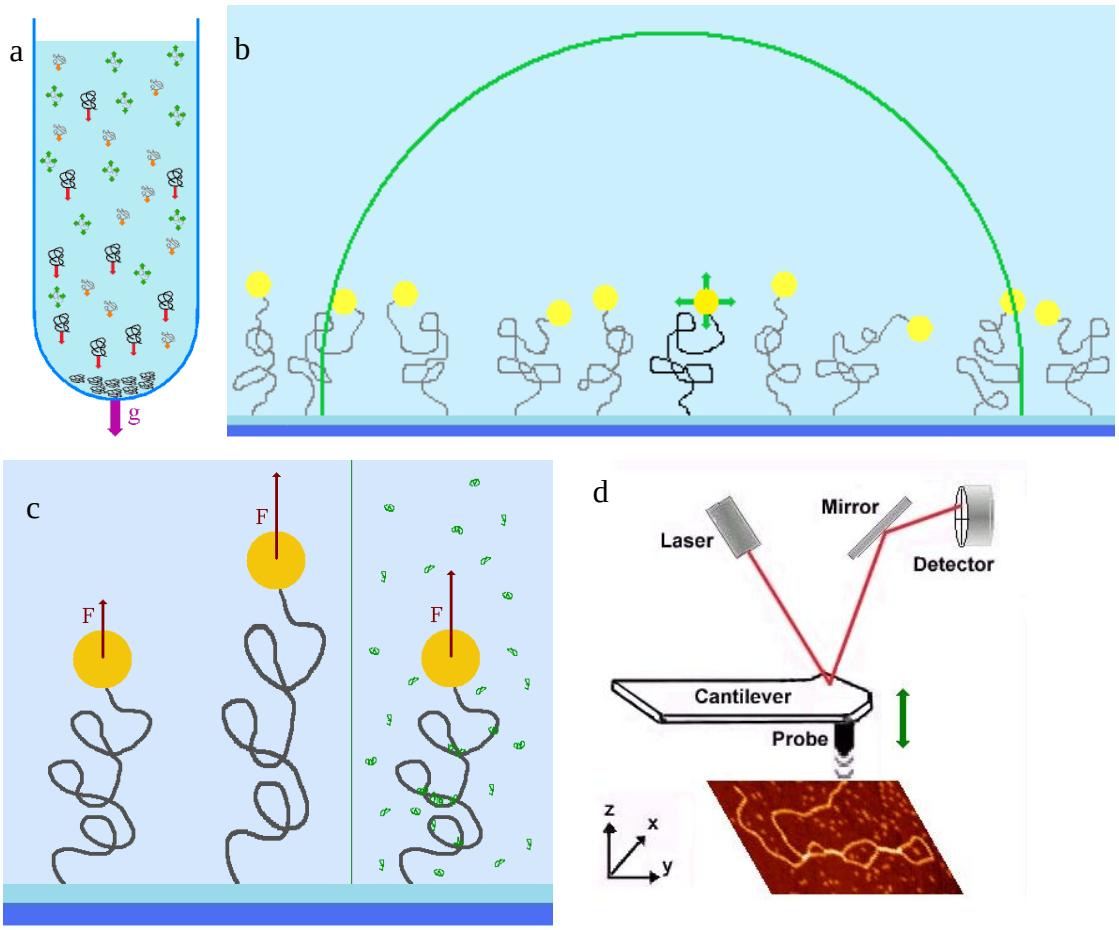

Figure 6.1: Representations of techniques commonly used in DNA compaction assays
a) Schematic representation of a sedimentation or precipitation assay. The most dense particles sediment first, and addition of NAPs and depletion increase the density of DNA coils. c) Beads tethered to a surface by a polymer can be microscopically followed to find changes in diffusion and end-to-end distance. d) In DNA pulling experiments an optical or magnetic trap is used to move a bead bound to DNA, and force/extension curves can be measured with and without protein. e) AFM detects the surfaces by means of a cantilever.

Another single-molecule technique to assess DNA compaction is the tethered particle motion experiment (Figure 6.1b). Beads are bound to single DNA molecules tethered to a

surface. Positions of many beads are tracked and analysed to give highly accurate distributions for the centre-of-mass position of the beads. These can be analysed in terms of the configurational properties of the DNA chains (reviewed by Nelson, 2007). While in tethered-particle motion assays, the DNA under observation is not under the influence of external forces, in other experiments tethered DNA is stretched and rotated by exerting forces on the beads, either using laser traps or magnetic fields (Figure 6.1c).. Typically these experiments are done to investigate phenomena that occur at various levels of force rather than determining DNA coil sizes in the absence of external forces. Analysis of bead positions is typically done by optical microscopy, which is adequate to determine typical extensions on the order of a μm or more. The DNA coils preferentially used in these experiments, such as 48.5 kDa λ DNA, have a size well below optical resolution if they are compacted to the same final DNA concentration as in the bacterial nucleoid, which means that only moderate degrees of compaction can be quantified.

Quite some work on the effect of nucleoid proteins on DNA configurations has also been done using Atomic Force Microscopy or AFM (Figure 6.1d). AFM observes DNA immobilized on a surface, rather than free in solution. Often, samples are dried before measurement. Both the surface attachment and drying steps may influence the DNA configurations, which makes the deduction of changes in DNA coil volume induced by NAPs in solution problematic. On the other hand, more local effects can be analysed successfully, such as angles of DNA bending induced by NAP binding and NAP-induced DNA stiffening. All of the methods described above have been used on nucleoid proteins, as we discuss below. Yet none has been specifically designed to quantify the extreme degrees of compaction of DNA that occur when the bacterial chromosomal DNA is compacted into the tiny volume of the bacterial nucleoid. Nevertheless, here we summarize the information on compaction that we extracted from these measurements. Before we do so, we must note that at physiological ionic strength, electrostatic interactions of DNA are screened to a large extent. Some authors have also studied the effects of NAPs on DNA configurations at low ionic strengths. This is problematic because non-specific electrostatic interactions become very important at low ionic strengths and the basic NAPs start to form dense, non-specific condensates as any polycation would do. Therefore, we will mainly compare results that have been obtained at higher ionic strengths.

Study	*DNA* Type	*Protein* Species	C nM	*Buffer*	*Force* pulling pN	*End-to-end distance* No protein µm	Max. protein µm
van Noort *et al*. 2004	modified pSFV1 10 kbp 3.2 µm long 1.82×10^{-2} μm^3 coil	HU *E. coli*	40	60 mM KCl 20 mM Hepes pH7.9	1 0.5 0.09 0.05 0.009	2.7 2.4 1.7 1.0 0.5	1.8 1.5 0.8 0.3 0.2
Xiao *et al*. 2011	λ-DNA 48,5 kbp 15.5 µm long 0.19 µm3 coil	HU *E. coli*	500	PBS buffer	0.8 0.3 0.1 0.05	14.1 12.8 8.7 6.4	12.8 10.7 4.1 2.7
Ali *et al*. 2001	λ-DNA Idem Xiao *et al.*	IHF *E. coli*	1250	10 mM TrisHCl 0.2M KCl 5% DMSO 0.1 mM EDTA 0.2 g/l casein pH 8.0	1 0.1 0.015	14.2 9.2 2.5	13.8 7.4 1.5
Skoko *et al*. 2006	λ-DNA Idem Xiao *et al.*	FIS *E. coli*	20	20 mM HEPES 0.1 M KGlu 500 nG BSA 5% glycerol pH 7.6	1 0.45 0.2 0.03	14.1 12.5 9.6 6.7	12.1 9.4 6.1 3.2
			13000 6000 1000 500 200		0.6 0.3 0.2 0.1 0.06	14.5 12.9 11.5 8.2 6.2	<0.5 <0.5 <0.5 4.8 4.4
Amit *et al*. 2003	λ-DNA Idem Xiao *et al.*	H-NS *E. coli*	250	Idem Ali *et al.*	1 0.5 0.1 0.05 0.02	14.6 13.0 8.5 5.6 2.4	14.9 13.6 9.4 6.6 3.0
			4000		1 0.5 0.1 0.05 0.02	14.6 13.0 8.5 5.6 2.4	15.8 15.5 12 10.1 6.4
Liu *et al*. 2010	ΦX174 DNA 5,386 bp 1.7 µm long 7.2×10^{-3} μm^3 coil	H-NS *E. coli*	600	5 mM KCl	1 0.5 0.1 0.06	14.2 12.8 8.2 5.7	15.0 14.7 12.5 11.3
				600 mM KCl	1 0.5 0.1 0.06	14.2 12.8 8.2 5.7	14.2 12.8 8.2 5.7
				50 mM KCl	0.8 0.4 0.1 0.05	13.7 12.7 8.4 5.7	14.3 13.7 11.0 8.9
				50 mM KCl 5 mM MgCl	0.8 0.4 0.1 0.05	13.7 12.7 8.4 5.7	14.0 13.1 <4 <4

Table 6.1: An overview of DNA compaction in single molecule force extension experiments for the NAPs HU, IHF, FIS and H-NS.

Dps

We will start our overview on DNA compaction by NAPs with a nucleoid protein that undoubtedly induces dramatic DNA compaction: the nucleoid protein Dps. It is thought to

protect the genomic DNA under conditions that are adverse for bacterial growth. The Dps protein interacts with DNA through a tail of basic lysine residues (Ceci *et al*., 2004), without inducing significant deformations in the DNA. Dps is present at low levels during early growth, and increases dramatically to about 180,000 copies per cell during late stationary phase in *E. coli* (Azam *et al*., 1999). These high concentrations of Dps induce protective biocrystallization of DNA (Wolf *et al*., 1999), which is physiologically relevant if organisms are exposed to a severe environment. DNA-Dps assemblies have been shown to be crystal-like objects with sizes >100 nm diameter in EM pictures. The crystals are thought to contain most genomic DNA *in vivo* (Wolf *et al*., 1999). Dps also compacts DNA into a crystalline phase *in vitro*. The ordered packaging is thought to thread DNA between Dps dodecamers (Minsky, 2004) and appears to reduce DNA coil volume by orders of magnitude, but the available data does not allow us to make a more quantitative estimate.

HU

Many nucleoid proteins induce DNA bending, and some of the studies include experiments that give quantative information about the extent of NAP-induced DNA compaction. Among the major bacterial nucleoid proteins, HU is especially well studied. Using magnetic tweezers force-extension experiments and AFM imaging, van Noort *et al.* (2004) find that 40 nM of HU induces moderate compaction of 10 kbp DNA. At this concentration, the end-to-end distance decreases by a factor of about three under low forces, implying the coil volume is compacted by about one order of magnitude. At higher concentrations (500 to 1000 nM), AFM imaging shows that HU fully coats linear DNA and forms a helical filament that is significantly stiffer than naked DNA according to the force extension measurements. Similar experiments have been performed with longer λ DNA (table 6.1) (Xiao *et al*., 2011). Using a somewhat different buffer these authors find that the moderate compaction persist up to HU concentrations of 500nM.

Homologous nucleoid proteins do not necessarily behave the same with respect to DNA compaction: HUBst from thermophylic *Bacillus stearothermophilus* (~60% homology with *E. coli* HU, Drlica and Rouviere-Yaniv, 1987) has been reported to compact DNA to a significantly greater extent than *E. coli* HU. A fluorescence microscopy study showed (Endo *et al*., 2002) that HUBst compacts 166 kbp linear T2 DNA gradually. The median longest axis length decreases from ~2.6 to ~0.8 μm when HUBst concentration increases from 0 to 930 nM, implying a compaction factor of ~30 in terms of the coil volume (table 6.2). Another recent study on HUBst by Nir *et al*. (2011) used a tethered bead assays in PBS buffer, and a

2.7 kbp fragment of λ-DNA. These authors find that the median bead height decreased from 150 nm for 0 nM HU to ~90 nm for 500 nM HU (table 6.2). It increases again at higher HUBst concentration, confirming the stiffening effect also found for *E. coli* HU, but in apparent disagreement with the fluorescence microscopy study by Endo *et al*. (2002), which may have been caused by lack of a buffering agent.

Yet another HU homologue, TmHU from *Thermogata maritima* (61.1% homology with HUBst, Christodoulou and Vorgias, 2002), has been studied using force-extension experiments by Wagner *et al*. (2011). For 4 kbp plasmid DNA, the extension was found to decrease from 1.36 μm to ~0.4 μm at a force of 2 pN and a very high TmHU concentration of 10.5 μM. This corresponds to a compaction of the coil volume of one order of magnitude. The ionic strength of the buffer used by these authors was rather low, such that the observed effects might also be due to non-specific electrostatics.

In summary: HU is typically found to decrease coil volumes by approximately one order of magnitude at intermediate concentrations of HU, followed by stiffening and coil expansion at higher concentrations.

Study	*DNA*	*Protein*		*Buffer*	*Radius of DNA coil*	
	type	Species	C nm		No protein μm	Max. protein μm
Endo *et al*., 2002 *Fluorescence microscopy*	T2 DNA 166 kbp 53.12 μm long	HU *Bacillus stearothermophil*.	930	200 mM NaCl	2.6	0.8
Nir *et al*., 2011 *Tethered particle motion*	λ-DNA fragment 2.7 kbp 0.86 μm long	HU *Bacillus stearothermophil*.	500	50 mM NaPhosphate 50 mM NaCl 10 mM EDTA 0.02% Tween pH 7.5	0.15	0.09
Ali *et al*., 2001 *Tethered particle motion*	IHF-site fragment 1288 bp 0.41 μm long	IHF *E. coli*	500	As described in Table 6.1	x	x

Table 6.2: Volume reduction by HU and IHF in fluorescence microscopy and tethered particle motion experiments.

IHF and FIS

The other DNA-bending nucleoid proteins have been the subject of fewer studies, but some experiments have been performed for IHF and FIS. Magnetic tweezers experiments on IHF binding to λ-DNA (Ali *et al*., 2001) show that at a high concentration of 1250 mM IHF, the DNA extension decreases by ~4 times at a low force of at ~0.015 pN, corresponding to a compaction of the DNA coil volume by less than an order of magnitude (Table 6.1). In tethered bead experiments, the decrease in DNA extension levels off at ~500 nM of IHF, and again the final compaction factors of the DNA coil volume are less than an order of

magnitude (Table 6.2). FIS, another major DNA bending nucleoid protein, has also been subjected to various single molecule studies. In DNA stretching experiments, FIS collapses λ-DNA in 100 mM KGlu at low forces and protein concentrations of >1 μM (Skoko *et al*., 2005). In a follow-up paper Skoko *et al*. (2006) report that at a low force of ~0.03 pN, FIS decreases the extension of λ-DNA from 6.7 μm to 3.2 μm at 20nM of FIS and to 4.4 μm at 200nM of FIS and double force. Both cases correspond to compaction factors of the coil volume of at most one order of magnitude. In the same paper, Skoko *et al.* also quantify the collapse initially described in the first paper (Table 6.1) and find that at least 1 μM of FIS is required to abruptly reduce the end-to-end distance of DNA to <0.5 μm, which is the resolution of the experiment. This means that "collapse" should be taken to mean that the DNA concentration inside the condensed λ-DNA coil is higher than about 1 g/L (assuming a spherical coil with a 250 nm radius). Hence the optical resolution is still very far away from the level of compaction inside bacterial nucleoids, which corresponds to DNA concentrations of around 100 g/L. Hence, while it is very interesting that an apparent "collapse transition" is observed, at this stage it is still uncertain what degree of compaction is achieved for this case.

H-NS

H-NS is the most important NAP in the context of this thesis. In the introduction we discussed a number of AFM studies of H-NS, where it seems to compact plasmid DNA by introducing DNA-DNA bridges (for example Dame *et al*., 2001). The existence of these bridges was proven conclusively by single molecule experiments with two strands of stretched DNA (Dame *et al*., 2006), but that set-up does not determine compaction by H-NS. Here we review the results of a number of force-extension measurements of DNA in the presence of H-NS focussing in particular on the extent of compaction.

Although initial microscopy data (AFM and EM) indicated that the H-NS dimer mainly binds in a bridging mode, the DNA force-extension curves in the presence of H-NS by Amit *et al.* (2003) suggest that there are also conditions in which DNA does not form bridges. These authors find that H-NS binding increases the end-to-end distance of DNA coils, presumably by stiffening the DNA. Maximal stiffening at high (4 μM) concentrations of H-NS corresponds to a volume increase of the DNA coils by a factor of order 10. Recently, it was argued by Liu *et al*. (2011) that the mode of H-NS DNA binding may depend on solution conditions, with a particularly prominent role for the concentration of divalent ions. From DNA force extension curves in the presence of H-NS, Liu *et al*. also find that H-NS increases

the end-to-end distance of DNA coils, but only in absence of Mg^{2+}, and especially at lower salt concentrations. At higher salt (200 mM KCl) but still in the absence of divalent cations, no apparent DNA stiffening is observed from the force-extension curves, at least not up to a concentration of 600 nM H-NS (Table 6.1). When Mg^{2+} is added at high H-NS concentrations, the end-to-end distance of the DNA coils drops below the value of naked DNA. AFM imaging also confirms that the binding mode of H-NS depends on solution conditions, and that both bridging and non-bridging binding modes occur.

Dramatic compaction or collapse to end-to-end distances below the (optical) resolution of the instrument occurs at critical Mg^{2+} concentrations that depend on the force: 10mM Mg^{2+} at a force of 0.2pN and 5mM Mg^{2+} at a force of 0.1pN. Again, compaction to coil sizes below the optical resolution may still be very far from extreme degree of compaction that occurs in the *E. coli* nucleoid, and which corresponds to DNA concentrations of around 100g/L.

All studies mentioned so far have focused on one single NAP. It is widely believed that at least in regulation gene expression, NAPs work together. A similar cooperative effect of multiple types of NAPs may also be important in determining the organization of DNA in the bacterial nucleoid. Maurer *et al*. (2009) have combined H-NS, HU and IHF with λ and 1 kbp DNA and studied its local effects on DNA by AFM. While this approach does not tell much about extreme compaction of very large DNA, it is useful for determining the local structure of mixed NAP/DNA complexes. For combinations of two NAPs and λ DNA, irregular NAP/DNA fibres were observed, but when all three NAPs bind DNA simultaneously, regularly folded stretches were found of up to 700 nm long (Maurer *et al*., 2009).

Archaeal NAPs

The nucleoids of archaea are not contained by membranes, much like bacteria, and also have a range of different nucleoid associated proteins. But, much less is known about archaeal nucleoid proteins, as compared to their bacterial counterparts. Here we only mention two nucleoid proteins from the Archaea that have received some attention in the biophysical literature. The first one is the 7 kDa basic protein Sso7d from *S. Solfataricus* (and its homologues from related genera). This protein has also been studied in this thesis, in Chapter 5. The second protein is the 10kDa basic protein called Alba or Sac10b that is more widespread in the Archaea. The Sso7d protein, and its homologues, introduces a sharp bend into double stranded DNA via the insertion of hydrophic residues into the major groove

(Baumann *et al*., 1994). Small angle X-ray studies (Krueger *et al*., 1999) have shown that full coating of dsDNA with Sso7d does not lead to the compaction of large DNA coils. In chapter 5, we arrive at a similar conclusion based on light scattering studies of complexes of linearized plasmid DNA with Sso7d. The protein Alba interacts with DNA in more complicated way: EM images show both coating of single dsDNA and bridging of two dsDNA, depending on protein concentration (Lurz *et al*., 1986; Jelinska *et al*. 2005). Hence, at least under some conditions, Alba is a DNA bridging protein, and may lead to compaction of large DNA coils, as has been observed for H-NS in the presence of Mg^{2+} (Liu *et al.*, 2011).

Presently, the influence of these and other archaeal nucleoid proteins are also being investigated using single molecule DNA force-extension measurements (Remus Dame, *personal communication*) and such experiments may give more quantitative information on stiffening and compaction of DNA induced by them.

6.4 Conclusion

In summary, from the available data it is not at all clear that nucleoid proteins are the dominant driving force for DNA compaction in prokaryotes. Instead, single molecule DNA force extension measurements indicate that many nucleoid proteins simply coat and stiffen DNA, or induce compaction of around one order of magnitude (in terms of the coil volume), which is only a small contribution towards the final degree of DNA compaction that is achieved in the bacterial nucleoid, and which corresponds to DNA concentrations of around 100 g/L. In a few cases, the single molecule experiments (both fluorescence microscopy and force-extension measurements) find DNA collapse down to coil sizes below the resolution of the experiments: H-NS at higher concentrations of Mg^{2+}, and FIS. Since the local DNA concentration in a coil of e.g. λ-DNA that has been collapsed into a sphere with a radius of around 250 nm is still only about 1 g/L, the actual degree of compaction may still be orders of magnitude away from the actual degree of DNA in bacterial nucleoids.

For determining actual degrees of compaction, one approach would be to use fluorescence microscopy on isolated bacterial nucleoids, as we have done in Chapter 4. The size of the bacterial nucleoid is just on the boundary of the resolution of fluorescence microscopy, so degrees of compaction comparable to those in the bacterial nucleoid can be determined at least semi-quantitatively for this case. In this thesis, we have only applied the method for H-NS in the absence of Mg^{2+} or other multivalent cations, for which no collapse

occurs in the absence of macromolecular crowding, but it would be very interesting to extend these measurements to conditions and nucleoid proteins for which collapse reported, in particular FIS, and H-NS in the presence of multivalent cations.

References

Ali, B.M.J., Amit, R., Braslavsky, I., Oppenheim, A.B., Gileadi, O. and Stavans, J. 2001. Compaction of single DNA molecules induced by binding of integration host factor (IHF). Proc. Natl. Acad. Sci. USA 98(19): 10658-10663

Amit, R., Oppenheim, A.B. and Stavans, J. 2003. Increased bending rigidity of single DNA molecules by H-NS, a temperature and osmolarity sensor. Biophysical Journal 84(4): 2467-2473.

Azam, T.A., Iwata, A., Nishimura, A., Ueda, S. and Ishihama, A. 1999. Growth phase-dependent variation in protein composition of the *Escherichia coli* nucleoid. Journal of Bacteriology 181(20): 6361-6370

Baumann, H., S. Knapp, T. Lundback, R. Ladenstein, and T. Hard. 1994. Solution structure and DNA-binding properties of a thermostable protein from the archaeon Sulfolubus solfataricus. Nat. Struct. Biol. 1:808-819.

Bohrmann, B., M. Haider, and E. Kellenberger. 1993. Concentration evaluation of chromatin in unstained resin-embedded sections by means of low-dose ratio-contrast imaging in STEM Ultramicroscopy 49:235-251.

Ceci, P., Cellai, S., Falvo, E., Rivetti, C., Rossi, G. L. and Chiancone, E. 2004. DNA condensation and self-aggregation of *Escherichia coli* Dps are coupled phenomena related to the properties of the N-terminus. Nucleic Acids Research 32:5935-5944.

Christodoulou, E., and Vorgias, C. E. 2002. The thermostability of DNA-binding protein HU from mesophilic, thermophilic, and extreme thermophilic bacteria. Extremophiles 6:21-31

Cunha, S., Woldringh, C.L. and Odijk, T. 2001. Polymer-mediated compaction and internal dynamics of isolated *Escherichia coli* nucleoids. Journal of Structural Biology 136(1): 53-66

Dame, R.T., Wyman, C. and Goosen, N. 2001. Structural basis for preferential binding of H-NS to curved DNA. Biochimie 83(2): 231-234

Dame, R.T., Noom, M.C. and Wuite, G.J.L. 2006. Bacterial chromatin organization by H-NS protein unravelled using dual DNA manipulation. Nature 444:387-390.

Drlica, K. and Rouviere-Yaniv, J. 1987. Histone-like proteins of bacteria. Microbiological Review 51:301-319.

Endo, T., Sasaki, N., Tanaka, I. and Nakata, M. 2002. Compact form of DNA induced by DNA-binding protein HU. Biochemical and Biophysical Research Communications 290(1): 546-551

Jelinska, C., Conroy, M. J., Craven, C. J., Hounslow, A. M., Bullough, P. A., Waltho, J. P., Taylor, G. L. and White, M. F. 2005. Obligate heterodimerization of the archaeal Alba2 protein with Alba1 provides a mechanism for control of DNA packaging. Structure 13:963-971.

Krueger, J.K., McCrary, B.S., Wang, A.H.J., Shriver, J.W., Trewhella, J. and Edmondson, S.P. 1999. The solution structure of the Sac7d/DNA complex: a small angle X-ray scattering study. Biochemistry 38: 10247-10255

Liu, Y. J., Chen, H., Kenney, L. J. and Yan, J. 2011. A divalent switch drives H-NS/DNA-binding conformations between stiffening and bridging modes. Genes & Development 24:339-344.

Lurz, R., Grote, M., Dijk, J., Reinhardt, R. and Dobrinski, B. 1986. Electron-microscopic study of DNA complexes with proteins from the archaebacterium *Sulfolubus-acidocaldarius*. EMBO Journal 5:3715-3721.

Maurer, S., Fritz, J. and Muskhelishvili, G. 2009. A Systematic In Vitro Study of Nucleoprotein Complexes Formed by Bacterial Nucleoid-Associated Proteins Revealing Novel Types of DNA Organization. Journal of Molecular Biology 387:1261-1276.

Minsky, A. 2004. Information content and complexity in the high-order organization of DNA. Annual Review of Biophysics and Biomolecular Structure 33: 317-342.

Murphy, L.D. and Zimmerman, S.B. 1995. Condensation and cohesion of λ DNA in cell extracts and other media: Implications for the structure and function of DNA in prokaryotes. Biophysical Chemistry 57(1): 71-92

Nelson, P.C. 2007. Colloidal particle motion as a diagnostic of DNA conformational transitions. Current Opinion in Colloid & Interface Science. 12: 307-313.

Nir, G., Lindner, M., Dietrich, H. R. C., Girshevitz, O., Vorgias, C. E. and Garini, Y. 2011. HU Protein Induces Incoherent DNA Persistence Length. Biophysical Journal100:784-790.

van Noort, J., Verbrugge, S., Goosen, N., Dekker, C. and Dame, R. T. 2004. Dual architectural roles of HU: Formation of flexible hinges and rigid filaments. Proc. Natl. Acad. Sci. USA 101(18): 6969-6974

Skoko, D., Yan, J., Johnson, R. C. and Marko, J. F. 2005. Low-force DNA condensation and discontinuous high-force decondensation reveal a loop-stabilizing function of the protein Fis. Physical Review Letters 95(20): ???

Skoko, D., Yoo, D., Bai, H., Schnurr, B., Yan, J., McLeod, S. M., Marko, J. F. and Johnson, R. C. 2006. Mechanism of chromosome compaction and looping by the *Escherichia coli* nucleoid protein Fis. Journal of Molecular Biology 364:777-798.

Wagner, C., Olbrich, C., Brutzer, H., Salomo, M., Kleinekathofer, U., Keyser, U. F. and Kremer, F. 2011. DNA condensation by TmHU studied by optical tweezers, AFM and molecular dynamics simulations. Journal of Biological Physics 37:117-131.

Woldringh, C.L. and Nanninga, N. Structure of nucleoid and cytoplasm in the intact cell. In: N. Nanninga (Ed.) Molecular Cytology of *Escherichia coli.* London: Academic Press; 1985, pp. 161–197.

Wolf, S. G., Frenkiel, D., Arad, T., Finkel, S. E., Kolter, R. and Minsky, A. 1999. DNA protection by stress-induced biocrystallization. Nature 400: 83-85.

Xiao, B.T., Zhang, H.Y., Johnson, R.C. and Marko, J.F. 2011. Force-driven unbinding of proteins HU and Fis from DNA quantified using a thermodynamic Maxwell relation. Nucleic Acids Research 39:5568-5577.

Yoshikawa, K., and Matsuzawa, Y. 1995. Discrete phase transition of giant DNA dynamics of globule formation from a single molecular chain. Physica D 84: 220-227.

Chapter 7

Summary & Samenvatting

7.1 Summary

In this dissertation we discuss H-NS and its connection to nucleoid compaction and organization. Nucleoid formation involves a dramatic reduction in coil volume of the genomic DNA. Four factors are thought to influence coil volume: supercoiling, DNA charge neutralization, macromolecular crowding and DNA deformation by NAPs. This study focuses mainly on the latter two factors, and on their interplay. We investigate both direct and indirect changes in DNA coil volume as a result of H-NS binding to DNA. H-NS / DNA binding is thought to be influenced by the self-association of H-NS, hence DNA self-association (both in bulk and on DNA) has also been investigated.

Chapter 2 focuses on the known cooperative character of H-NS-DNA binding. The molecular origin of the cooperativity is poorly understood. High concentrations of H-NS are known to oligomerize extensively in the absence of DNA. Some models propose that cooperativity is caused by the same protein-protein interactions that cause oligomerization in solution, whereas others propose cooperativity may be induced by the DNA substrate. We have mutated some parts of H-NS we believed to be important in oligomerization to investigate the role of H-NS protein-protein interactions in cooperative DNA binding, and studied the oligomerization and DNA-binding properties of these mutants. The D68VD71V mutant has two aspartic acids in the linker region replaced by valines, making the linker significantly more hydrophobic. The double linker mutation D68VD71V dramatically enhances H-NS oligomerization in solution, and its temperature-dependence is changed as well *in vitro*. Yet there is only a moderate effect on DNA binding properties, which does point in the direction of enhanced cooperativity, as expected. This suggests that protein-protein interactions have a much larger effect on H-NS self-association in solution than on the DNA binding properties.

Chapter 3 discusses the influence of the bacterial nucleoid protein H-NS on DNA coil sizes in solution, using Light Scattering, for both supercoiled and linear pUC18 DNA. We clearly find H-NS binding: the intensity of light scattered by the DNA coils increased upon the addition of H-NS. But, H-NS did not have a significant effect on the effective hydrodynamic radius of the coils. Our results suggest that under the conditions of our experiment (in particular the buffer conditions: 10mM Sodium Phosphate buffer, pH 7, 100mM NaCl), the H-NS proteins most likely did not cause extensive bridging of dsDNA,

since this most certainly would have led to a significant effect on the DNA coil sizes. This absence of bridging in the absence of multivalent cations is consistent with single molecule DNA force measurements performed for similar buffer conditions by other authors. We also find that, although H-NS alone does not have a dramatic effect on DNA coil sizes in solution (for our solution conditions), it does have an interesting synergetic effect on polymer-induced condensation of DNA. Condensation of H-NS/DNA complexes was measured by their sedimentability in solutions of polyethylene glycol (PEG). In the absence of H-NS the critical concentration of PEG needed to condense DNA is approximately 15%, whereas the critical concentration is remarkably lower, about 3.5%, at near saturation concentrations of H-NS.

Chapter 4 is concerned with the effect of binding of H-NS and macromolecular crowding on nucleoid compaction. An osmotic shock method using ampicillin was used to isolate the *Escherichia coli* nucleoids intact, disrupting the peptidoglycan layer. These nucleoids were stained with DAPI and photographed using confocal microscopy. This showed a decrease in the volume of the isolated nucleoids when polyethylene glycol (PEG) concentrations became higher. The addition of small amounts of H-NS appeared to enhance the compaction due to macromolecular crowding induced by PEG. Remarkably, in the absence of PEG, H-NS did not affect the compaction of the nucleoids even at higher concentrations. The results are consistent with previous experiments done on DNA-binding proteins HU and Sso7d by other research groups. Therefore, our results confirm a general enhancement of macromolecular crowding effect of cytoplasm by nucleoid-associated proteins binding.

In Chapter 5 we focus on an archaeal NAP. Like bacteria, archaea have NAPs that bend DNA and form extended helical protein-DNA fibers. These do not condense the genomic DNA directly, but some NAPS strongly promote DNA condensation by macromolecular crowding, such as the bacterial HU. Using theoretical arguments, we show that this synergy can be explained by the larger diameter and lower net charge density of protein-covered DNA filaments compared to naked DNA. Therefore the effect should be nearly universal in prokaryotes. We illustrate this general effect by demonstrating that Sso7d, a 7 kDa basic DNA-bending protein from the archaeon *Sulfolobus Solfataricus,* does not significantly condense DNA by itself, using light-scattering to determine coil volumes. However, the Sso7d-coated DNA fibres are much more susceptible to macromolecular crowding-induced condensation. Clearly, if DNA-bending nucleoid proteins fail to condense DNA in dilute solution, this does not mean that they do not contribute to DNA condensation in the context of the crowded living cell.

7.2 Samenvatting

Deze samenvatting bestaat uit een introductie voor leken, en een samenvatting van wat ik zelf heb gedaan. In de lekenintroductie leg ik alle begrippen die ik in mijn onderzoek gebruik uit. Dit gedeelte is bedoeld voor mensen zonder specialistische kennis van scheikunde, biologie en natuurkunde. Het tweede gedeelte is een korte uitleg van wat ikzelf heb gedaan.

7.2.a *Lekenintroductie*

In levende cellen is DNA het grootste molecuul. Het is een polymeer, dat wil zeggen dat het is opgebouwd uit bouwstenen die samen lange ketens vormen, in het geval van DNA altijd onvertakt. De bouwstenen van DNA zijn nucleïnezuren. De hoofdketen of ruggengraat bestaat uit een negatief geladen fosfaatgroep en een goed oplosbare suiker, met daaraan een hydrofobere base adenine (A), thymine (T), cytosine (C) of guanine (G). Die basen gaan graag waterstofbindingen aan met tegenoverliggende basen, zodat een antiparalelle dubbele keten ontstaat; A vormt twee waterstofbindingen met T en C drie met G. Individueel zijn waterstofbindingen niet zo sterk, maar het effect accumuleert snel omdat elke base een binding aangaat ofwel een basepaar vormt. Dit is energetisch zo gunstig dat DNA in de natuur (dat wil zeggen in een waterige oplossing) bijna altijd voorkomt als een verbinding van twee antiparallelle ketens, die een dubbele helix vormen. Één wenteling van de helix bestaat uit ~10.5 bp (basepaar) en is 3.4 nm lang. Helixvorming heeft ook gevolgen voor het gedrag van het molecuul. Een enkele opgeloste DNA keten is heel flexibel, de dubbele helix juist niet. Als je een enkele keten zou vergelijken met bindtouw, dat je kunt knopen en opproppen, dan is een dubbele helix als een tuinslang, stijf en moeilijk op te rollen. Vanwege die stijfheid neemt DNA enorm veel ruimte in als willekeurige kluwen. De grote lengte van DNA-ketens draagt daar ook aan bij; het erfelijk materiaal ofwel genoom van de meeste bacteriën bestaat uit één cirkelvormig chromosoom van een paar miljard baseparen, dat uitgerekt in de orde van één millimeter meet, terwijl het menselijk genoom uitgestrekt meer dan een meter lang is.

Opgeloste ketens zoals DNA ordenen zich niet spontaan, en hun driedimensionale structuur verandert ook gemakkelijk. We noemen de structuren die een driedimensionale, willekeurige kluwen kan aannemen de conformatie. DNA is het grootste molecuul in de cel, maar het is klein genoeg om beïnvloed te worden door Brownse- of warmtebeweging (de

willekeurige beweging van deeltjes in een vloeistof of gas). Daarom beschouwen we de gemiddelde conformatie van een keten. Dat betekent dat er een gemiddeld kluwenvolume is. Aangezien de gemiddelde kluwen naar een bolvorm neigt, wordt het formaat meestal aangegeven in de vorm van een straal. Polymeerkluwens in een goed oplosmiddel zijn ijl; een groot gedeelte van het volume van het kluwen wordt in feite ingenomen door oplosmiddel. Hoe stijver een polymeer, hoe meer oplosmiddel in het kluwen zit. Als de stijfheid en de lengte van een molecuul bekend zijn, kunnen we de gemiddelde straal en het volume van een vrije kluwen berekenen, mits het oplosmiddel goed is. In het geval van DNA moet ook rekening worden gehouden met de grote negatieve lading van de fosfaatgroepen in de keten, die elkaar afstoten. Die lading draagt sterk bij aan het grote volume van DNA kluwens, tenzij die oplossing veel ionen bevat. De positieve ionen worden aangetrokken door de negatieve fosfaatgroepen op het DNA, en schermen zo de lading van het DNA zelf af.

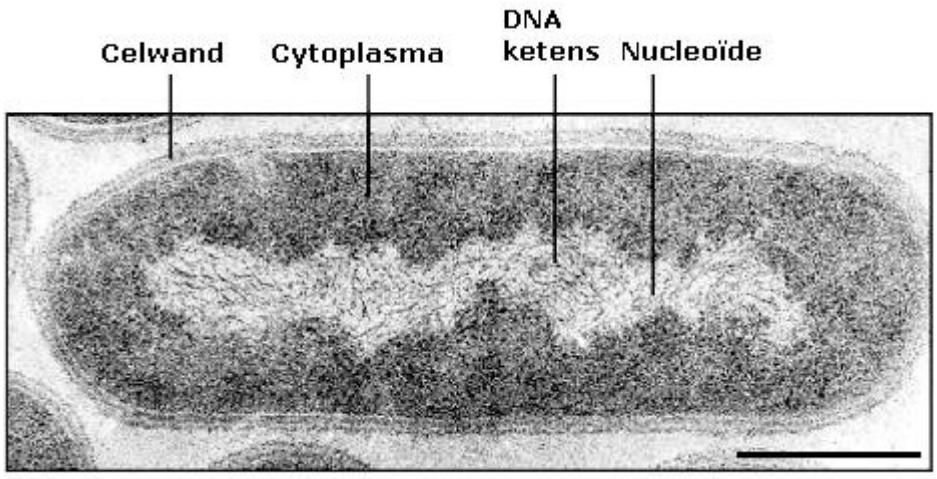

Figuur 7.1: Een elektronenmicroscopisch beeld van een intacte *E. coli* cel. De nucleoïde neemt slechts ~15% van het celvolume in beslag. Dit preparaat is gekleurd om de DNA ketens zichtbaar te maken en het cytoplasma donker te kleuren. Schaalaanduiding 0.5 μm.

Toch is het DNA in een levende cel geordend. Cellen zijn klein vergeleken met het volume van een DNA kluwen ter grootte van een genoom, maar het erfelijk materiaal neemt slechts een deel van een cel in beslag. In eukaryote cellen zoals de onze is de situatie relatief goed bekend; al het DNA bevindt zich in de celkern of nucleus omringd door membranen, en het is opgerold rond eiwitten genaamd histonen, die zich weer verder ordenen. Prokaryote cellen zoals bacteriën hebben kleinere genomen dan eukaryoten. Toch past een ongeorganiseerde DNA kluwen er niet in, omdat prokaryote cellen ook veel kleiner zijn, meestal een paar micrometer lang (Figuur 7.1). In prokaryoten is het DNA ook niet door de

hele cel verspreid. Al het genomische DNA bevindt zich in nucleoïde. In de modelbacterie *Escherichia coli* (*E. coli*) neemt de nucleoïde ongeveer 15% van het celvolume in. De nucleoïde is niet omringd door een membraan, en heeft een onregelmatige vorm. Het volume van een even lange vrije DNA kluwen is minstens 100 maal groter dan een bacteriële cel. Het volume van DNA in een nucleoïde kan 1000 tot 10.0000 maal verminderen. We noemen de volumereductie van DNA compactie of, in extreme gevallen, condensatie. In tabel 7.1 staan enkele voorbeelden van DNA compactie. Figuur 1.1 van de introductie laat een *E. coli* cel zien met het DNA rondom uitgespreid. Het bacteriële DNA is zichtbaar georganiseerd in domeinen die een rozet vormen.

Soort DNA	Lengte DNA		Vrije kluwen DNA		Volume nucleus/	Volume
	baseparen	contour	Straal	Volume	nucleoïde	voorbeeldcel
	aantal	Nm	nm	nm^3	nm^3	nm^3
E. coli plasmide	2686	886	121.5	7.5×10^6	/	/
(lineair)	1.0×10^4	3300	234.5	5.4×10^7	/	/
E. coli genoom	4.6×10^6	1.5×10^6	5.0×10^3	5.0×10^{11}	2.0×10^8	1.5×10^9
Humaan genoom	3.0×10^9	1.0×10^9	1.3×10^5	9.0×10^{15}	6.9×10^{11}	4.0×10^{14}

Tabel 7.1: Een vergelijking van ideale volumes van DNA kluwens met experimenteel bepaalde volumes van celkernen of nucleoïden. De waarden zijn benaderingen, afhankelijk van oplosmiddel voor ideale kluwens, en afhankelijk van celtype en groeicondities voor celvolumes.

In fysische termen kan men de vorming van een nucleoïde zien als een voorbeeld van fasescheiding. De meest bekende vorm van fasescheiding is scheiding van waterige en olieachtige vloeistoffen, maar ook polymeren kunnen in twee fasen scheiden als ze in hoge concentratie aanwezig zijn. Zonder invloed van buitenaf streven systemen naar vermindering van orde, ofwel verhoging van entropie (de energie die niet beschikbaar is voor arbeid). Fasescheiding lijkt in strijd met toename van entropie, maar over het hele systeem gerekend kan het de vrijheid van moleculen verhogen. Het blijkt dat polymeren die voldoende in vorm verschillend, elkaar zodanig in de weg zitten dat hun totale entropie verhoogd wordt door fasescheiding in een fase rijk aan het éne polymeer en een fase rijk aan het andere polymeer. In dit proefschrift dragen we bewijs aan voor de veronderstelling dat de vorming van het bacteriële nucleoïde ook gezien kan worden als een soort van fasescheiding waarbij de belangrijkste polymeren verschillen in vorm zijn: aan de ene kant, de vele min of meer bolvormige eiwitten, die niet binden aan DNA, en aan de andere kant, het DNA (bedekt met DNA-bindende eiwitten). De concentraties van macromoleculen, of polymeren, in levende

cellen zijn inderdaad zeer hoog, zodat het niet gek is om faseschеiding te verwachten. Gemiddeld is elk macromolecuul (eiwit, RNA, DNA, etc.) maar door een paar laagjes watermoleculen gescheiden van het volgende macromolecuul, zodat in de cel met recht gesproken kan worden van “macromoleculaire drukte”, of, in de terminologie van de engelstalige vakliteratuur, van “macromolecular crowding”. Deze macromoleculaire drukte, die dus een drijvende kracht is voor faseschеiding, is aanwezig zolang de bacteriële cel intact is. Een breuk in het celmembraan veroorzaakt daarom onmiddellijke expansie van het DNA

Ondanks de afstoting tussen de negatief geladen ketens en de stijfheid van DNA kan het molecuul gemakkelijk compact worden. In de cel worden kleine biopolymeren zoals eiwitten, RNA’s en suikers uit de DNA-rijke fase ofwel de nucleoïde verwijderd door macromoleculaire drukte. We concentreren ons hier op eiwitten, die in groten getale aanwezig zijn in de celvloeistof. De stroperige celvloeistof is geen goed oplosmiddel voor DNA. In slechte oplosmiddelen, onder hoge zoutconcentraties en bij hoge depletie vormt DNA zelfs vloeibare kristallen. Die drie factoren moeten zorgen voor de 1000-10.000-voudige volumereductie van het DNA, samen met DNA-bindende eiwitten. Deze factoren functioneren zolang de bacteriële cel intact is, maar een breuk in het celmembraan veroorzaakt onmiddellijke expansie van het DNA.

Nucleoïden bevatten niet alleen DNA, maar ook eiwitten die DNA binden en het genoom reguleren. De transcriptie-, translatie- en reparatie-eiwitten hebben weinig effect op het volume van de nucleoïde. De klasse van gyrase-eiwitten heeft wel een belangrijk effect op DNA; gyrases winden het DNA op, zodat het in elkaar gedraaide plectonemen gaat vormen (zie figuur 1.4). Dit verkleint het volume van de kluwen. Een vierde klasse DNA-bindende eiwitten staat centraal in de andere hoofdstukken; de nucleoïde-associërende eiwitten (NAPs). Zij reguleren de expressie van genen en hebben een rol in de organisatie van DNA. Bacteriële NAPs vervormen het DNA, meestal door DNA te buigen of bruggen te vormen tussen strengen DNA.

In dit werk staat het nucleoïde-associërende eiwit H-NS centraal. H-NS staat voor histonachtig nucleoïde-structurerend eiwit. Het is een belangrijk eiwit; het is met maximaal 20.000 kopieën aanwezig, maar giftig als de concentratie verhoogd wordt. H-NS reguleert de expressie van groepen genen door hun promotoren te binden of los te laten, maar het heeft geen sterke voorkeur voor één specifieke DNA sequentie. Een aantal van de H-NS gecontroleerde genen zijn betrokken bij de virulentie van pathogene bacteriën zoals *Salmonella*, bekend als veroorzaker van voedselvergiftiging. Buiten een gastheer zijn deze pathogenen niet virulent; ze produceren geen toxines en blijven niet kleven. De omgeving

moet veranderen, zoals verhoging van de temperatuur of osmotische druk. De binding van H-NS aan promotoren van virulentiegenen verandert bij een toename van de temperatuur naar lichaamstemperatuur en reguleert daarmee de eerste stap in de virulentie cascade van *Salmonella*. Wij zijn geïnteresseerd in deze temperatuurschakelaar.

H-NS bevindt zich in de nucleoïde. Het bindt DNA zwak, maar H-NS bedekt veel DNA omdat er zo veel kopieën van zijn. H-NS heeft twee domeinen; het ene domein heeft dimerizering oftewel semi-permanente binding van een ander H-NS eiwit als voornaamste functie, terwijl het andere domein DNA bindt (zie figuur 1.5). Deze domeinen worden verbonden door een niet gevouwen streng aminozuren die we de schakel noemen. Met twee DNA-bindingsplekken in het kunnen bruggen tussen DNA strengen worden gevormd, maar door de zwakke DNA-binding kunnen die ook weer makkelijk loslaten. Als een dimeer een ander dimeer bindt, versterkt dat de DNA-binding van beide. Vorming van grotere deeltjes noemen we multimerizering of oligomerizering. H-NS kan oligomeren van tientallen dimeren vormen, die lange stukken DNA bedekken (zie figuur 1.7). Dit veroorzaakt condensatie van kleine stukjes DNA, maar details over het effect van brugvorming door H-NS op grote schaal is weinig bekend. Dit is het belangrijkste onderwerp van deze dissertatie.

In deze dissertatie willen we meten hoe groot H-NS oligomeren en kluwens DNA zijn. We gebruiken daarvoor een aantal technieken, waarvan dynamische lichtverstrooiing (DLS) de belangrijkste is. De techniek meet de beweging ofwel diffusie van deeltjes in oplossing, door het meten van veranderingen in de lichtverstrooiing door deeltjes. De diffusie is gerelateerd aan een straal (ervan uitgaande dat de deeltjes ongeveer bolvormig zijn). De techniek kan ook de grootte van deeltjes in mengsels meten, zolang verschillen in volume vrij groot zijn en er maar een paar groepen deeltjes zijn.

7.2.b *Samenvatting van deze dissertatie*

Dit onderzoek is begonnen met de studie van H-NS oligomerizering in oplossing, en we willen dit fenomeen verbinden aan de coöperatieve binding van DNA door H-NS. Wij zijn geïnteresseerd in de rol van eiwit-eiwit interacties versus eiwit-DNA interacties in oligomerizering. Daarom hebben we een mutant gemaakt waarvan het schakeldomein veel hydrofober is dan normaal H-NS. We hebben de hydrofiele zwakke asparaginezuren op aminozuur positie 68 en 71 vervangen door valines, die hydrofoob zijn. Omdat die posities omringd zijn door nog meer hydrofobe aminozuren geeft de mutatie een hydrofoob cluster dat het hele schakeldomein minder goed oplosbaar maakt, zodat het sterk gaat plakken aan andere

hydrofobe domeinen. De mutant is bijna functioneel, want overproductie is bijna even toxisch voor de cel als ongemuteerd (wild type of *wt*) H-NS.

Wij zijn de eersten die DLS gebruikten om oligomerizering van *wt* H-NS te meten in hoofdstuk 2. We hebben bevestigd dat *wt* H-NS oligomeren vormt waarvan het merendeel een geschatte omvang van 5 tot 20 dimeren heeft, afhankelijk van de H-NS concentratie. We vonden ook veel grotere deeltjes, maar het is niet duidelijk of die fysiologisch relevant zijn. De omvang van de oligomeren is zwak temperatuurafhankelijk, maar het verband is grofweg lineair. De omvang halveert tussen 16˚C en 40˚C, in plaats van een scherpe daling rond de 30˚C. Deze temperatuursafhankelijkheid verandert door kleine modificaties aan de N-terminus van H-NS. De toevoeging van twee kleine aminozuren GA onderdrukt de temperatuursafhankelijkheid van de oligomeeromvang. Diezelfde toevoeging heeft echter geen invloed op DNA-binding *in vitro*, of op giftigheid. Dit betekent dat H-NS eiwit-eiwit interacties geen belangrijke rol in de thermoregulatie van het bacteriële genoom door H-NS spelen. De hydrofobere schakelmutant creëert veel grotere oligomeren met stralen tot 35 nm. Hun omvang hangt minder af van de eiwitconcentratie. De straal van deze hydrofobere oligomeren is wel temperatuurafhankelijk, maar dat verband is niet linear. Het effect van de schakelmutatie op DNA binding is klein. Al met al kan de temperatuurafhankelijke regulatie door H-NS niet afhangen van interacties tussen verschillende dimeren. Ook is het duidelijk dat het gedrag van H-NS zonder DNA niet direct gerelateerd kan worden aan het gedrag in aanwezigheid van DNA.

Hoofdstuk 3 van deze dissertatie richt zich op interacties van H-NS met DNA, en vooral het effect van H-NS op DNA condensatie onder "macromoleculaire drukte". Als vereenvoudigd model voor het lange genomische DNA gebruiken we de plasmide pUC18 (2686 bp) in lineaire en in elkaar gewonden vorm. In DLS experimenten zien we dat H-NS aan DNA bindt door de hogere intensiteit van het verstrooide licht, maar binding van H-NS verkleint het volume van DNA kluwens weinig. We zien wel dat H-NS soms intermoleculaire bruggen vormt tussen kluwens DNA. Dit lijkt geen direct effect op DNA condensatie te hebben maar het kan belangrijk zijn voor genregulatie en mogelijk ook voor de vorming van domeinen of lussen (introductie figuur 1.1). H-NS heeft wel een sterk condenserend effect op DNA dat al bloot staat aan "macromoleculaire drukte". We simuleren dat met het inerte polymeer PEG. PEG condenseert DNA kluwens sterk door depletie, maar die condensatie neemt toe als H-NS ook aanwezig is. Dit effect is synergistisch en verlaagt de hoeveelheid polymeer nodig voor sedimentatie van 15% naar 3.5%. Kortom, H-NS kan een belangrijke bijdrage aan de compactievan DNA leveren door de negatief geladen keten te binden. Het is

nog steeds onduidelijk of DNA-deformatie door brugvorming ook een rol speelt in condensatie en vorming van de nucleoïde.

Hoofdstuk 3 gaat over het effect van macromoleculaire drukte en H-NS op de compactie van nucleoïden. Wij hebben de nucleoïde van *Escherichia coli* intact geïsoleerd door gebruik van osmotische schok en disruptie van de peptidoglycanenlaag door ampicilline. Deze intacte nucleoïden werden gekleurd met DAPI en gefotografeerd met een confocale microscoop. Het volume van de geïsoleerde nucleoïden verminderde bij verhoging van de concentratie polyethylene glycol (PEG). Toevoeging van kleine hoeveelheden H-NS versterkte deze compactie door macromoleculaire drukte. H-NS alleen heeft echter vrijwel geen effect op het volume van nucleoïden, zelfs in hogere concentraties. Dit is consistent met de resultaten van andere NAPs, zoals HU. Deze resultaten bevestigen dat binding van DNA door NAPs het volumeverkleinende effect van macromoleculaire drukte (zoals aanwezig in het cytosol) versterkt. In hoofdstuk 5 hebben we gekeken we naar een ander nucleoïde-associërend eiwit, Sso7d. Dit eiwit is niet afkomstig uit bacteriën maar uit een archaeon. Archaea zijn prokaryoten. Ze zijn klein, net als bacteriën, maar hun metabolisme lijkt meer op dat van eukaryoten. De DNA-bindende eiwitten van archaea hebben eigenschappen uit beide rijken; sommige archaea hebben eiwitten die nauw verwant zijn met eukaryote histonen, maar andere hebben een homoloog van het bacteriële DNA-buigende eiwit HU, en sommige eiwitten komen exclusief voor in een familie van archaea. Sso7d en homologen komen voor onder verschillende Archaea. Het eiwit buigt DNA, maar draagt maar beperkt toe aan DNA condensatie in oplossing. Toevoeging van polymeren zodat macromoleculaire drukte ontstaat leidt echter tot dramatisch versterkte DNA condensatie. Het is duidelijk dat ook dit eiwit kan bijdragen aan condensatie in de stroperige, volle celvloeistof.

Deze dissertatie focust op het condenserend effect van nucleoïde-associërende eiwitten en macromoleculaire drukte op nucleoïden. Wij stellen voor dat synergie tussen macromoleculaire drukte en nucleoïde-associërende eiwitten een algemeen mechanisme voor condensatie is, dat ook geldig is voor andere nucleoïde-associërend eiwitten zowel in bacteriën als archaea. In de literatuur zijn aanwijzingen te vinden dat dit geldt voor de bacteriële eiwitten HU en FIS, en dat combinaties van buigende en bruggen vormende eiwitten een sterk effect hebben op condensatie. Dit geeft een algemeen model voor de vorming van nucleoïden in bacteriën en mogelijk ook in archaea.

Acknowledgement

This work was supported financially by grant number 805.47.181 of the Dutch Science Foundation (NWO), in the context of the programme from Molecule to Cell (MtC). Several chapters of this thesis are the result of two collaborations. The first collaboration is with our project partners prof. Theo Odijk (Delft University of Technology), Dr. Conrad Woldringh (University of Amsterdam) and Anna Wegner, my fellow PhD student in this NWO project. The work described in Chapters 3 and 4 was done jointly with Anna Wegner, with equal contributions from us both, for both chapters. We also collaborated with Dr. Roberto Spurio and Mara Giangrossi both of the Laboratory of Molecular Genetics, School of Bioscience and Biotechnology, University of Camerino. The various *E coli* strains overproducing both wild type and mutant H-NS came from their laboratory, and protein purification was done with their help, at the University of Camerino. Also, they contributed to Chapter 2 by providing part of the experimental data (electrophoretic mobility shift assays, *in vitro* transcription assay and DNAse I footprinting).

Dankwoord

Terugkijkend op mijn promotie realiseer ik me hoeveel mensen er een rol in hebben gespeeld. Wetenschappelijk onderzoek is teamwerk, ook al moet je het uiteindelijk zelf doen. Gedurende het proces voel je je soms eenzaam, maar gelukkig heb ik altijd mensen gehad die mij een handje hielpen of gewoon luisterden. Als eerste wil ik mijn ouders bedanken, die mij van jongs af aan hebben gestimuleerd om nieuwsgierig te zijn, en dingen uit te zoeken. Mam, bedankt voor de manier waarop je hebt aangemoedigd om vragen te stellen en vooral heel veel te lezen. Gedurende mijn promotie had je altijd tijd om naar me te luisteren, advies te geven (ook al luisterde ik niet) en mijn successen te delen. Pa, ik weet dat je het hartstikke leuk vindt dat ik ook de chemie in ben gegaan, en uiteindelijk zelfs nog reologie ben tegengekomen. Mathijs, je bent de beste broer die ik me kan voorstellen. Bedankt voor alle hulp, de computerprobleempjes die jij zó oploste, de discussies over wetenschap, het doorlezen van mijn dissertatie en artikelen om mijn grammatica te controleren en alle andere dingen. Ik wil alleen nog zeggen dat ik heel trots ben op je en je het allerbeste toewens met je eigen promotie bij Wiskunde in Groningen. Oma, zonder jou zou het niet hetzelfde zijn.

Renko, ik heb onze samenwerking altijd als prettig ervaren. Ik heb heel veel van je geleerd en ik hoop dat je ook iets hebt gehad aan mijn biochemische inbreng. Ik kon altijd bij je binnenlopen, en jouw commentaar op mijn experimenten was altijd waardevol. Ook heb ik onze discussies over wetenschap in Corsica en Italië erg gewaardeerd. Frans Leermakers, je bent pas in een laat stadium bij mijn onderzoek betrokken geraakt, maar ik waardeer je inbreng heel erg, net als het eerdere advies aan de koffietafel. Je was ook een fantastische reisgenoot tijdens de PhD trips. Je bent een grote steun geweest bij de laatste loodjes, die spreekwoordelijk zwaar waren. Martien, Fysko is een fantastische groep en jij bent degene die het mogelijk maakt. Theo, je bent een bijzonder mens en een bijzondere wetenschapper. Ik denk vaak terug aan onze interessante discussies in de mooie binnenstad van Leiden.

Anna Wegner, we hebben heel veel en heel direct samengewerkt. Je hield altijd de moed erin tijdens de eindeloze fotoseries van nucleoïden. Ik heb het altijd leuk gevonden om labwerk te doen in Amsterdam, ondanks de eindeloze verhuizingen van het SILS lab, of met jou samen te werken in Wageningen. Ik weet dat het traject jou ook erg zwaar is gevallen. Ik schrijf je in het Nederlands, want ik weet hoe hard je gewerkt hebt aan je talen. Tanneke,

bedankt voor je hulp bij het plannen van de laatste experimenten. Jij, Conrad en Jojanneke waren een grote hulp bij het experimentele werk in Amsterdam.

Roberto, I want to thank you again for you aid and support of the biochemical part of this thesis, as well as your critical reading of several articles. I really enjoyed my visits to the Microbiology lab in Camerino. I learned a lot about protein isolation from you. I am very grateful for you encouragement and quick replies to my questions. Thanks for picking me up at the most ridiculous times. The conferences I attended in Camerino were really good. This brings me to Claudio, who organized these conferences with Anna-Maria. Thank you for hosting me, and introducing me to various speakers. Mara, thanks for the footprinting, the other experiments and commenting on some of my work. Anna, you were a great help around the lab. Maurizio, Gaetana, Lolita, Cinzia, Marco, Ulysse, Alesandra, and all the other people, thanks for your help and showing me a great time.

Willy van den Berg, je hebt mijn experimenten bij Biochemie ruimhartig gefaciliteerd en veel tijd voor me vrijgemaakt. Ans Geerling, bedankt voor alle hulp met de Sso7d experimenten. Esio, I know how much you hated Dutch weather, but you still braved it with me to do experiments all over "de Dreijen". You played a crucial role in the Sso7d story, and I enjoyed cooperating with you.

Petya en Bas, jullie waren mijn eerste kamergenoten. Jullie hebben me op weg geholpen bij het moeilijke begin en het was een gezellige kamer, mede dankzij het briljante idee van Bas om een la te vullen met snoep. Ik heb veel plezier gehad in onze discussies over speculatieve fictie en (populaire) wetenschap, ook al raakte onze onderzoeksonderwerpen elkaar eigenlijk niet. I wish you and Paulina the best in Gouda. Dmitri and Yunus, you were great roommates. I enjoyed our discussions about culture differences as well as the barbeques you organized. Hans Lyklema, ik vond het heel erg fijn om je kamer en je wijsheid te mogen delen. Ik bewonder dat je nog zo betrokken bent bij Fysko en heb leuke herinneringen aan je deelname aan de PhD trip naar Zweden. Ik vond het ook heel leuk om wat meer te horen over de geschiedenis van het lab en Wageningen.

Paulina and Mark, I enjoyed the organization of the PhD trip to Switzerland and France. I learned a lot by contacting all these foreign universities and from cooperating with you. I'm sure we are rightly proud of the resulting trip, especially the interesting labs we

visited and how we managed to do it all under budget. Evan, Yuan, Cecilia, Dmitri, Yunyou and Monica, I really enjoyed your company on the trip, both the serious meetings and the fun stuff. Cecilia, I enjoyed talking politics in the Louvre, and Yuan, I'll never forget your look of surprise at those snails.

Mentioning PhD trips, I would like to thank Bas, Wiebe and Joris, organizers of the previous PhD trip to Sweden and Denmark. Saskia, ik kon altijd vertrouwen op je goede advies, in deze en andere zaken, en wens jou en Wiebe heel veel geluk. Pascal, ik heb altijd veel plezier gehad in onze discussies over everything geeky. Agata, I'm sorry for accidentally acquiring your desk, and I think back fondly of your photography and the mills. Suomi and Surrender, that recipe was really great. Lyakat, I enjoyed the tourism and the discussions about religion and philosophy. Arnout, Ilja, Marat, Bart, Yun Yan, Erika, Sabine, Johan, Thao, Armando, Wolf, Lennart, Christian, Huanhuan, Harke, Jeroen, Katarzyna, Bram, Gosia and all the others, you are all great colleagues, and I want to thank you for making my time at Fysko as enjoyable as it was.

Beste Josie, bedankt voor het luisterend oor en de hulp met alle mogelijke formulieren. Ik kon altijd bij je binnenlopen en dat heeft veel voor mij betekend. Je bent echt het zonnetje van Fysko, en je rol kan niet overschat worden. Ik wens je het allerbeste met je gezondheid. Mara, je stond altijd voor me klaar als ik rare dingen wilde bestellen (ook al had ik nooit gedacht dat droogijs op dinsdag raar was) of als ik zware dingen van hot naar her verplaatste. Als ik wilde weten wat er voor nieuws was, wist ik bij wie ik terecht kon. Anita, bedankt voor je hulp met de financiële kant van de PhD trip, en de formulieren die een onvermijdelijk gedeelte zijn van een promotie. Ronald, bedankt voor je computerhulp. Remco, je hebt me ontzettend geholpen met statische lichtverstrooiingsexperimenten. Bert, bedankt voor je hulp met pakketjes. Frans, ik heb het altijd leuk gevonden om onderwijs te geven met jou, en je hebt me er veel over geleerd. Anton, je was altijd bereid om een helpende hand toe te steken in het lab. Rhoda en Anneke, jullie hebben nooit genoeg waardering gekregen voor jullie harde werk voor onze leefomgeving.

About the author

Kathelijne Wintraecken was born on the 25th of May 1982 in Zeist, the Netherlands. She has one younger brother. She attended "De Griffel" for primary education, then took gymnasium-level secondary education at "De Breul", both in Zeist. Having graduated in 2000, she continued her education at Utrecht University, studying Chemistry. She got her Chemistry Bachelor in 2004 with a thesis on the binding of the leukocyte β_2 integrins to von Willebrand Factor performed at the Department of Haematology at UMC Utrecht. She did the major research project of het master in Biomolecular sciences in the Membrane Enzymology section of the Bijvoet Centre, Utrecht University, where she characterized Ros3p and its role in P-type ATPase dependent lipid transport. For her minor project she identified novel genes in Alg1/Alg2 pathway and a possible function for Rrf-2 by a genome-wide RNAi screen in *C. elegans* in the Hubrecht Laboratory, Utrecht. She completed her Master in 2005, and found a PhD project in the Laboratory for Physical Chemistry and Colloid Science at Wageningen University in 2006. She researched the role of H-NS and macromolecular crowding in compacting prokaryote DNA under supervision of Renko de Vries. The results are in this thesis.

Levensloop

Kathelijne Wintraecken is op 25 mei 1982 in Zeist geboren. Ze kreeg een jongere broertje in 1985. Na 8 jaar op de basisschool “De Griffel”, ging ze naar het gymnasium van “De Breul”, beide in Zeist. In 2000 ontving ze haar gymnasiumdiploma, en begon meteen daarna aan de studie Scheikunde aan de Universiteit Utrecht. Ze behaalde haar Bachelordiploma in 2004 met als scriptie de binding van leukocyt β_2 integrines aan Von Willebrand Factor bij Hematologie in het UMC Utrecht. Tijdens haar Master Biomolecular Sciences koos ze voor een hoofdvak bij Membraanenzymologie in het Bijvoet Centrum van de Universiteit Utrecht, waar ze de rol van Ros3p in P-type ATPase-afhankelijk lipidentransport karakteriseerde, en voor haar minor onderzoeksproject deed ze een genoom-wijde RNAi screen in *C. elegans* in het Hubrecht Laboratorium te Utrecht, waarbij ze nieuwe genen in de Alg1/Alg2 cascade identificeerde en een mogelijke functie van Rrf-2 voorstelde. Gedurende haar bachelor- en masterfase was ze actief in de facultaire medezeggenschap. Ze rondde haar master af in 2005. Ze vond een interessant promotieproject bij het Laboratorium voor Fysische Chemie en Kolloïdkunde aan de Universiteit Wageningen in 2006, en onderzocht de rol van H-NS en macromoleculaire drukte in de volumereductie van bacterieel DNA onder begeleiding van Renko de Vries. De resultaten van het onderzoek staan in deze dissertatie.

List of publications

J. E. Bessa Ramos, Jr., K. Wintraecken, A. Geerling, and R. de Vries. 2007. Synergy of DNA-bending nucleoid proteins and macromolecular crowding in condensing DNA. Biophysical Reviews and Letters (BRL) 2:259-265.

Overview of training activities

Conferences

Annual Dutch Meeting on Molecular and Cellular Biophysics	Lunteren	2006
Excerpts of Molecular Biology	U. v. Camerino, Italy	2006
ECIS conference Ven	Lund University, Sweden	2007
Annual Dutch Meeting on Molecular and Cellular Biophysics	Lunteren	2007
Excerpts of Molecular Biology	U. v. Camerino, Italy	2007
Soft Matter Springschool	FZ-Jülich, Germany	2008
Annual Dutch Meeting on Molecular and Cellular Biophysics	Lunteren	2008
Excerpts of Molecular Biology	U. v. Camerino, Italy	2008
Lorentz: The physics of genome folding and function	Leiden	2008
Annual Dutch Meeting on Molecular and Cellular Biophysics	Lunteren	2009
DNA and chromosomes	CEA, France	2009
Excerpts of Molecular Biology	U. v. Camerino, Italy	2009
Annual Dutch Meeting on Molecular and Cellular Biophysics	Lunteren	2010

General courses:

MSc Lectures Colloid Science, PCC	Wageningen	2006
Part of MSc course Research Methods, PCC	Wageningen	2006
Workmeetings Physical Chem., PCC	Wageningen	2006-2011
Colloquia Physical Chem, PCC	Wageningen	2006-2011
Presentation course	Wageningen	2007
Endnote course	Wageningen	2007
Fire extinction instruction	Wageningen	2010

Other activities

PhD Study trip to Sweden and Denmark	2007
PhD Study trip to Switzerland and France (part of organizing committee)	2009

Cover design and photography by Kathelijne Wintraecken
Printed by Wöhrmann Print Service, Zutphen